Université de Montréal

Dissecting the dynamic of Noc2p and its partners in pre-60S particles maturation

par
Katherine Cléroux

Département de biochimie
Faculté de Médecine

Mémoire présenté à la Faculté des études supérieures
en vue de l'obtention du grade de Maître ès Sciences
en biochimie
option génétique moléculaire

Avril, 2014

Résumé

Plusieurs études ont permis la caractérisation de la structure et de la fonction du ribosome. En ce qui attrait à la biogénèse du ribosome, nombreux aspects restent à être découverts et compris de façon plus dynamique. En effet, cette biogénèse englobe une variété de voies de modifications et d'assemblages requises pour la maturation des ARNr et pour leurs liaisons avec les protéines ribosomales. De ce fait, les protéines Noc ont été caractérisées comme des facteurs d'assemblages et ont permis la découverte d'une des premières indications sur l'ordre spatio-temporel de la maturation du ribosome. Ainsi, en utilisant la levure comme modèle, notre objectif est d'étudier d'avantage l'échange des complexes composés des protéines Noc ainsi que leur localisation intranucléaire. Ainsi, la nature des interactions de Noc2p avec Noc1p et Noc3p et l'influence de l'arrêt du transport intranucléaire ont été étudiés en utilisant des promoteurs inductibles, la microscopie à fluorescence, des immunobuvardages, qRT-PCR et des purifications par affinité.

Mots-clés :

Biogénèse du ribosome, maturation du ribosome, voie d'assemblage, ordre spatio-temporel, Noc1p, Noc2p, Noc3p, Rix7p

Abstract

Several studies have been performed to characterize the ribosome as far as to understand its structure and its function. However, major aspects of ribosome biogenesis remain elusive or gave only a static picture of the process. In fact, ribosome biogenesis involves dynamic processing and assembly pathways that are required for rRNA modification and folding, in addition to rRNA binding with some ribosomal proteins. One set of assembly factors, the Noc proteins, allowed one of the first indications about the spatio-temporal ordering of ribosome maturation. By using yeast as model, our objective is to provide a dynamic picture of the Noc proteins complexes exchange and nuclear localization by determining the nature of Noc2p interactions with Noc1p and Noc3p and by studying the influence of reversibly arrested intranuclear transport on these proteins and on Rix7p, an AAA-ATPase. In order to achieve these aims, inducible promoter, fluorescent microscopy, western blot, qRT-PCR and affinity purification analyses were used.

Keywords:
Ribosome biogenesis, ribosome maturation, assembly factors, spatio-temporal ordering, Noc1p, Noc2p, Noc3p, Rix7p.

Table of contents

List of tables

List of figures

Abbreviations

Amp	ampicillin
ATP	adenosine triphosphate
bp	base pair
d	deoxy-
DEPC	diethylpyrocarbonate
DNA	deoxyribonucleic acid
dNTP	desoxyribonucleo
DTT	dithiothreitol
EDTA	ethylendiaminetetra acetic acid
g	gram
GAL	galactose
GDP	guanosine diphosphate
GFP	green fluorescent protein
GTP	guanosine triphosphate
HIS	histidine
H_2O	double destilled water, sterile
IPTG	isopropyl-D-thiogalactopyranoside
Kan	kanamycyn
kb	kilobase pair
kDa	kilo Dalton
L	liter
LSU	large subunit
LB	luria broth

M	molar
MET	methionine
pMET	MET25 promotor
µ	micro (10^{-6})
m	mili (10^{-3})
min	minute
mRNA	messenger ribonucleic acid
MS	mass spectrometry
OD	optical density
o/n	over night
ORF	open reading frame
PAGE	polyacrylamide gelelectrophoresis
PCR	polymerase chain reaction
qRT-PCR	quantitative real-time polymerase chain reaction
RNA	ribonucleic acid
rRNA	ribosomal ribonucleic acid
rpm	rotations per minute
r-protein	ribosomal protein
RT	room temperature
SD	synthetic dropout
SDS	Sodium dodecyl sulphate
sec	second
snoRNA	small nucleolar RNA
snoRNP	small nucleolar ribonucleoprotein
SSU	small subunit

TEMED	N, N, N', N' –tetramethylethylendiamine
Tris	Tris-(hydroxymethyl)
tRNA	transfer RNA
WT	wild-type

À Bruno,

Acknowledgments

First, I want to thank the person who makes this possible, Marlene Oeffinger. Thank you for giving me this huge opportunity and believing in me during my entire master. It was an honor to work with and for you. I will always remember you as the good and understanding boss, the special Yoga teacher and the cat lover. Thank you for your understanding about my possible switch into the world of teaching… but I will always have the science passion!

I would like also to say a big thank you to the member of the lab. Karen Wei, thank you to showed me quite everything! Pierre Zindy, thank you for being with me every early morning and to helped me with the qRT-PCR and the microscopy stuff. Your help saved me many times. I would like to thank Christian Trahan and Mathew Karmar for sharing your knowledge in general. You were very helpful. Finally, a special thank to Carolina Lisbeth Agular, who shared coffee and lunch time with me and especially for the 24 hours-long experiments. It was a pleasure to work with all of you!

In addition, I would like to thank my friends. Mes amies de toujours, merci d'être tout simplement là… friendship never end! Mes amies de biochimie, merci d'avoir toujours été à l'écoute... étant donné que vous êtes les seules qui peuvent vraiment me comprendre!

Finally, I want to thank my family who was always so much supportive. Maman, même si tu ne comprenais pas toujours se que je faisais, merci d'avoir été présente, de m'avoir soutenue et d'avoir toujours accepté mes choix. Bruno, mon amour, merci de m'avoir supporté, d'avoir su me guider dans mes nombreuses remises en question et de m'avoir fait autant rire dans nos moments fous. Une chance que tu es là pour moi ! Finalement, un petit merci tout spécial à Gino et Maurice, nouveaux dans ma vie, mais qui m'apportent beaucoup de bonheur.

1 Introduction

1.1 The Ribosome

The ribosome was discovered in 1955 by the Nobel laureate George Emil Palade who described it as small particles in the cytoplasm, associated with the endoplasmic reticulum membrane [1]. Through his work, ribosomes were found to be the biological protein synthesis machinery in cells. Since many years, a lot of structural and biological studies have allowed to understand the structure of the mature ribosome and its components. It is known that all prokaryotic and eukaryotic ribosomes are composed of ribosomal RNA (rRNA) and ribosomal proteins (r-proteins), in addition to having the same molecular function [2]. Due to additional regulatory steps during translation in eukaryote, these two ribosomes differ in structure and complexity [2]. In *Escherichia coli,* ribosome is composed of two unequal subunits namely the small 30S subunit (which contains the 16S rRNA) and the large 50S subunit (which contains the 5S, 23S rRNAs) [2]. In comparison , the eukaryotic ribosome of the budding yeast *Saccharomyces cerevisiae* is made of two unequal subunits, the small 40S subunit (which contains the 18S rRNA) and the large 60S subunit (which contains the 5S, 5.8S and 25S rRNA) [3]. Furthermore, these two subunits contain about 79 r-proteins that form the mature 80S ribosome, such as 33 in the small subunit and more than 46 in the large subunit (Figure 1.1) [4]. Synthesis of these proteins as well as rRNAs are made in equimolar amounts [5]. Thereby, mature 80S eukaryotic ribosome is much larger and complex, with more than 5500 nucleotides of rRNA and 79 r-protein, compared to the mature 70S prokaryotic ribosome with about 4500 nucleotides of rRNA and 54 r-proteins [6]. These differences in complexity are due to the large number of proteins that interact with ribosomes and to the diversity of cellular processes where ribosomes play a role [7]. This aspect will be elaborated later in the manuscript.

Since 2000, when the first structural model of eukaryotic ribosome was constructed using cryo-electron microscopy, our knowledge of ribosomal function and structure has increased significantly [8]. In fact, 33 r-proteins have been shown to exist in all domains of life, including 15 proteins of the small subunit (Rps2p-5p, Rps7p-15p, Rps17p and Rsp19p) and 18 of the large subunit (Rpl1p-6p, Rpl10p-15p, Rpl18p, Rpl22-24 and Rpl29p-30p) [9]. It has been shown that r-proteins contain a high amount of positively charged lysines and

arginines in their loops and tails [9]. Indeed, the specificity of interaction between r-proteins and rRNA was first shown for the Rpl11p-rRNA complex and revealed that the interaction is mainly determined by complementarities of the charges and shapes of the surface, but not by amino acid composition or combination [9]. Moreover, it has been shown that r-proteins are involved in compactization of rRNA into correct structures which determine the shape and features of ribosomal particles [9]. Crystal structures of yeast ribosomes allowed to show that RNA are present in the core of each subunit, with r-proteins enshrined on the surface (Figure 1.1) [4]. Sites for ribosome functions such as peptidyltransferase center, polypeptide exit tunnel, GTPase binding site in large subunit (LSU) and tRNA-binding site have been identified in bacterial, archeaeal and euckaryotic ribosome structures [4]. Indeed, r-proteins were found to be responsible for specific functions of the ribosome through their participation in more than half of the known inter-subunit bridges [9].

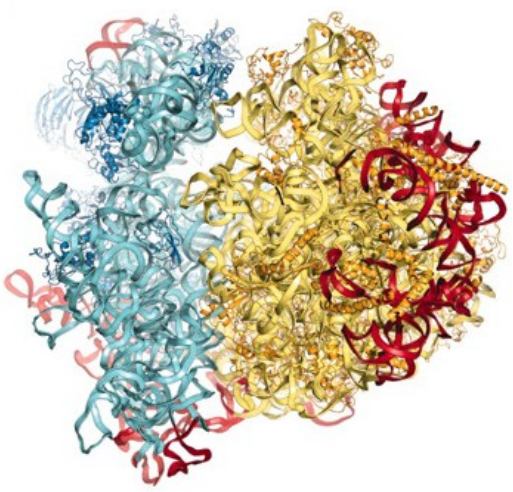

Figure 1.1. X-ray structure of the *S.cerevisiae* 80S ribosome

Proteins and rRNAs of the 40S subunit are colored in dark and light blue respectively. Proteins and rRNAs of the 60S subunit are colored in dark and pale yellow respectively. [7]

Although our understanding of the ribosomal composition and function has much significantly evolved, ribosomal biogenesis pathway remains elusive owing to a complex maturation and a tight regulation. Assembly of r-proteins and rRNA in ribosomal particles has been proposed to result in two principles: the incorporation of r-proteins is made step-by-step and the formation of ribosomal particles is accompanied by conformational changes in rRNA

structure [9]. However, eukaryotic ribosome formation is known to include the assembly of 5500nt of rRNA and about 79 r-proteins, in addition to requiring about 76 small nucleolar RNAs (snoRNA) and 200 different assembly factors [4]. This formation has been shown to be an extremely dynamic and expensive process for a cell and to required stringent inspection by specific control mechanisms coupled to nuclear export of pre-rRNPs [4]. Therefore, ribosome biogenesis will be under the microscope in this manuscript, especially the dynamic aspect of the assembly pathway.

1.2 Ribosomal DNA transcription

Synthesis of the eukaryotic ribosome has been extensively studied in the yeast *Saccharomyces cerevisiae* because of its easy experimental accessibility by biochemical and genetic methods [2]. Ribosome biogenesis is a dynamic process and is known to start in a specialized compartment of the nucleus called the nucleolus, which is composed of three substructures: fibrillar center (FC), dense fibrillar component (DFC) and granular component (GC) [10]. Ribosomal DNA (rDNA) is ~9.1 kb long and is present in 100 to 200 tandem copies on chromosome XII, located in the FC substructure [3, 11]. rRNA has been shown to elongate into the cortex of this substructure and to enter into the surrounding DFC to be processed, modified, folded and assembled with r-proteins by specific dynamic pathways from the nucleolus to the cytoplasm [11, 12]. As shown in Figure 1.2, a single rDNA unit is composed of an autonomously replicating sequence (ARS), the bidirectional promoter (E-pro), the 5S rRNA gene, which is transcribed by RNA polymerase III (Pol III) and flanked by two nontranscribed spacers (NTS1 and NTS2), and finally the 35S pre-rRNA operon, which is transcribed by RNA polymerase I (Pol I) [2, 3, 5, 13]. The 35S pre-rRNA contains the mature sequence of the 5.8S, 18S and 25S rRNAs separated by two internal transcribed spacers (ITS1 and ITS2) and flanked by two external transcribed spacers (5'-ETS and 3'-ETS) [3]. While the sole function of RNA polymerase I is to transcribe the 35S rRNA gene precursor, it has been shown that its function can be replaced by RNA polymerase II following select mutations [14].

In exponentially growing cells, only ~50% of rDNA is transcriptionally active [15]. By using a psoralen photo-crosslinking assay, in which cells are treated with a DNA intercalating

agent and UV-cross-linked (discussed in results and method section), rDNA genes were shown to adopt two distinct chromatin states that coexist throughout the entire cell cycle [15, 16]. Thus, rRNA gene can be psoralen-accessible or psoralen-inaccessible, which corresponds to transcriptionally active or inactive rDNA genes, respectively [15]. This transcriptionally inactive fraction has been shown to be important for the integrity of the rDNA locus since actively transcribed rDNA is sensitive to mutagen-induced DNA damage [15]. Moreover, experiments investigating chromatin dynamic have shown that replication is required to convert rDNA to a transcriptionally inactive state, and that Pol I transcription is required to establish an open-conformation, transcribed rDNA chromatin state [15]. This open-conformation rDNA was shown to be stabilized outside of S-phase by the HMG box protein Hmo1, which is believed to interfere with replication-independent nucleosome assembly [15]. It has been shown that when cells enter the diauxic shift, which is a transition triggered by nutrient depletion and characterized by massive reprogramming in metabolism that prepares cells for long-term survival during stationary phase, Pol I-mediated transcription of rDNA is repressed [16]. rDNA that becomes transcriptionally repressed has been found to return to a closed chromatin state until cells are provided with fresh nutrients [16].

Recent studies have taken this further by providing evidence that active rDNA genes are devoid of nucleosomes [16, 17]. ChIP experiments demonstrated that log and post-log cells have a severe difference in histones occupancy, including a 10-fold increase in H2B and H4 across the transcribed 35S region [16]. In this study, H2B and H4 were used and considered as indicators of the H3/H4 tetramer and H2A/H2B dimer respectively, which strongly implies that the entire nucleosome is likely removed during Pol I transcription [16]. In fact, it has been already shown that nucleosomes are acetylated and disrupted ahead of the polymerase during Pol II transcription elongation [16]. This disruption/reassembly cycle is known to require several proteins such as the histone deacetylase Rpd3p and histone chaperon/elongation factors Spt6p, Asf1p and FACT [16]. While Rpd3p has also been shown to associate with both the rDNA promoter (IGS2) and transcribed 35S regions, its depletion was found to cause a decrease in both H2B and H4 acetylation and in the loading of these histones onto rDNA genes [16]. Indeed, this factor was suggested to be important for maintaining the entire nucleosome structure [16]. Meanwhile the depletion of the FACT

component Spt16p was shown to be defective for loading of H2B only, suggesting that FACT is mainly responsible for assembling of the H2A/H2B dimer onto rDNA [16]. Due to the fact that the H3/H4 tetramer is known to assemble before H2A/H2B, a model has been proposed where Rpd3 could be responsible for either H3/H4 deposition or for maintaining stability of the nucleosome, while FACT could be required for H2A/H2B deposition [16]. Another recent study has developed a new purification technique enabling compositional and structural analyses of the multicopy rDNA gene cluster. Indeed, the autonomously replicating sequence (ARS), the 5S rRNA gene, the bidirectional promoter (E-pro) region and the 35S rRNA gene were found to exhibit distinct histone modification patterns [13]. As an example, histone H3 K4 tri-methylation was enriched across the ARS region, whereas histone H3 K36 tri-methylation was preferentially found across the E-pro and 35S rDNA [13]. Analyses of proteins co-purifying with rDNA domains allowed for the identification and classification of 250 to 350 proteins associated with each of the four rDNA subdomains (Figure 1.2). In fact, yeast strains were constructed to constitutively express a LexA-TAP fusion protein and specific rDNA domains or a complete rRNA repeat were flanked by RS element and include LexA-binding sites [13].

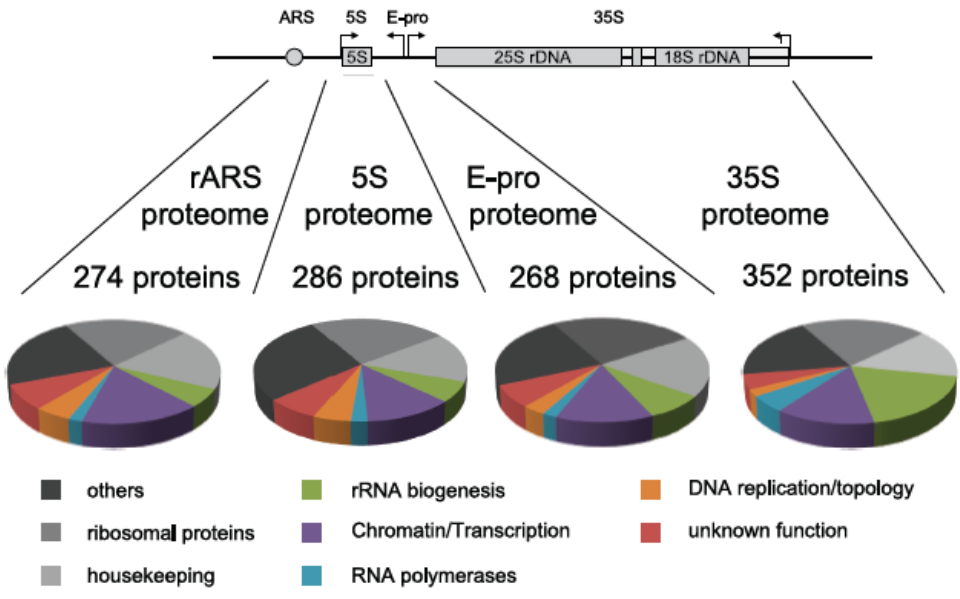

Figure 1.2. Compositional analysis by comparative MS and classification of proteins co-purifying with distinct rDNA chromatin domains

Proteins co-purifying with LexA-TAP were subjected to iTRAQ analyses in direct comparison with control purifications [13]. Identified proteins were categorized according to their biological function. The pie charts depict the relative fraction for each protein class in the purification. The data represent the summary of three independent biological replicates.

In addition to transcription, ribosomal synthesis involves several post-transcriptional processing and assembly steps to ensure 40S and 60S subunit maturation. With the aim of providing a large number of 35S pre-rRNA transcripts, Pol I needs to efficiently elongate and maintain a high synthesis rate through the rDNA region [18]. It has been shown that Pol I transcription elongation rate is closely linked to the downstream events of the pre-rRNA processing pathway [18]. Indeed, mutation of the Pol I subunit Rpa135p was shown to have a 90% reduced elongation rate and to result in a multitude of rRNA processing permutations, in addition to a reduced 60S subunit level [18]. Thus, these results provided evidences for the link between Pol I transcription and pre-rRNA processing [18]. Further evidence came via electron microscopy analysis. Due to the tandem arrangement of rDNA, pre-rRNAs have been shown to adopt a characteristic Christmas tree-like structure by EM, whereas rDNA and Pol I molecules form the stem and rRNAs are the branches extending out from transcribing Pol I molecules along the rDNA [19]. In addition, identification of co-transcriptional assemblies of r-proteins and ribosomal factors has been possible by visualization of ball- or knot-like structures, which are believed to be compacted pre-rRNA transcripts [19]. Moreover, a new purification technique allowing for compositional and structural analyses of the multicopy rDNA gene cluster, revealed several different r-proteins and pre-rRNA biogenesis factors in each actively transcribed rDNA region, supporting once again the co-transcriptional aspect of the pre-rRNA processing (Figure 1.2) [13]. Finally, by using the temperature-sensitive (*ts*) allele *rpa190-2* of RPA190, which is an essential gene encoding for the largest subunit of Pol I, *in situ* electron microscopy was used to study the effect of an rDNA transcription arrest [10]. Interestingly, this arrest has been shown to result in a dramatic nuclear reorganization, where the nucleolus was spatially rearranged and the pre-rRNA processing machinery dispersed [10]. In fact, some amount of Nop1p and Gar1p, core components of the box C/D and box H/ACA small nucleolar ribonucleoprotein complexes (snoRNP), respectively, were found re-localized to the nucleoplasm, while some still remained in the intermediate-electron-dense domain of

the segregated nucleoli [10]. Under normal conditions, both proteins are known to be involved in early pre-rRNA processing steps and are localized exclusively within the nucleolus. Indeed, rDNA transcription is now known to be required in order to maintain the structural integrity of the nucleolus as well as the early pre-rRNA processing machinery [10].

1.3 Ribosomal processing pathway

As it is being transcribed by Pol I, the nascent pre-rRNA is modified by about 75 different snoRNPs that target specific sites for pseudouridylation and 2'-O-ribose methylation, and assembled with *trans*-acting factors [2, 5]. The 35S pre-rRNA is co-transcriptionally assembled with a number of processing and assembly factors in addition to r-proteins devoted to the 40S biogenesis pathway and form the 90S particle [3, 12]. Following these early modifications and assembly steps, there are at least 11 endonucleolytic and exonucleolytic cleavages that process the precursor to remove external (ETS1 and 2) and internal spacer (ITS1 and 2) regions and generate mature 5' and 3' ends of the 5.8S, 18S and 25S rRNAs [20]. Indeed, pre-rRNA processing is carried out by a dynamic pathway, which involves more than 200 proteins, and which occurs in a hierarchical manner in the context of pre-ribosome particles.

1.3.1 90S processing

It has been showed that about 30% of the length of Pol I transcripts are completed before pre-rRNA processing is initiated [21]. The modular subcomplexes UTP-A, UTP-B and UTP-C, consisting of processing and assembly factors, some small subunit r-proteins and more than 20 other assembly factors, progressively assemble onto the primary transcript co-transcriptionally and form the first ribosomal particle called the 90S particle [2]. As shown in Figure 1.3 B, the 3' external spacer (ETS) is immediately cleaved at the B_0 site by the endoribonulcease Rnt1p, and the pre-rRNA simultaneously undergoes a large number of covalent modifications carried out by the box C/D and box H/ACA snoRNPs [2, 22]. SnoRNP complexes are composed of small nucleolar RNA (snoRNAs), which select the site to be modified by base pairing with the pre-rRNA target site, and RNA binding proteins, which are known to catalyze the modification reaction on the pre-rRNA [2, 23]. Based on their

conserved sequence and structural elements and their associations with specific proteins, snoRNPs can be divided in two classes named box H/ACA and C/D, which catalyze site-specific pseudouridylation and 2'-O-methylation of rRNA, respectively [23]. In fact, box H/ACA snoRNPs are composed of common core proteins (Cbf5, Nop10, Nhp2 and Gar1p) that base pair with the rRNA by a pseudouridylation loop where the unpaired uridine is converted to pseudouridine by the the pseudouridine synthase Cbf5p [23]. Next, the C/D box snoRNPs are known to be composed of a common core proteins (Snu13, Nop56, Nop58 and Nop1) [23]. It is known that the rRNA nucleotide five base pairs from the box D is 2'-O-methylated by Nop1p, the yeast homologue of Fibrillarin [23]. 35S pre-rRNA processing has been shown to require a subset of snoRNPs, comprising the box H/ACA snoRNPs snR30/U17 and snR10 and the boxC/D snoRNPs U3, U14, U8 and U22 [23].

Thereafter, the 35S pre-rRNA is cleaved at sites A_0, A_1 and A_2, which are dependent on the small-subunit (SSU) processosome, a 2.2 MDa RNP complex composed of the U3 snoRNA and more than 30 proteins [24]. The cleavage at site A_0 produces the 33S precursor, and, afterwards, a cleavage at site A_1 yields the 32S pre-rRNA allowing for the precise removal of 5' ETS [2, 25]. Cleavage at site A_2 in the internal transcribed spacer 1 (ITS1) leads to the separation of the 32S pre-rRNA into 20S and $27SA_2$ pre-RNAs, which are part of the pre-43S and pre-66S particles, respectively [2]. These are the earliest pre-40S and pre-60S particles, and from here on out the separate pathways are marked by dramatic differences in particles compositions [2, 12]. It should also be noted that these early processing events are irreversible, which suggest a point of regulatory control [2, 25].

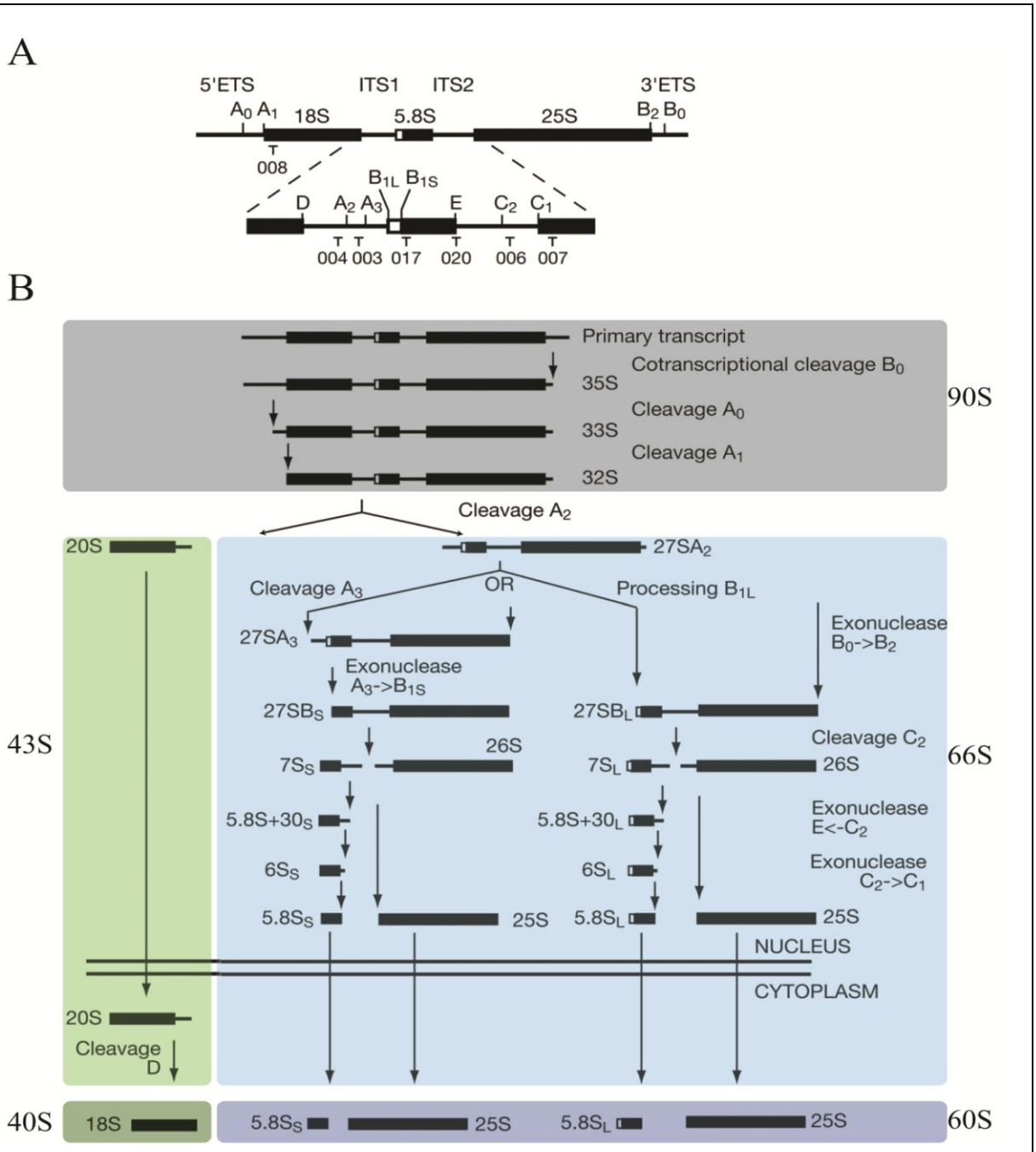

Figure 1.3. Schematic *Saccharomyces cerevisiae* processing pathway.

A) Location of the ETS and ITS sequences, rRNA regions and processing site. B) Pre-rRNA processing pathway showing steps which are performed in the 90S particle (gray), in the 66S particle (light blue) and in the 43S particle (light green). The 40S subunit contains 18S rRNA (dark green) and the 60S subunit contains 5.8S, 25S and 5S rRNAs (dark blue). Modified from [24, 26]

1.3.2 Pre-40S processing

In *S.cerevisiae*, the 20S rRNA within the pre-43S particle was shown to be directly exported from the nucleolus to the cytoplasm after cleavage at site A_2, where 3'end maturation of 18S rRNA occurs, whereas its 5'end has been already formed through the removal of the 5'ETS in the nucleus [24]. Thereafter, particle composition is known to change when further modifications are carried out. The methyltransferase Dm1p has been found to methylate conserved adenosines near the 3'end of the 18S rRNA, and endonucleolytic cleavage at site D has been shown to require the nuclease Nob1p as well as factors Rio1p, Rio2p, Tsr1p and Fap7p [2, 27]. The Bud23p methyltransferase is also part of this complex; Bud23 catalyzes N7-methylation of guanosine 1575 and Nep1p, which is responsible for the N1-methylation of the hyper modified m1acp3Ψ 1191 base [28].

1.3.3 Pre-60S processing

Pre-60S rRNA maturation is much more complex than that of the 18S rRNA, since it comprises the maturation of two rRNAs, 5.8S and 25S, as well as two distinct processing pathways (major and minor), and requires several non-ribosomal processing factors, including exo- and endonucleases. As for the major pathway, it is known that the MRP RNase induces the cleavage at site A_3 resulting in 85-90% of $27SA_2$ pre-rRNA, which is then endonucleolytically cleaved to form the $27SA_3$ precursor [4, 29]. The timing of this cleavage was found to occur posttranscriptionally, and to be linked to events at the 3' end of the 35S pre-rRNA [29]. Moreover, A_3 cleavage requires the presence of the non-ribosomal protein Rrp5p, which binds adjacent to sites A_2 and A_3 and which is also required for A_0, A_1 and A_2 cleavage [29]. Indeed, the C-terminal domain of Rrp5p appears to be required for the A_0-A_2 cleavages on the pathway of 18S rRNA processing, whereas the N-terminal domain was demonstrated to be required for A_3 cleavage along the 5.8S/25S rRNA processing pathway. This clearly illustrates the complexity and dynamic of the ribosomal biogenesis pathway [29]. Thereafter, the 5' to 3' exonucleases Rat1p, Xrn1p, Rrp17p and the cofactor of Rat1p, Rei1p, are required to generate the $27SB_s$ pre-rRNA and thus the 5' end of the major form of the 5.8S rRNA, $5.8S_{SHORT}$ [4, 30, 31]. In contrast, the minor pathway is known to start with

endonucleolytic processing at the B_{1L} site. In fact, 10-15% of $27SA_2$ pre-rRNA is not processed by the MNP RNAse, but directly cleaved at the B_{1L} site by an unknown endonuclease, which generates the $27SB_L$ pre-rRNA [4].

Simultaneous with formation of the 5'end of 5.8S rRNA into both major and minor pathways, the 3' to 5' exonuclease Rex1p generates the 3'end of 25S rRNA at the B_2 site [32]. Subsequently, cleavage at the C_2 site, again by an as yet unknown endonuclease, allows separations of 7S and 26S pre-rRNAs, the two large subunits rRNAs precursors [4]. The mature 3' end of the 5.8S rRNA is generated by a multistep process, involving the exosome component Rrp6 and the exonucleases Rex1p and Rex2 [4]. The 5' end of 25S rRNA is generated by Rat1p and Rrp17, which carry out exonuclease digestion from the C_2 to C_1 site [4].

1.4 Assembly pathway

Ribosomes were shown to contain ~79 r-proteins. In addition, research groups have identified a large number of non-ribosomal proteins involved in ribosome biogenesis. There are more than 200 non-ribosomal proteins, such as GTPases, DExD/H-box ATPases, AAA-type ATPases, nucleases, rRNA-binding proteins and RNA helicases that participate in rRNA processing, folding and assembling of the rRNA with ribosomal proteins at different stages of maturation [20, 33]. These proteins are believed to assemble with the pre-ribosomes in a transient manner [34]. Maturation of the pre-40S particle occurs mainly in the cytoplasm, while the pre-60S particle matures mostly in the nucleus and continues after its exportation into the cytoplasm [5]. In fact, pre-ribosomes start off in the nucleolus, traverse into or through the nucleoplasm to the nuclear periphery, and are finally exported to the cytoplasm [5, 33, 35]. It is believed that this spatial movement of maturing pre-ribosomes is linked to specific temporal maturation events, which underscores the importance of coordinating the processing and assembly steps. To date, little is known about the integration of processing steps with rRNA folding and assembly. By using affinity purification methods, several studies isolated and characterized different complexes associated with assembly factors, in addition to identifying their approximate positioning along the maturation pathway [2, 33, 34]. However,

ribosome biogenesis is a highly dynamic process, and so far most of these studies provided only a static image of the process and limited information on the pathway's dynamics [34].

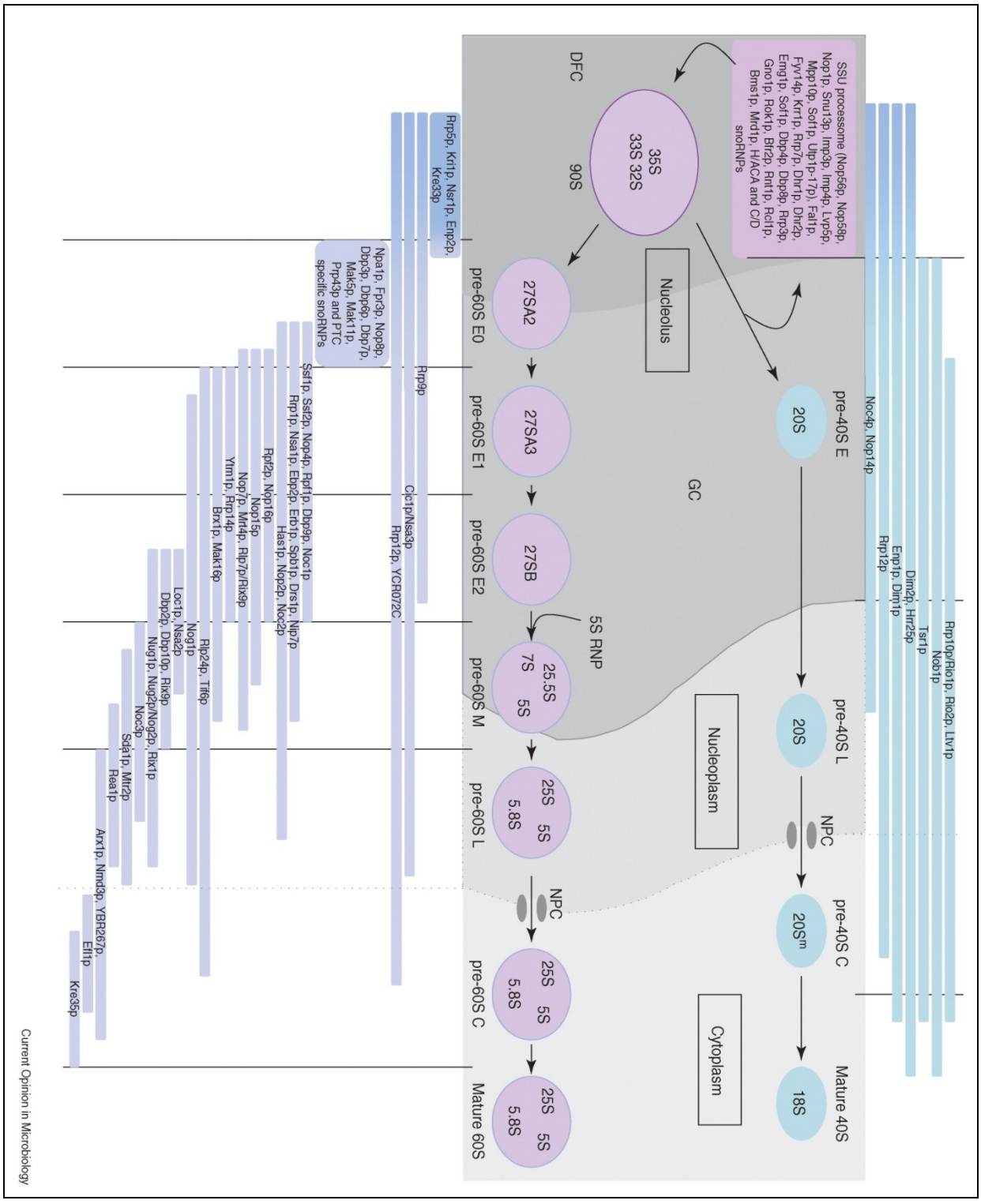

Figure 1.4. Assembly of non-ribosomal proteins with the different pre-ribosomal particles.
The upper and lower panels indicate 40S and 60S non-ribosomal proteins, respectively. The central panel illustrates the different pre-ribosomal particles in their sub-cellular locations. Pre-ribosomes are classified as early (E), middle (M), late (L) and cytoplasmic (C). Nuclear pore complexes (NPC) allow pre-ribosomes passage from the nucleoplam to the cytoplasm [33].

1.4.1 Pre-40S assembly

As mentioned above, pre-40S maturation occurs mainly in the cytoplasm, and the particle is exported directly following the A_0, A_1 and A_2 cleavages. Thereafter, composition of the pre-40S drastically changes, where a group of non-ribosomal factors are dissociated whereas a novel set are associated and further r-proteins are recruited [2]. Rrp12p, a protein that was found in 90S complexes but also in pre-40S particles, is essential for maturation of the small subunit, and is believed to facilitate the export of pre-ribosome particles to the cytoplasm. [5]. This protein was also found in association with some pre-60S proteins (Nop4p, Nop15p and Noc1p), being one of the very few ribosome biogenesis factors involved in the maturation of both subunits [5].

The pre-40S particle was shown to already display typical morphological 'landmarks' of mature 40S subunits, while still lacking the typical "beak" structure [2]. At this point, the Enp1p-Ltv1p-Rps3p subcomplex and Hrr25p are known to promote phosphorylation/dephosphorylation events that finally allow the stable association of Rps3p, and the formation of the mature 40S subunit structure, including the 'beak' [2].

1.4.2 Pre-60S assembly

Pre-60S subunit maturation is known to be much more complex and to require many more non-ribosomal proteins that associated with the large number of different pre-ribosomal particles. In fact, distinct pre-60S particles have been characterized by affinity purification of definite non-ribosomal proteins. However, it is still unclear whether these particles are all along the same, or parallel, pathways.

In the nucleolus, the earliest pre-60S particles that have been identified are associated with Npa1p and Ssf1p. The Npa1p particle contains $27SA_2$ pre-rRNA and ~40 non-ribosomal proteins, such as early pre-60S factors (Noc1p and Nop4), snoRNP components, RNA helicases and some 90S-associated factors [2]. In contrast, the Ssf1p particle is composed of $27SA_2$ and 27SB pre-rRNA, and ~30 non-ribosomal proteins, such as early factors Noc1p and Rrp5p, but no snoRNP components [2]. There is also Rpf1p that has been found in the Ssf1p particles but only associated with 27SB pre-rRNA intermediates [5]. Thereafter, another pre-60S particle has been isolated with Nsa1p, where the exchange of the Noc1p-Noc2p to Noc2p-Noc3p complex has already been made (see section 1.6) [2]. This intermediate particle contains the 27SB pre-rRNA only, the AAA-ATPase Rix7p and the Ytm1p-Erb1p-Nop7p subcomplex in addition to the 5'-3'exonucleases Rat1p, Rrp17p and Xrn1p, which participate in the 5' trimming of the $27SA_3$ pre-rRNA [2, 31, 36]. The proteins Rpf2p and Rrs1p are both part of this particle, and have been shown to mediate the incorporation of the 5S rRNA:Rpl5p complex as well as Rpl11p into the pre-ribosome [2, 37]. Moreover, 5S rRNA is found in Nug1p and Nog2p associated complexes, but not with Ssf1p associated complex [5]. As mentioned previously, there are two distinct processing pathways (major and minor) that can lead to the formation of the 27SB pre-rRNA. Mostly, these two pathways were shown to require the same non-ribosomal factors, except for the so far unknown endonuclease that cleaves at the B_{1L} site [34].

In the nucleoplasm, the pre-60S particle has been isolated using Rix1p as bait, which allowed visualization of drastic compositional changes at this point. Several intermediate factor such as Erb1p, Ytm1p, Nop2p, several DExD/H-ATPases and the Noc2p-Noc3p complex were found to have been dissociated and replaced by different factors such as Rea1p, Rsa4 and Nug2 [2]. This simplification of protein composition is consistent with the 5S rRNA association, and with the formation of the 7S pre-rRNA that occurs after the C_2 cleavage [5]. In fact, the Rix1p particle contains the nearly mature 25S and 7S/5.8S rRNAs, which indicates that processing of the 27SB pre-RNA has been almost completed [2]. On top of this major compositional change, ATP-dependent structural rearrangements have been found to occur through the dynein related AAA-ATPase Rea1p/Mdn1p and the Rix1p-Ipi1p-Ipi3p complex [33].

Later pre-60S particles contain Arx1p, and can be found in both the nucleo- and cytoplasm, indicating the transitioning aspect of this particle; moreover, Arx1p has also been found associated with export factors Nmd3p and Mtr2p [5]. This particle also contains more mature 5.8S rRNA than 7S pre-rRNA [2]. It has been shown that the AAA-ATPase Drg1p binds the Arx1p-containing particle only once it has reached the cytoplasm [2]. This binding triggers Nog1p and Rlp24p release [2]. The later, solely cytoplasmic pre-ribosomal particle is characterized by the presence of Lsg1p/Kre35p [2]. This particle contains some cytoplasmic factors and a diminished amount of Arx1p, whose release depends on Rei1p, Ssa1/Ssa2p and Jjj1p [2, 4]. Another protein of the Lsg1p/Kre35p particles is Tif6p, the ortholog of the mammalian protein eIF6, which is functionally linked to the cytoplasmic GTPase Efl1p [2, 5]. Interestingly, Tif6p is an essential nucleolar protein that relocates to the cytoplasm when Efl1p is depleted in cells, and dissociates from the cytoplasmic pre-60S particle through the GTPase activity of Efl1p and Sdo1p [2, 5].

Some assembly factors are only transiently associated with distinct pre-60S particles, while others are found across several maturation steps. This is the case with Nsa3p/Cic1p, which is present in both late 90S particles and early pre-60S particles [5]. Another example is Rlp24p, which is found in the nucleolar, nucleoplasm and cytoplasm pre-60S complexes [5].

The enormous number of non-ribosomal proteins involved in the ribosome biogenesis has been a puzzle for some time, however, is most likely due to the coordination of the ribosomal synthesis with other cellular process such as growth rate and stress response [2]. Interestingly, although, the majority of these proteins are essential for cell viability, it seems that mutation or depletion of some of them does not affect the viability of the cell but more the growth rate [5, 31]. Indeed, there is a concept of overlapping and parallel pathways to ensure the production of ribosome in the cell, that would not only explain this particular phenomenon, but also the existence of more than 200 ribosome biogenesis factors in yeast [38].

1.5 Coordination and quality control system

Ribosomes are essential to a cell's viability, and ribosome biogenesis needs to be regulated in conjugation with other cellular pathways. In yeast, it is known that at least 60% of

the RNA polymerase II transcription and 90% of mRNA splicing are dedicated to mRNAs encoding r-proteins and non-ribosomal protein factors [4, 39]. All these mRNAs are processed and exported from the nucleus, translated, and the proteins then imported into the nucleus, where they associate with nascent pre-rRNAs [4]. Moreover, pre-rRNAs also need to be processed, modified and assembled as two separate and distinct subunits. Overall, 2000 ribosomes are produced per minute that correspond to 200,000 ribosomes per yeast cell, and about 4000 ribosomal subunits are exported from the nucleus to the cytoplasm every minute [39]. Therefore, cells need to expend a lot of energy to ensure the production of ribosomes.

It also demonstrates the incredible coordination that is required to ensure that correct ribosomes are made, as malfunctioning ribosome could cause mistakes during translation that may have deleterious effects for any cell or organism, as it has been recently shown in the cases of ribosomopathies and even cell cycle arrest in yeast [4, 33]. Indeed, there may be some ribosomal factors that have a role in quality control steps during ribosome biogenesis, or even in overlapping and alternative pathways, that allow pre-ribosomes to still be matured correctly by a minor factor if major ones are absent or not available at the necessary levels [40]. However, how pre-ribosomes are quality controlled, and whether any checkpoint exists, is poorly understood to date. It is known that pre-ribosome, containing mal-processed pre-rRNAs, can be degraded by the exosome, following targeting and polyadenylation by Trf4/5p-Air1/2p-Mtr4p polyadenylation (TRAMP) complex [41, 42]. Moreover, it has been shown that release of Tif6p during late steps of pre-60S maturation is coupled to verification of P-site integrity [41]. This formation of sub-complexes is one possibility of quality-control system because it can physically block the binding-site of ribosomal proteins or other assembly factors [40]. Other proteins, such as the Noc proteins, are known to function together or, like Ssf1p and Nop7p, interact directly with the pre-rRNA [39]. Based on our knowledge about the translocation of pre-ribosomes, it is certainly conceivable that some of these proteins, or sub-complexes, are involved in the coordination of the controlled spatio-temporal movement of pre-ribosome, from nucleolar compartment to the next, through the nucleoplasm to the nuclear pore [5, 31, 33]. However, these kinds of control mechanisms remain, to this date, largely unexplored.

It is known that about 20% of ribosome assembly factors are nucleoside triphosphate hydrolyzing enzymes, such as kinases, ATPases and GTPases [40]. These enzymes are believed to provide the energy needed to confer directionality to the maturation pathway [2]. Ribosomal assembly requires one GTPase during pre-40S maturation (Bms1p), and five during pre-60S maturation (Nog1p, Nug1p, Nug2p/Nog2p, Ria1p and Lsg1p) [2, 20, 40]. Interestingly, these proteins contain an RNA-binding domain in addition to their GTPase domain, suggesting that they may be able to bind to the pre-rRNA directly, in the absence of bridging interactions via other factors [20]. From previous biochemical and genetic work, some possible functions for these proteins have been speculated on; one is that the energy from the GTP hydrolysis can be used to remove proteins or to promote a conformational rearrangement within the nascent ribosome [20]. But these studies have not been able to confer the exact function of these proteins [20].

In addition, seven DExD/H-box ATPases were found to be involved in pre-40S maturation (Dbp4-8p, Dhr1-2p, Fal1p, Rok1p, Rrp3p), ten in pre-60S maturation (Dbp2-3-6-7-9-10p, Drs1p, Mak5p, Mtr4p/Dob1p, Sbp4p), and two in the maturation of both subunits (Has1p, Prp43p) [2]. Although their precise roles remain unclear, these proteins are known to act as ATPases and can be viewed as chaperon/modulators of RNA or RNP structures [2].

There are also three kinases implicated in pre-40S maturation (Hrr25p, Rio1-2p), where recently Hrr25p has further been related to phosphorylation of Tif6p during pre-60S maturation [2, 40]. Moreover, both pre-40S and pre-60S maturation pathways involve two ATP-binding cassette (ABC) proteins, Arb1p, Rli1p [2]. This superfamily of proteins is known to use ATP hydrolysis to transport proteins against a concentration gradient [2].

Finally, there are three AAA-ATPases required during pre-60S maturation, Drg1p/Afg2p, Rea1p/Mdn1p and Rix7p [2]. These proteins are known to use ATP hydrolysis to potentially stimulate structural rearrangement, or protein dissociations from the particles through transmission of the tension of a nucleotide-dependent conformational switch to bound substrate proteins [2, 40].

1.5.1 AAA-ATPase Rix7p

Rix7p was the first AAA-ATPase characterized during pre-60S maturation. It is also the earliest acting in the 60S subunit biogenesis pathway [43]. Rix7p contains two AAA ATPase domains (D1 and D2) and one putative bipartite nuclear localization signal (NLS) [44]. Cdc48p has been identified as a yeast homologue of Rix7p; Cdc48p is known to recognize ubiquitinated proteins and dissociate them from unmodified binding partners [45]. However, sequence conservation of Rix7p is restricted to the two AAA ATPase domains, but not to the N-terminal domain [43]. Indeed, the highly homologous domain D1 is known to promote hexamer formation and to be a relatively stiff structure, whereas domain D2 is known to harbor the ATPase activity and perform conformational changes following ATP hydrolysis [45]. By mutating conserved residues implicated in ATP binding and ATP hydrolysis, the D1 domain was shown to require ATP or ADP binding, but not ATP hydrolysis to perform its function [41]. On the other hand, the D2 domain was shown to required both ATP and ADP binding as well as ATP hydrolysis [41].

Due to its N-terminal domain, Rix7p shows a nuclear localization in normal condition [44]. Nevertheless, its intranuclear localization has been shown to change depending on the growth condition and nutrient availability (See Figure 5) [44]. Using fluorescent microscopy and growth density analysis, cells containing GFP-tagged Rix7p were grown to stationary phase and Rix7p-GFP was shown to concentrate in the nucleolus [44]. However, after entering stationary phase, cells were transferred to fresh medium and Rix7p-GFP was then shown to follow a transient perinuclear location [44]. Finally, when cells were grown until they reached an exponential phase, Rix7p-GFP was shown to have an overall nuclear distribution [44]. These localization changes have been suggested to correlate with some adjustments and alterations of ribosome biogenesis in response to nutrient availability [44].

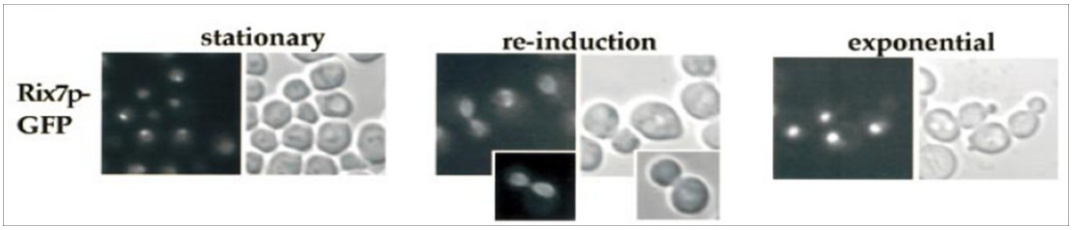

Figure 1.5. Rix7p-GFP localization under different growth conditions monitored by fluorescent microscopy.

Yeast cells were grown in YPD medium at 23°C (A) Stationary phase (B) Re-induction in fresh medium for 3 h (C) Exponential phase [44].

Using the temperature-sensitive (ts) mutant strain *rix7-1* and the large subunit reporter Rpl25p-eGFP, Rix7p has been predicted to have a role in pre-60S ribosomal export [44]. Indeed, at restrictive temperature (37°C), Rlp25p-eGFP was retained in the nucleolus and nucleoplasm, suggesting a defect in pre-60S export from the nucleus to the cytoplasm [44]. Moreover, sucrose density gradient profiling of polysomes in *rix7-1* under restrictive conditions revealed a significant decrease of free 60S subunits, indicating a role in 60S biogenesis [44]. Northern blot, primer extension and pulse-chase analysis have indicated that Rix7p is not essential for pre-rRNA processing itself, but rather for structural rearrangement and stability of the pre-60S particles [44].

More recently, Rix7p has been shown to be genetically linked to Nsa1p, an essential pre-60S factor and conserved WD repeat protein that is known to bind pre-60S particles containing 27SA pre-rRNA [40, 45]. By mutation of the N-terminus of Rix7p in a GFP-tagged Nsa1p strain, fluorescent microscopy analysis showed that Nsa1p cannot be efficiently removed from late nucleolar pre-60S particles, and stays associated with aberrant cytoplasmic pre-60S particle [45]. Thus, Rix7p was suggested to be essential for removal of Nsa1p from pre-60S particle during pre-ribosomal maturation [45]. Moreover, Nsa1p removal by Rix7p coincides with compositional changes on the pre-60S particle; Nop7-TAP associated particles isolated in a *rix7* mutant were found to be more complex than wild-type complexes, and to be composed of a set of very early factors such as Rrp5p, Noc1p, and Nop4p [45]. In addition, the later nucleoplasmic Rix1p particle was found to contain reduced quantities of the usual factors, such as Nug1p, Nog2p and Rsa4p in a *rix7* mutant background [45]. Overall, Rix7p

has been proposed to detect the structural integrity of pre-60S particles and lead them into a clearance or check point, which, if the particles are correct, leads to Nsa1 removal and change in particle composition, including structural rearrangements [40, 41, 45].

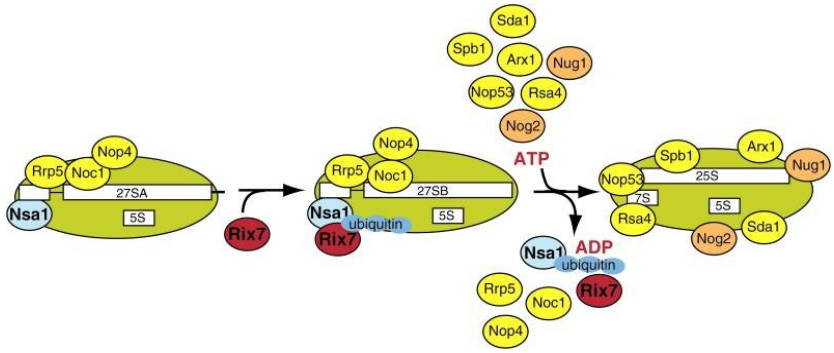

Figure 1.6. Potential model for Rix7p remodeling of pre-60S particle.

Nsa1p and other early 60S assembly factors such as Rrp5p, Noc1p and Nop4p are bound to pre-60S subunit containing 27SA rRNA. Rix7p interacts with Nsa1p to remove it from the particle and this coincides with loss of the early and binding of later 60S-assembly factors. Orange: Energy-consuming factors. Yellow: Assembly factors. [40]

1.6 The Noc proteins

The Noc proteins (Noc1p, Noc2p, Noc3p and Noc4p) were heavily studied at the beginning of the last decade, and provided one of the initial clues about the spatio-temporal dynamic of ribosome maturation. In fact, mass spectrometric analysis of a large nucleolar substructure co-purified with RNA Polymerase I (Pol I) and Pol I-dependent transcription factors in a single chromatographic fraction, allowed for the identification of several nucleolar proteins implicated in pre-rRNA processing. Among these were the Noc proteins (NucleOlar Complex-associated proteins) [46, 47]. Later on, it was shown that, indeed, Noc1p, Noc2p and Noc3p are involved in intranuclear transport as well as export of pre-60S particles, and that Noc4p is required for the nuclear export of the pre-40S particles [47, 48]. Using the 3D-PSSM server (http://www.sbg.bio.ic.ac.uk/~3dpssm/), the Noc proteins were determined to be constituted of α-helical repeats, similar to HEAT/Armadillo repeats, with a confidence range of 70%-90% [49]. About 0.2% of eukaryotic proteins contain HEAT or Armadillo repeats,

including Rrp12p, Utp10p, Utp20p and Sda1p, all of which are essential for ribosome biogenesis, however, there is no detectable sequence similarity between these and the Noc proteins [49, 50]. Because some HEAT-repeats proteins, such as Rrp12p, play role in the export of both ribosomal subunit export, α-helical repeats of the Noc proteins could provide a possible explanation about their function [49, 50].

Interestingly, pre-60S particles associate with either Noc1p and Noc2p, or Noc2 and Noc3p, but never Noc1p and Noc3p, in a seemingly strict temporal order during ribosome biogenesis [47]. Finally, essential roles for the Noc proteins could potentially be inferred from their conserved homologues in human cells. Their dynamic common functions and distinct differences will be discussed in more detail in the following paragraphs. Noc1p/Mak21p

1.6.1 Noc1p/Mak21p in *S.cerevisiae*

Noc1p, also called Mak21p, presents in ~1500 molecules per cell, was first identified in studies on the "killer character" of the yeast *Saccharomyces cerevisiae* [51, 52]. Indeed, by testing the propagation of the M_1 dsRNA, which encodes the secreted polypeptide "killer toxin" and immunity to this toxin, ~30 MAK genes (MAintenance of Killer) were identified [53]. Mutation of MAK genes resulted in the loss of M_1 propagation [52]. Of these 30 genes, 20 were also found to affect 60S ribosomal subunit biogenesis, amongst them MAK21, but none were found to affect 40S subunit synthesis [52]. MAK21, or NOC1, is located on chromosome IV and is essential for cell viability in yeast [52]. Mutations in MAK21/NOC1 induce a decrease of free 60S ribosomal subunit on a polysome gradient [52]. Depletion of Mak21p/Noc1p, using a inducible/repressible GAL1 promoter, increases the doubling time by ~4.8-fold after 40 hours of growth in repressive glucose medium [52]. However, it is possible to delete the first 228 amino acids at the N-terminus as well as the last 127 amino acids from the C-terminus of Mak21p/Noc1p without affecting its function in ribosome subunit formation [52].

Using fluorescence microscopy, GFP-tagged Noc1p was found to be present in crescent-like nucleolus, and co-localized with the well-known nucleolar marker Nop1p [47, 54]. In addition, immunoelectron microscopy using Protein A-tagged Noc1p showed that 80%

of Noc1p was concentrated in the nucleolus, compared to 85% of Pol I [47]. In fact, polysome sucrose gradients have shown that Noc1p co-sediments with 90S complexes, and remains associated with 66S particles, which corresponds to early steps during ribosome biogenesis [47]. Moreover, an increase in temperature to 37°C caused accumulation of Noc1p into 90S particle due to a slowdown in ribosome biogenesis [47]. Affinity purification of Tap-tagged Noc1p coupled with Northern blot and primer extension analyses, revealed the co-purification of $27SA_2$ and 35S pre-rRNAs and, albeit less efficient, of $27SB_S$ and $27SB_L$ pre-rRNAs [55]. Moreover, Chromatin Immunoprecipitation (ChIP) analysis has shown that Noc1p associates specifically with the 25S rRNA coding region on 35S primary transcripts [55]. This suggests that Noc1p is recruited to the earliest particles, and not present in intermediate and late particles [55]. In addition, peptide count analysis of RNA polymerase subunits from mass spectrometry (MS) analysis of proteins co-purifying with Noc1p-TAP and Pol I affinity purification from chromatin fractions of formaldehyde-treated yeast cells, demonstrated that Noc1p is part of Pol I-associated rDNA chromatin, and is co-transcriptionally recruited to nascent pre-rRNA [55]. Finally, down-regulation of pre-rRNA synthesis using a *ts* mutant expressing defective Pol-I transcription factor Rrn3p under restrictive temperature has shown a 40% reduction of Noc1-TAP protein levels [54]. In contrast, expression levels of other TAP-tagged proteins such as Nop7p, Rix1p, Arx1p, Enp1p and Rio2p, all of which are either intermediate to late pre-60S complex components or 40S synthesis factors, was comparable in the wild-type and mutant backgrounds. Redistribution of Noc1p localization was also observed in this *rnr3* mutant, showing an intra-nuclear redistribution, probably due to changes in nucleolar structure [54]. Indeed, Noc1p still co-localized with the nulceolar marker Nop1p, and both overlapped significantly with the DAPI stained nucleoplasmic region when pre-rRNA synthesis was down-regulated [54].

As previously mentioned, Noc1p was found to play a role in 60S ribosomal subunit biogenesis, when growth of the temperature sensitive *noc1-1* strain under restrictive temperature conditions for 6 hours induced a reduction of 60S/40S ratio of polysome [47]. In addition, Northern blot analysis showed impairment in the rRNA processing pathway, leading to a reduction of the mature 25S and 5.8S rRNAs; indeed, a strong reduction of 27SB, 7S and 6S pre-rRNA was observed [47]. However, synthesis of the $27SA_2$ and 20S prRNA precursors

continued at a reduced rate, suggesting a delay in the three early cleavages sites A_0, A_1 and A_2, while primer extension analysis showed the continuation of A_3, B_{1L} and B_{1S} cleavages, demonstrating that the *noc1-1* strain is not primarily defective in pre-rRNA processing, suggesting a potential role in assembly or transport of the pre-60S subunit [47]. In addition, a 60S subunit export assay in *noc1-1* cells under restrictive temperature revealed a retention of Rpl25p-eGFP in the nucleolus, suggesting again that Noc1p is either involved in subunit transport, and possibly in the correct assembly of 60S ribosomal subunits [47].

1.6.1.1 Homologs of Noc1p in higher eukaryotes

Noc1p shares significant amino acid similarity throughout its 1025 residues with some open reading frames (ORFs) of unknown function in mouse, *Caenorhabditis elegans*, and *Schizosaccharomyces pombe*, but especially with a human CCAAT-box-binding transcription factor called CBF or CEBPZ for CCAAT/enhancer-binding protein zeta (See Figure 7) [52]. A NCBI Blast showed that Noc1p has 94% sequence similarity and 29% identity to human CBF (hCBF) [56]. hCBF is a transcription factor that specifically binds to the HSP70 CCAAT element and stimulates transcription from the HSP70 promoter in a CCAAT-element-dependent manner [57, 58]. Moreover, the human HSP70 promoter is transcriptionally activated by adenovirus E1a, which needs to interact with residues 1 to 192 of hCBF to induce transcription [58]. To determine if Noc1p shares a similar function to hCBF, expression from the SSA3 promoter was tested, since Ssa3p is the yeast homolog of human Hsp70 [52]. No decrease in the expression from the SSA3 promoter was detected in *ts noc1-1* strain, which suggested that Noc1p is not required for Ssa3p expression [52]. hCBF also interacts with E1a and p53 via its N-terminal region, which is not homologous to Noc1p and also absent in the *S. pombe* homolog [52]. Furthermore, subcloning of hCBF to test complementation of *noc1-1* showed that hCBF was not able to rescue the *noc1-1* mutant phenotype [52]. Finally, no specific role for hCBF in ribosome biogenesis was found in human cells [52]. Thus, while Noc1p shares high amino acid similarities with hCBF, no functional overlap seems to exist.

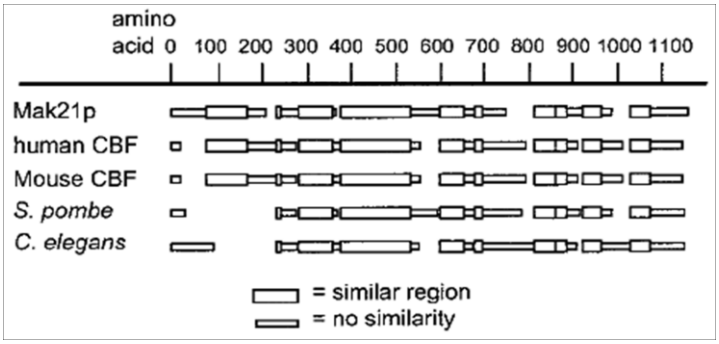

Figure 1.7: Representation of homologous regions of Noc1p/Mak21p with its different homolog.

Homologous regions of Noc1p/Mak21p with the mouse hCBF and ORFs form S. pombe and C. elegans were determined by using Multiple Alignment Construction and Analysis Workbench (MACAW) [52, 59].

Another Noc1p homolog is the protein Swa2p, with 31% sequence identity and 53% similarity at the amino acid level [60]. SWA2 is expressed ubiquitously in the *Arabidopsis thaliana* in actively dividing tissues and female gametophytes [60]. The protein contains a C-terminal nuclear localization signal and an N-terminal nucleic acid-binding domain and was suggested to be involved in ribosome biogenesis, transcription and RNA metabolism, based on the presence of motifs such as CCAAT-BOX binding factor (CBF) and DNA Topoisomerase I in eukaryote (TOPEUc) [60]. Analyses demonstrated nucleolar localization of Swa2p, and a physical interaction with At2g18220, one of the two yeast Noc2p homologues in *Arabidopsis* [60]. Although, similar to Noc1p, *swa2* mutations impaired cell growth and division, SWA2 failed to functionally complement the yeast *noc1-1* mutant [60].

1.6.2 Noc2p in *S. cerevisiae*

The second member of the Noc protein family that is part of a large nucleolar substructure is Noc2p. It is an essential and highly abundant protein (~ 29,000 molecules per cell) composed of 710 amino acids [51]. Its gene locus is located on the chromosome XV [47, 51]. Initially, Noc2p was identified by a screen from a bank of 900 randomly generated temperature sensitive mutants to test for factors required for ribosomal export (rix) [61]. A library of mutants was analyzed for nuclear accumulation of Rpl25p-eGFP at restrictive temperature [61]. Out of these, 20 mutants, such as *rix3-1,* were shown to exhibit a Rpl25p-

eGFP nuclear accumulation phenotype [61]. Indeed, *rix3-1* cells showed an accumulation of Rpl25p-eGFP in two ways: between the nucleolus and nucleoplasm, and between the nucleoplasm and the cytoplasm, suggesting that the protein exists in two subsets [47]. Later, this mutant was complemented by the ORF YOR206W, which was already known to correspond to the nucleolar complex associated protein, Noc2p [46, 47].

Using fluorescent microscopy, N-terminally GFP-tagged Noc2p was shown to exhibit a predominantely nucleolar localization, with a weaker distribution throughout the nucleoplasm [47]. In fact, immuno-EM indicated an intermediate distribution for Noc2p with 60% nucleolar and 40% nucleoplasmic [47]. In addition, sucrose gradient analysis showed that Noc2p associated with 90S pre-ribosomes, and after cleavage at site A_2 remained associated with the 66S pre-ribosome [47]. Unlike Noc1p, however, Noc2p was not detected associated with Pol I-containing particles, suggesting that Noc2p is not part of primary transcript containing, Pol I-associated complexes [55]. To date, it is not well understand if this result is due to limitations in sensitivity, or if Noc2p is truly not recruited co-transcriptionally to nascent pre-rRNA [55]. Indeed, affinity purification using Noc2p-TAP predominantly co-purified 27SA and 27SB pre-rRNAs, which correspond to late 90S and early to intermediate steps in pre-60S maturation [62]. Consistent with that, Noc2p-TAP co-purification also showed an underrepresentation of Rpl2p, Rpl43p and Rpl39p, all of which are described to play roles in 7S pre-rRNA processing at later pre-60S maturation steps [62]. Interestingly, increasing levels of Noc2p were detected in complexes co-purified with Nog1p-TAP from individual mutants that lacked expression of either RPL25, RPL43 or RPL2, while 7S pre-rRNA levels co-purified with Noc2-TAP increased after depletion of either rpL2 or rpL43 [62]. In addition, depletion of rpL25 induced a strong delay in ITS2 cleavage at site C_2, causing a reduction in 7S and 25.5S pre-rRNA production from 27SB pre-rRNA [62]. In contrast, RpL2 and RpL43 are both required for conversion of 7S into 5.8S rRNA, and absence of these proteins does not block 7S pre-rRNA production [62]. Therefore, it has been suggested that release of Noc2p from the intermediate pre-60S particle is affected by lack or absence of rpL2, rpL25 and rpL43 [62].

As mentioned, in *ts* NOC2 mutants, Rpl25p-eGFP is accumulated in the nucleus at two distinct stages [47]. In addition, absence of functional Noc2p causes a reduction in the ratio of

60S to 40S subunits, indicating a defect in 60S subunit synthesis [47]. In the *noc2-1* strain, Northern analysis after 2 hours at 37°C showed an impairment in 25S and 5.8S rRNA processing, and a strong reduction of 27SB, 7S and 6S precursors; however, all earlier cleavages at sites A_0, A_1, A_2, A_3, B_{1L} and B_{1S} appeared to have been carried out accurate at the nucleotide level, suggesting that Noc2p is not responsible for pre-rRNAs cleavages but may be involved in correct assembly and transport of pre-60S particle [47]. However, a mild accumulation of the 35S pre-rRNA and a low level of the 23S rRNA were detected; 23S is an aberrant precursor species found when processing at sites A_0-A_2 is delayed, which is a common phenotype for 60S mutants, in which these earlier steps do not seem to occur co-transcriptionally anymore, but rather take place after transcription of rDNA and transcript modification has been completed [48][Tollervey et all, unpublished data].

1.6.2.1 Homologs of Noc2p in higher eukaryotes

An NCBI Blast search (http://blast.ncbi.nlm.nih.gov/Blast.cgi?PROGRAM=blastp &PAGE_TYPE=BlastSearch&LINK_LOC=blasthome) showed that Noc2p has 31% sequence identity to the mouse protein NIR, also called NOC2L, NET7 or NET15. NIR is a 749 amino acids long protein that is ubiquitously expressed during mouse embryogenesis as well as in adult mouse tissues [63]. It contains two inhibitor of histone acethyltransferase (INHAT) domains, one at its N-terminal and one at its C-terminal end, as well as a putative bipartite NLS [63]. It was shown that either full-length protein or both INHAT domains alone bind efficiently to nucleosomes, and block acetylation of the core histones H3 and H4 [63]. Using a LexA/Gal-reporter, promoter-recruited NIR has been demonstrated to be able to repress basal and activated transcription in a cell line and promoter-independent manner [63]. Moreover, compared to other INHAT domain containing proteins such as PELP1 and Set/TAF1β, NIR functions independently of HDAC activity [63]. Interestingly, amongst proteins identified by MS analysis to associate with NIR, was the tumor suppressor p53 as a NIR-interacting transcription factor. Microscopy confirmed their colocalization in the nucleus. Moreover, these two proteins were found to interact directly *in vitro* by GST-pulldown assays, where p53-interaction domain binds to the central part of NIR, and *in vivo* using NIR-TAP purification [63]. Thus, NIR is the first p53-interacting INHAT. In later experiments, it has

been shown that Aurora B also binds to NIR to form an Aurora-NIR-p53 complex [64]. Finally, NIR was shown *in vivo* to be a *bona fide* co-repressor of p53, that blocks histone acetylation at p53-regulated target promoters, and to be involved in the regulation of p53-dependent apoptosis [63]. Depletion of NIR dramatically inhibited cell growth and activated p53 possibly by de-repression of p53 acetylation [64].

Independently, TAp63γ, the major trans-activating form of p63, containing the N-terminal transactivation domain, central DNA binding domain and C-terminal oligomerization domain, was found to physically interact with NIR [65]. It was shown that NIR binds to TAp63 and acts as a repressor of TAp63-mediated transactivation. Moreover, synchronization of human diploid fibroblasts indicated that NIR transcription and protein levels were cell cycle dependent [65]. Indeed, NIR transcript levels are lowest in G1 and gradually increase during G2/M phase, while protein levels are lowest during S phase and increase during G2/M. Since both p53 and TAp63 can induce a G1/S arrest by trans-activating p32, it has been suggested that p53, TAp63 and NIR may be interconnected through a feedback loop in proliferating cells. However, it has also been determined that neither p53 nor TAp63 are directly regulating NIR expression [65].

As for its homology to Noc2p, NIR co-localizes predominantly with fibrillarin in the nucleolus and localizes more weakly throughout the nucleoplasm [64]. Nuclear fractionation determined that NIR is part of both the pre-40S and pre-60S particles in human cells [64]. Moreover, silencing of NIR expression induced an inhibition of 18S, 28S and 5.8S rRNA processing [64]. In addition, NIR was found associated with U3 snoRNA, which base pairs with 47S rRNA and facilitates processing of 18S rRNA; yet NIR knockdowns did not affect U3 snoRNA levels [64].

1.6.3 Noc3p in *S.cerevisiae*

Similar to Noc1p and Noc2p, Noc3p was first identified through a screen from a bank of 900 randomly generated *ts* mutants searching for factors required for ribosomal export, and by mass spectrometry of proteins co-purifying with Pol I [46, 61]. Indeed, Noc3p (NucleOlar Complex associated protein 3) is 663 amino acid essential protein with an abundance of ~

11,700 molecules per cell [51]. The NOC3 (YLR002c) gene is located on chromosome XII, and database searches showed that Noc3p is composed of a basic helix-loop-helix (bHLH) motif and two bipartite nuclear localization signals [47, 66].

Subsequent, yeast genetic screens were carried out to identify unknown initiators of DNA replication [66]. NOC3 was found to be one of the five multicopy suppressors that could rescue the lethal phenotype of an *mcm5/cdc46-1 ts* mutant, demonstrating an interaction between Noc3p and the replication-initiation protein Mcm5p, a subunit of the MCM protein complex [66]. Reciprocal affinity purifications using HA-tagged Noc3p revealed that the protein forms a complex with the initiation complex *in vivo*[66]. In fact, Orc1p and MCM proteins, such as Mcm2p and Mcm5p, could be isolated with Noc3p-HA, and conversely, Noc3p-HA could be co-purified using an anti-Mcm5 antibody. Moreover, plasmid loss in a *temperature-sensitive* degron (*td*) Noc3p mutant indicated that Noc3p may be required for the initiation of DNA replication [66]. Additional flow cytometric analyses showed that compared to the wild-type, *noc3-td* mutant cells were strongly delayed in entering S phase [66]. Synchronization experiments with hydroxyurea (HU), which inhibits ribonucleotide reductase and causes an arrest in early S phase, demonstrated that Noc3p is dispensable for DNA replication following HU arrest and release [66]. Thus, these data suggest an essential role of Noc3p for chromosomal DNA replication at the initiation level, and a minor, non-essential role during elongation of DNA replication [66]. Finally, Noc3p was also demonstrated to be essential for the recruitment of Cdc6p and MCM proteins and maintaining MCM proteins on chromatin [66]. All these results strongly suggest that Noc3p is a component of the pre-replication (pre-RCs) and post-replication complexes (post-RCs), similar to the Origin Recognition Complex (ORC) [66]. In fact, as cells enter S phase, MCM proteins, Cdc45p and other proteins are known to migrate with the replication forks and dissociate from chromatin after carrying out their roles, leaving ORC and Noc3p on autonomously replicating sequences, forming post-RCs [67]. A yeast functional proteomic screen has identified Ipi1p, Ipi2p and Ipi3p (IPI complex) as replication-initiation proteins that play essential roles in pre-RCs assembly and maintenance by acting downstream of ORC and Noc3p, and upstream of MCM proteins [67].

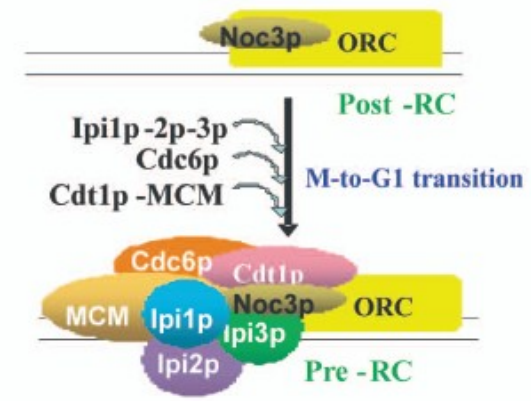

Figure 1.8. Hierarchical of replication-initiation proteins.

Sequential assembly of pre-RC proteins, where IPI proteins allow the directly connection of ORC and Noc3p to the other pre-RC components and where Cdc6p to Cdt1p-MCM proteins assemble [67].

Immuno-EM showed that ~ 40% of PrA-Noc3p was distributed in the nucleolus, while ~ 60% was nucleoplasmic [47]. GFP-Noc3p showed an entirely nuclear distribution [47]. Chromatin-binding assays have demonstrated that Noc3p is a chromatin binding protein together with ORC, Cdc6p, Cdt1p, Cdc45p and the MCM proteins [66]. Furthermore, Noc3p was found to bind chromatin throughout the cell cycle at a constant level, suggesting that like ORC, it is constitutively chromatin bound [66]. Using ChIP assays, Noc3p was shown to bind specifically to autonomously replicating sequence (ARSs) elements *in vivo* at different phases of the cell cycle, in the same way as ORC [66]. Reciprocal experiments using *ts* mutants revealed that ORC is required for stable chromatin association of Noc3p.

In addition to chromosomal DNA replication, Noc3p was also shown to participate in ribosome biogenesis. The 60S/40S subunit ratio was significantly reduced in a *noc3-1 ts* mutant when shifted to the restrictive temperature [47]. Sucrose gradient centrifugation in combination with Western and Northern blot analyses demonstrated that Noc3p co-sedimented with 27S and 7S pre-rRNA; thus, compared with the two earlier Noc proteins, Noc1p and Noc2p, Noc3p appears to be associated only with later 66S particles [47]. Northern hybridization, primer extension and pulse-chase labeling experiments showed pre-rRNA processing phenotypes supporting this hypothesis, revealing a defect in the 25 rRNA/5.8S

rRNA maturation pathway [47]. A mild accumulation of 35S pre-rRNA and reduction of $27SA_2$ and 20S pre-rRNAs synthesis rates demonstrated a delay in the early cleavages A_0, A_1 and A_2 [47]. A strong reduction in 27SB, 7S and 6S pre-rRNA was also observed while A_3 cleavage was blocked [47]. In contrast, 25S rRNA was reduced in Noc1p and Noc2p mutants. whereas an accumulation of the 25S rRNA was observed in *noc3-1* mutant [47]. Taken together, these results suggest that Noc3p, similar to Noc1p and Noc2p, is not primarily involved in pre-rRNA processing, but possibly in the correct assembly of 60S ribosomal subunits [47]. When the 60S subunit reporter Rpl25p-eGFP was used to test the efficient 60S subunit export, *noc3-1* cells exhibited accumulation of this reporter throughout the nucleolus and the nucleoplasm, indicating that Noc3p may participate in a late step prior to pre-ribosomes export from the nucleoplasm into the cytoplasm [47].

1.6.3.1 Homologs of Noc3p in other organisms

The homolog of yeast NOC3 in *Schizosaccharomyces pombe,* $noc3^+$ ($Spnoc3^+$), is an essential protein and required during DNA replication, cell cycle progression and ribosome biogenesis [68]. Moreover, it has been shown that SpNoc3p and Noc3p are functionally homologous proteins, essential for the complete maturation of the 60S subunit [68].

Noc3p shares ~30% sequence similarity with the mammalian protein Fad24 (factor for adipocyte differentiation, clone number 24) [69]. At its C-terminal, Fad24 contains a basic leucine zipper (bZIP)-like domain and a NOC domain [69]. As for Noc3p, Fad24 localizes to the nucleus, but is enriched within nuclear speckles [69]. Overexpression of Fad24 in NIH3T3 cells promoted adipogenesis in the presence of a ligand for the peroxisome proliferator-activated receptor γ [69]. However, no function in ribosome biogenesis for Fad24 has been reported so far.

1.6.4 Noc4p in S.cerevisiae

Noc4p is an essential 63kDa protein abundant at ~1630 molecules per cell [51]. It was found to be enriched in isolated large nucleolar subcomplexes, and GFP-tagged Noc4p localized within the nucleolus [46, 48].

Affinity-purification analysis showed that Noc4p formed a heterodimeric complex with Nop14p, a 98 kDa protein, which had previously been shown to play a role in 40S subunit biogenesis [48]. Noc4p was detected in fractions corresponding to 90S particles, 43S pre-ribosomes and 40S subunits on sucrose density gradients, supporting its role in 40S biogenesis [48].

Noc4p is a member of the early small subunit processome (SSU) [48]. To characterize the effect of r-protein assembly events on association of Noc4p with early pre-ribosomes, mutants of several SSU r-protein genes under the control of the inducible/repressible GAL promoter were expressed in a Noc4p-TAP strain. Under permissive conditions (Galactose), Noc4p-TAP co-purified with early SSU rRNA precursors such as 32S and 35S pre-rRNAs [70]. Under repressive conditions, when either Rps11p, Rps9p, Rps22p or Rps15p were depleted, Noc4p-TAP was still efficiently co-purifying large amounts of accumulating 32S and 35S pre-rRNAs [70]. However, depletion of either Rps13p, Rps14p or Rps5p, lead to a severe reduction in the efficiency co-purification of 32S and 35S (by a factor of 10), suggesting that the assembly of Rps13p, Rps14p and Rps5p onto the pre-rRNA primary transcript has to occur in order to allow downstream association of Noc4p with the 90S pre-ribosome [70].

A *ts noc4-1* mutant was used to test defects in rRNA processing. Under restrictive conditions, free 40S subunits were shown to be significantly decreased in this strain, whereas the level of 60S subunits increased [48]. These results show the opposite effect of what has been observed in *noc1-1*, *noc2-1* and *noc3-1* mutants. In addition, in *noc4-1* cells, 20S pre-rRNA and mature 18S rRNA were significantly reduced after 4h at restrictive temperature, whereas 27S and 7S pre-rRNA and mature 25S rRNA were not affected [48]. Moreover, *noc4-1* showed a block at the early cleavage steps A_0, A_1 and A_2 by a reduction in the 20S, 32S and $27SA_2$ pre-rRNA species [48]. Similar to *noc2-1*, *noc4-1* also showed a slight accumulation of 23S precursor RNA, and thus post-transcriptional assembly of the 90S components onto the primary rRNA transcript and a delay in processing at sites A_0-A_2 [48].

Using the Rps2p-eGFP and Rpl25p-GFP reporter for the export of the small and large subunits, respectively, Rps2p-eGFP was found to significantly accumulate in the nucleus in

the *noc4-1* strain at restrictive temperature, whereas the nuclear export of Rpl25p-eGFP was not impaired [48]. This suggested that Noc4p is indeed involved in pre-40S maturation, and is also required for efficient export of the small subunit to the cytoplasm. Interestingly, further affinity purification experiments of FLAG-tagged r-proteins binding to 18S rRNA and co-isolation of 20S pre-RNA in a *noc4 ts* strain, showed that not only are certain assembly events required for Noc4p assembly into pre-ribosomes, but the presence of Noc4p itself is needed for the efficient assembly of the SSU 3' (head) domain [70].

1.6.4.1 Homologs of Noc4p

Homologs for Noc4p have been identified in different species. In humans, Nucleolar Complex-Associated Protein 4-Like, Noc4L or Net49 is located in the nucleolus and at the nuclear membrane [48]. The protein was initially identified through an RNAi screen, which was performed in HeLa cells, using a list of proteins with a potential function in human ribosome biogenesis [71]. 153 targets were found to display a phenotype relating to ribosome biogenesis defects, and in a Noc4L knockdown, the reporter Rps2-YFP were accumulated in the nucleoli and nucleus, indicating a specifically pre-40S maturation defect [71].

1.6.5 The dynamics of Noc protein exchange

As discussed above, the Noc proteins are essential for cell growth, and all four proteins are highly conserved with homologs from yeast to human [47]. The data up-to-now has suggested that Noc1p, Noc2p and Noc3p are involved in intranuclear transport and export of the pre-60S particles, and that Noc4p is required for the nuclear export of the pre-40S particle [47, 48].

Noc1p, Noc3p and Noc4p have an evolutionary conserved domain of 45 amino acids in length (Noc-domain) [47]. Interestingly, overexpression of this conserved domain causes an accumulation of Rpl25p-eGFP reporter in the nucleolus [47]. This phenotype is the same that has been observed in *noc1-1* and *noc3-1 ts* mutants , where Rpl25p-eGFP accumulated throughout the nucleolus and the nucleoplasm [47]. Yet while Noc4p also contains the conserved domain, Rpl25p-eGFP export has not been found to be impaired in *noc4-1 ts* mutants [47, 48]. However, Rps2p-eGFP significantly accumulated in the nucleus, denoting a

role in pre-40S transport. Furthermore, no defect in pre-rRNA processing was detected when the Noc-domain was overexpressed [47]. Together, these results suggested that the Noc-domain of Noc1p, Noc3p and Noc4p could play a role in the retention of precursors, either pre-40S or pre-60S, in the nucleolus without affecting pre-rRNA processing [47]. Interestingly, Noc2p does not shown to contain this conserved Noc-domain [47]. Nevertheless, an accumulation of Rpl25p-eGFP at two different stages, between the nucleolus and nucleoplasm, and between the nucleoplasm and the cytoplasm could be visualized in a *noc2-1 ts* mutant, indicating defects in pre-60S transport, from the nucleolus to the nucleoplasm as well as to the cytoplasm [47].

Figure 1.9. Sequence comparison of the conserved Noc-domain in Noc1p, Noc3p and Noc4p.
Comparison of the conserved 45 amino acid long Noc-domain from Noc1p, Noc3p and Noc4p homologues. The numbers indicate the position of the domain within the respective protein [47].

In pre-60S subunit maturation, Noc1p, Noc2p and Noc3p gave some of the first indications about a spatio-temporal nature of the ribosome biogenesis pathway. Milkereit et al. found that the intranuclear movement of pre-60S ribosome required a dynamic interaction between the Noc proteins in the form of two heterodimeric complexes, Noc1p-Noc2p and Noc2p-Noc3p [47]. These complexes act as a prerequisite for specific maturation steps [47]. High-salt affinity purifications were used to purify Noc2p-PrA and co-purifying Noc1p and Noc3p [47]. However, Noc1p and Noc3p do not purify with each other, only with Noc2p [47]. Indeed, Noc2p interacts directly with either Noc1p or Noc3p, but in two very distinct subcomplexes [47]. Functional linkage between Noc proteins was shown using *noc1-1, noc2-1* and *noc3-1 ts* mutant strains, where each was viable at 23°C [47]. However, a combination of *noc2-1* with *noc1-1,* and *noc2-1* with *noc3-1* resulted in synthetic lethality [47]. Yet, a

combination of *noc1-1* with *noc3-1* was not found to be lethal [47]. Thus Noc2p has a genetic functional link with both Noc1p and Noc3p [47]. Immuno-EM of PrA-tagged Noc proteins showed their ultrastructural localization and distribution; These analyses revealed a nucleolear distribution along the dense fibrillar component for all of the Noc proteins, but showed different distributions in the nucleoplasm; Noc1p is concentrated solely in the nucleolus, Noc2p is also concentrated in the nucleolus but also exhibits a weaker nucleoplasmic localization, while Noc3p is more evenly distributed between the nucleolus and the nucleoplasm (Figure 10) [47]. Using a combination of *ts* Noc mutant and GFP-tagged Noc proteins, effects in the intranuclear distribution of the different Noc protein were tested (Figure 10). In *noc1-1* cells, Noc2-GFP concentrated strongly in the nucleolus, whereas Noc3-GFP localization showed no significant change [47]. In *noc2-1* cells, Noc1-GFP was redistributed throughout the entire nucleoplasm, whereas, once again, Noc3-GFP localization showed no change [47]. This data suggested that localization of Noc1p and Noc2p depends on their complex formation [47]. Finally in *noc3-1* cells, Noc1p and Noc2p were accumulated in the nucleolus, indicating that Noc2p localization depends on the functionality of both Noc1p and Noc3p [47]. Together, the Noc proteins display a dynamic intranuclear distribution, with the potential to shuttle between the nucleolus and the nucleoplasm [47].

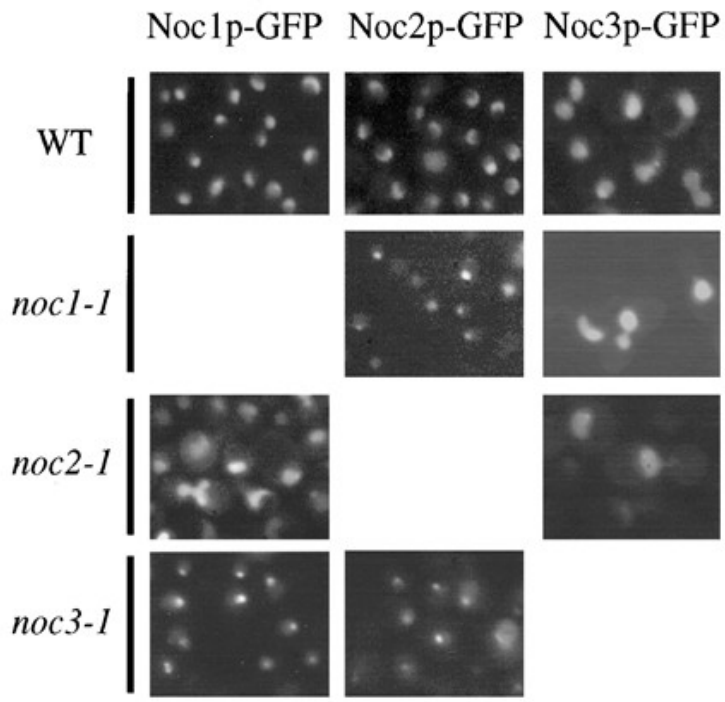

Figure 1.10. Intranuclear localization of Noc1p, Noc2p and Noc3p.

Visualization of *in vivo* distribution of the three 60S Noc proteins (Noc1p, Noc2p and Noc3p) in wild-type and in *noc ts* mutants cells, using GFP-tagged fusion proteins and fluorescence microscopy [47].

During transition from the nucleolus to the nucleolus/nucleoplasm border, many factors are dissociated causing a significant simplification of the complex composition [35]. Noc1p was suggested to be present with Noc2p in an early nucleolar 90S/pre-60S particle, and to be replaced by Noc3p upon release of the pre-60S particle into the nucleoplasm, a theory that was confirmed by affinity purification analysis [35, 47]. Indeed, Noc1p was found to be enriched in the early nucleolar 90S/pre-60S complexes, compared to Noc3p, which was found in much lower amounts [35]. In later pre-60 pre-ribosomes, Noc1p was shown to be less present, whereas Noc3p was enriched [35]. As pre-ribosomes move further down the maturation pathway Noc1p was found to be largely lost and Noc3p increasingly enriched [35].

In the same way, the dynamic aspects between the Noc proteins, especially those implicated in pre-60S maturation, maybe a means to trigger exchange between different factors on pre-ribosomal complexes. Several genetic analyses and affinity purification

coupled with mass spectrometry analyses have been able to identify many interacting partners associated with Noc1p, Noc2p and Noc3p [72]. As seen in Table I and II, these three Noc proteins share several associated proteins, reflecting their common function and their proximity. However, interesting distinctions can be made that underline their differences and their dynamics. Noc1p was found to be associated with some components of the SSU processome, containing the U3 snoRNA that is involved in the processing of the pre-18S rRNA (Utp10, 13, 14, 21). These associations are not seen with Noc2p and Noc3p [73]. Moreover, Noc1p is more likely associated with histones and others factors involved in 18S rRNA synthesis, such as the DEAD box Hca4p, pointing towards its proximity to chromatin and early function in the pathway. Many ribosomal proteins were found to be associated with Noc1p but not with Noc2p and Noc3p. Some of them are ribosomal 40S subunit protein, which supports the link between previous observations of Noc1p as an early 90S complex protein.

Table I. Summary of non-ribosomal proteins physically and genetically associated with Noc1p, Noc2p and Noc3p pre-ribosomal particles.

Tagged Noc1p, Noc2p and Noc3p are listed in the top row. In the columns below each bait protein, co-purifying proteins identified by mass spectrometry are indicated vertically as gray rectangles and proteins that are in addition genetically linked by synthetic lethality analysis are indicated as dark green rectangles. Proteins genetically linked by negative genetic analysis are indicated as light orange rectangles that have also been identified by mass spectrometry are indicated as dark orange rectangle. Some functions of the associated proteins are indicated in the right vertical column. Data were merged and analyzed from the BioGRID interaction summary [35, 72].

	Preys	Bait			
	Associated	Noc1	Noc2	Noc3p	Comments
90S	NOP1				35S processing and methylation
	NOP10				
	NOP12				25S pre-rRNA synthesis
	NOP13				
	NOP56				Box C/D component
	NOP58				Box C/D component
	GAR1				Part of H/ACA snoRNP
	CBF5				Part of H/ACA snoRNP
	RIX1				60S biogenesis
	DBP2				
	ECM16				
	NHP2				
	RRP9				pre-rRNA processing; associated with U3 snRNP
	SNU13				
	SNR17A				snoRNA U3
	SNR17B				snoRNA U3
	MPP10				
	UTP10				Component of the SSU proteasome
	UTP13				Component of the SSU proteasome
	UTP14				Component of the SSU proteasome
	UTP15				Component of the SSU proteasome
	UTP21				Component of the SSU proteasome
	UTP22				Component of the SSU proteasome; tRNA export
	HCA4				DEAD box RNA helicase; 18S rRNA synthesis
	RDN37				
	PWP1				WD-40 repeats; iRNA processing
	KRI1				
	KRR1				
	SRP40				
	MRD1				
	NAN1				U3 snoRNP protein
	KRE33				SSU biogenesis
	SOF1				
	UTP20				
	MAK11				WD40 repeats
	RDN37				
	NOP9				Subunit of U3-containing 90S pre-ribosome
	NOP6				
	RRP5				Processing to 25S and 5.8S
	RRP12				
	MAK11				Early step 60S biogenesis
	NOC4				
	ORC1				origine recognition complex
	BMS1				GTPase; 35S pre-rRNA processing

	Preys	Bait			
	Associated	Noc1	Noc2	Noc3p	Comments
pre-66S	BRX1				Brx family, 25S maturation
	RRP1				involved in 25S maturation
	NSA2				associated with 26S proteasome
	NOP2				60S processing and synthesis
	NOP4				rRNA processing and methylation
	RLP7				C2 cleavage
	NOC1	X			60S intranuclear transport
	NOC2		X		60S intranuclear transport
	NOC3			X	60S intranuclear transport
	NOP15				
	NOP16				
	RPF1				Brix familym LSU maturation
	RPF2				
	CIC1				Interaction with proteasome components
	ERB1				WD40 repeats
	EBP2				
	YTM1				WD40 repeats; 60S biogenesis
	NSA1				
	TIF6				60S subunit biogenesis and stability
	LOC1				
	SSF1				A2 cleavage associated
	DRS1				
	NIP7				60S biogenesis
	NOG1				Putative GTPase
	SPB4				Putative ATP-dependent RNA helicase
	RIX7				Putative AAA-TAPase
	DBP10				DEAD box RNA helicase; ATP-dependent
	DRS1				
	HAS1				DEAD box RNA helicase
pre-60S	REX4				
	PUS7				Pseudouridine synthase
	IPI3				Rix1 complex; ITS2 processing
	NOP53				60S biogenesis
	AIR1				Zinc knuckle protein
	RRP17				exonuclease for 5'end rRNA processing
	NOP7				Pescadillo homolog
	PUF6				Pumolio-homology domain protein
	RSA3				
	URB1				
	RLP24				60S biogenesis
	RRS1				
	MAK5				
	NSR1				Nucleolar protein; pre-rRNA processing
	REI1				AAA-ATPase
	DBP3				DEAD box RNA helicase; ATP-dependent
	DBP7				DEAD box RNA helicase; ATP-dependent
	DBP9				DEAD box RNA helicase; 27S processing
	NUG1				Putative GTPase
	JJJ1				Co-chaperone; ribosome biogenesis
	SSB1				ATPase; ribosome-associated chaperone

Affinity capture MS
Synthetic lethality + Affinity capture MS
Negatif genetic
Negatif genetic + Affinity capture MS

Table II. Summary proteins physically and genetically associated with Noc1p, Noc2p and Noc3p pre-ribosomal particles.

Tagged Noc1p, Noc2p and Noc3p are listed in the top row. In the columns below each bait protein, copurifying proteins identified by mass spectrometry are indicated vertically as gray rectangles. Proteins that are genetically linked by synthetic lethality analysis are illustrated as light green and in addition mass spectrometry analysis are indicated as dark green rectangles. Proteins genetically linked by negative genetic analysis are indicated as light orange rectangles that have also been identified by mass spectrometry are indicated as dark orange rectangle. Genetic links from phenotypic suppression are indicated as bleu reactangle. Some functions of the associated proteins are indicated in the right vertical column. Data were merged and analyzed from the BioGRID interaction summary [35, 72].

	Preys	Bait			
	Associated	Noc1	Noc2	Noc3p	Comments
Ribosomal proteins	RPS14A				
	RPS16A				
	RPS18A				
	RPS21B				
	RPS22B				
	RPS24B				
	RPL1A				
	RPL2A				
	RPL3				
	RPL4A				
	RPL4B				
	RPL5				
	RPL6B				
	RPL7A				
	RPL7B				
	RPL8B				
	RPL11B				
	RPL12A				
	RPL13A				
	RPL13B				
	RPL15A				
	RPL16				
	RPL17B				
	RPL18B				
	RPL18A				
	RPL20A				
	RPL23A				
	RPL25				
	RPL26B				
	RPL27A				
	RPL28				
	RPL29				
	RPL30				
	RPL31A				
	RPL33B				
	RPL36B				
	RPL37A				
	RPP1A				
	RPP2B				
Histones	HHO1				Histone H1
	HTA2				Histone H2B
	HHT1				Histone H3
	HHT2				Histone H3
	HHF1				Histone H4
	HHF2				Histone H4

	Preys	Bait			
	Associated	Noc1	Noc2	Noc3p	Comments
Others	FPR3				Peptidyl-prolyl cis-trans isomerase
	FPR4				Peptidyl-prolyl cis-trans isomerase
	SAS4				Subunit of the SAS complex
	TSL1				
	MAG2				
	GIS2				
	SPB1				Putative methyltransferase
	UBC9				
	ULP2				
	SMT3				Ubiquitin-like protein; SUMO family
	MRT4				mRNA turover; ribosome biogenesis
	UBI4				Ubiquitin;
	BRE5				interacts with Ubp3p
	UBP3				ubiquitin-specific protease
	UBP10				
	YMR1				
	HRK1				
	PAB1				Poly(A) binding protein
	DSN1				MIND kinetochore complex component
	NUP116				
	SPC24				
	NAT3				
	YRA1				Poly(A) RNA-binding protein
	SFA1				
	SKI2				Putative RNA helicase
	SKI3				Ski complex component; TPR protein
	SKI6				Exosome non-catalytic core component
	STM1				
	PRP43				pre-mRNA splicing factor
	CHL1				
	SEC15				
	SEC7				
	LRP1				
	YOR1				ATP-binding cassette (ABC) transporter
	TUB3				Alpha-tubulin
	MCM2				Involved in DNA replication
	MCM5				Mcm2-7 hexameric helicase comple xcomponent
	MCM6				Involved in DNA replication
	RPA190				
	RPA135				
	SGS1				
	PTC1				
	ORC2				Origin recognition complex subunit
	ORC3				Origin recognition complex subunit
	ORC5				Origin recognition complex subunit

Affinity capture MS
Phenotype supression
Synthetic lethality
Synthetic lethality + Affinity capture MS
Negatif genetic
Negatif genetic + Affinity capture MS

As seen in Table I, Rrp5p has been shown to co-purify with both Noc1p and Noc2p [54]. Rrp5p is a component of the early 90S/SSU processome and acts as a *trans*-acting factor required for both SSU and LSU maturation [25]. Rrp5p was found to bind sequences on either side of the A_3 site on the pre-rRNA, and suggested to block pre-mature exonucleolytic processing [25]. Later, this early protein was shown to be genetically linked to both Noc1p and Noc2p, as a *rrp5* mutant is synthetically lethal with *ts* alleles of NOC1 and NOC2 [55]. Using affinity purification of FLAG tagged components concluded that Rrp5p does not bind to Noc2p, but interacts directly with Noc1p [55]. Noc1p was shown to interact directly with the N-terminal part of Rrp5p, which contains nine copies of a S1-type RNA-binding motif [55]. This N-terminal part was shown to be sufficient yet required to establish a specific physical interaction with Noc1p [55]. Taken together, the three proteins are suggested to form a hetero-trimeric protein complex, where Noc1p bridges between Noc2p and Rrp5p [55].

Furthermore, rRNA composition of pre-ribosome associated with Rrp5p-TAP and Noc1p-TAP particles contain highly the same components [55]. Indeed, 35S and 32S pre-rRNA as well as U3 snoRNA were found to be enriched, compared to later pre-LSU or pre-SSU RNA species that were found in lower amounts in both particles [55]. Moreover, 22 components of the SSU processome have been identified, such as CD box and H/ACA box snoRNP components (Table I, data not shown for Rrp5p) [55]. In addition, most of the large subunit biogenesis factors identified had already been shown not only to be required for early steps in large subunit maturation, but also for processing of the 5'-end of 5.8S rRNA and production and/or stabilization of 27SB pre-rRNA (Table I, e.g. Brx1p, Nop4p, Erb1p, Ebp2p, Ssf1p, Rlp7p and Rix7p; data not shown for Rrp5p) [55]. Moreover, no factors indicative for later 60S or 40S pre-ribosomes were identified in either Noc1p-TAP or Rrp5p-TAP particles (Table I and II, data not shown for Rrp5p) [55].

Binding hierarchies have been studied recently for the Rrp5p, Noc1p and Noc2p hetero-trimeric protein complex. In a strain where Rrp5p was depleted, Noc1p and Noc2p were still able to bind to nascent pre-ribosomes [55]. On the other hand, in cells that were depleted of either Noc1p or Noc2p, Rrp5p-TAP copurified the same RNA species as observed in normal condition, but U3 snoRNA, 35S, 32S and 23S pre-rRNA were enriched [55]. These results indicated that Noc1p and Noc2p are recruited to pre-ribosomes independently of

Rrp5p, yet the absence of the Noc1-Noc2 complex caused a clear delay in early processing steps and a possible prolonged dwelling time of Rrp5p on pre-ribosomes [55]. Recruitment of the trimeric complex has been finally proposed to occur co-transcriptionally in the same way as SSU processome components, however, it should also be noted that Rrp5p, Noc1p and Noc2p predominantly associate with large subunit (LSU) precursors after separation of the LSU and SSU pre-rRNA through cleavage within ITS1 [55].

Furthermore, subcomplex Rrp5p-Noc1p, in addition to subcomplex Nop12p-Pwp1p, which was found to crosslink to 5.8S rRNA, and Nop4p which crosslinks to domain III of 25S rRNA, has been suggested to hold the pre-ribosome in an immature state to prevent stable r-protein binding to domain I as well as pre-rRNA processing prior to the association of the helicase Has1p (Table I) [25]. In fact, in the absence of Has1p, levels of all early factors have been shown to increase within the Rpf2p-TAP associated particles, indicating an arrest at that stage [25]. Indeed, Has1p has been also suggested to drive the removal of early assembly factors from the pre-ribosome [25]. However, it has not been determined whether Has1p induces the Rrp5p-Noc1p-Noc2p dissociation or is involved in the switch between Noc1p-Noc2p to Noc2p-Noc3p.

1.7 The Project and its Objectives

1.7.1 Rationale and Previous Work

In past years, it has been shown that ribosome biogenesis is a highly energy-consuming process. Because assembly factors are not found in the mature ribosome, this requirement of energy may be due to the dynamic binding of assembly factors to the pre-ribosome, and the necessity for their removal. Moreover, evidence of a correlation between free energy and ribosome spatial progression has been shown by using a metabolic poison [31]. Indeed, cells were arrested at an ATP/GTP-dependent steps and nuclear transport disruption has been observed by visualizing the accumulation of fluorescently-tagged proteins in the nucleolus, the nucleoplasm or along the nuclear rim [31]. In light of this information, energy-dependent events have been hypothesized to be linked to spatial progression and remodeling of ribosomal particles.

Rix7p, a triple AAA-ATPase, which is present in Noc protein containing complexes, has been speculated to be involved in such energy-dependent remodeling steps [40]. It has been shown that ATP hydrolysis by Rix7p coincides with Nsa1p removal and a compositional change of the pre-60S particle, where some early factors such as Noc1p dissociate from the particle, and some later nuclear factors associate with the pre-60S ribosome [40]. Rix7p has recently been suggested to have additional substrates, due to its homology with the yeast Cdc48p, and it was proposed that the protein is able to detect the structural integrity of pre-60S particles and lead to a check point, which, if the particles are correct, results in Nsa1 removal and change in particle composition, including structural rearrangements [41]. Since the Noc proteins are known to be present at a stage that overlaps with the presence of Rix7p, subcomplex exchange between Noc1p-Noc2p and Noc2p-Noc3p could potentially coincide with this particle rearrangement, and even be facilitated by it. Since intranuclear movement of this pre-60S complex was suggested to require a dynamic interaction between the Noc proteins, indeed, ATP hydrolysis by Rix7p could be linked to the exchange of Noc1p for Noc3p as part of a checkpoint mechanism to release the complexes from the nucleolus into the nucleoplasm, leading to spatial movement of pre-60S complexes [47]. Up to now, however, it has not been determined whether ATP hydrolysis could be a cause, or even a consequence, of the Noc protein subcomplex exchange. In fact, the mechanism of the Noc subcomplex exchange has remained completely elusive.

1.7.2 The use of *ts* mutants and ribosome biogenesis

Previous data has been mostly generated using yeast *ts* mutant strains, to determine the genetic relationship of Noc2p with both, Noc1p and Noc3p, their spatio-temporal behavior and dynamic implication in ribosome biogenesis [47]. *Ts* mutations are missense mutations and have been a fundamental approach to study functions of essential genes [74]. By using haploid yeast cells containing specific missense mutations, a gene's function can be easily managed by shifting temperature; at low, permissive temperature (23°C), *ts* mutations retain the function of the gene under study, while at a high, repressive temperature (37°C), the gene loses its function [74]. However, it has been a longstanding question whether this temperature shifts affects cells more severely than previously thought. It is known that under heat-shock, many

gene expression pathways are altered, and ribosome biogenesis is briefly switched off [75, 76]. Even in strains were the gene carrying the missense *ts* mutation is not involved in ribosome biogenesis after shift to restrictive temperature, significant shifts in the ribosome maturation network were observed, and the entire network of r-protein disappeared since their expression was shut down (Figure 11) [Oeffinger, unpublished data].

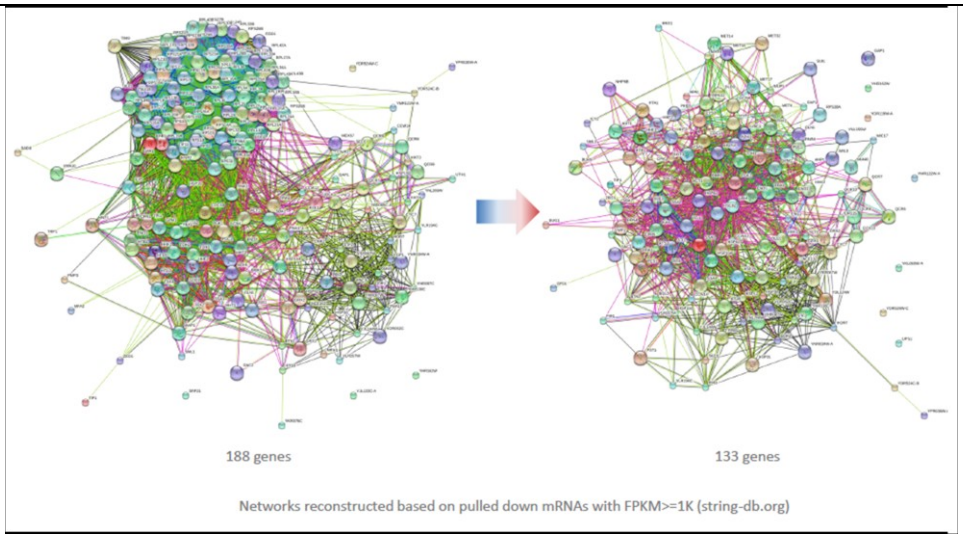

Figure 1.11. Changes in cellular expression networks after shift to restrictive temperature.
A Nab2-PrA/*mex67-5* strain was shifted to restrictive temperature for 30 minutes, and mRNAs co-purified with Nab2-PrA analyzed by RNA sequencing. Several changes in the gene expression pattern were observed, the most drastic the loss of expression of the r-protein gene cluster (upper left corner on the left image) [Oeffinger M., Unpublished].

This raises some questions about the accuracy of previous data on Noc proteins and shifts in ribosome biogenesis networks studied in the *ts* mutants. Thus, it is important to reevaluated previous conclusions that have been obtained by using *ts* mutants. To this aim, it is preferable to use inducible/repressible promoter systems that can regulate gene expression and that are not temperature-dependent, but also not carbon source dependent either. Indeed, the well known *GAL1* promoter, which is glucose-repressible, has been set aside because of the possibility that changes in the carbon source cause pleiotropic affects [77]. Instead, the MET25 promoter has been chosen since it is methionine-repressible. As it remains unclear to this point how Noc2p dissociates from Noc1p to form another, later, complex with Noc3p,

inducible promoter systems combined with microscopy, as well as affinity purification can be used to study this events in more detail, and elucidate how these proteins could be involved in the formation of subcomplexes may act as quality control checkpoints and, intranuclear pre-60S movement.

1.7.3 Aims and Objectives

Synthesis of eukaryotic ribosome has been mostly studied in the yeast *Saccharomyces cerevisiae* due to its easy experimental accessibility to biochemical and genetic methods [2]. Indeed, this organism has also been used in this project because of all the information already available on Noc proteins in this system. It has been shown by mass spectrometry and electron microscopy that the Noc proteins form two distinct subcomplexes over the nuclear, such as Noc1p-Noc2p and Noc2p-Noc3p. Indeed, I decided to study in particularly Noc2p in order to look at its influence on the ribosome maturation, since it is the intermediate protein of the two Noc subcomplexes. In the presence or absence of Noc2p, the dynamic and spatial movement of Noc1p, Noc3p and the AAA-ATPase Rix7p will be scrutinized. Moreover, I will determine the role of the ATP hydrolysis step by Rix7p on the Noc1p, Noc2p and Noc3p, and how this specific event relates to Noc1-Noc3 exchange. I will also determine links between Noc2p and its human homolog NIR.

This project is separated into four distinct aims.

1. **To determine the dynamic effect of Noc2p depletion on early steps of 60S ribosome biogenesis**

Since the pre-60S export function of Noc2p and intralocalization dependence between the Noc proteins have been tested by using a *noc2-1 ts* mutant, where ribsome biogenesis is potentially affected due to the stress conditions of the temperature change, I will reevaluate previous conclusions by using an inducible/repressible promoter system, that regulates NOC2 expression. Moreover, this system will be used to look at the possible regulation of Noc1p and Noc3p at their protein and their gene expression levels. Finally, I will also test a possible link between Noc2p and Rix7p.

1.1 Cellular depletion of Noc2p using an inducible/repressible MET25 promoter to determine its effect on

1.1.1 Localization of Noc1p, Noc3p and Rix7p.

1.1.2 Total levels of Noc1p, Noc3p and Rix7p.

1.1.3 Gene expression levels of Noc1p, Noc3p, Rix7p and others ribosome factors.

1.2 Determine the effect of Noc2p presence and absence on the spatial movement of pre-60S subunits using the Rpl11p-GFP reporter.

2. **To determine the influence of reversibly arrested intranuclear transport on Noc2p and its partner proteins Noc1p, Noc3p and Rix7p**

General influence of energy from nucleotide sources on different aspects of the Noc proteins and Rix7p. For this aim, I will reversibly arrest nuclear transport by using a metabolic poison, consisting of sodium azide and deoxy-d-glucose, which were shown to lead to a decrease of free ATP/GTP in the cell [78, 79].

2.1 Arrest of intranuclear transport via reversible depletion of cellular ATP and GTP levels to determine the

2.1.1 Localization of the Noc proteins and Rix7p

2.1.2 Total levels of the Noc proteins and Rix7p

2.1.3 Gene expression levels of the Noc proteins, Rix7p and other ribosome factors.

3. To determine compositional changes of selected pre-ribosomes

Affinity-purifications of Noc1p, Noc3p and Rix7p need to be performed in parallel, to pinpoint the Noc1p-Noc2p and Noc2p-Noc3p exchange, the possible role of Rix7p and to better understand the overall pre-ribosome environment.

4. To determine links between Noc2p and the function of its human homolog NIR

From an NCBI Blast search, Noc2p was shown to have 31% similarity to the human protein NIR, which contains two independent INHAT regions, one at its N-terminus and one at its C-terminus; these domains are known to efficiently bind to nucleosomes and block acetylation of the core histones H3 and H4 [63]. Indeed, I will test the possible role of Noc2p in transcription regulation by looking at the co-existence of the two distinct rDNA chromatin populations, dependent on the regulation of NOC2 expression.

4.1 Study how Noc2p depletion influences the rDNA chromatin state.

2 Materials and methods

2.1 Chemicals

Standard laboratory reagents were purchased mainly from Fisher and Sigma, and yeast media ingredients were purchase from Bio Basics.

2.2 Culture media

2.2.1 Bacterial culture media

- Liquid LB-Luria Broth: 1% (w/v) Bacto-tryptone, 1% (W/V) NaCl, 0.5% (W/V) Yeast extract, autoclaved. For agar plate, 2% agar was supplemented before autoclaving.

- SOC: 20mM glucose, 2.5 mM KCl, 10 mM NaCl, 10 mM $MgCl_2$, 10 mM $MgSO_4$, 2% (w/v) vegetal peptone, 0.5% (w/v) yeast extract, Autoclaved.

Antibiotics were added after autoclaving, depending on the selective marker.

Table III: List of the antibiotics for appropriate bacterial culture media

Antibiotic	Abbreviation	1000X stock (mg/mL)
Ampicillin	Amp	50
Gentamicin	Gen	20
Kanamycin	Kan	50

2.2.2 Yeast culture media

Yeast media is dependent on a selective or auxotrophic marker for the strain and the experimental purpose. For all of them, 1:500 ampicillin was added prior to use, in order to prevent bacterial contamination.

- Standard yeast media (YPD): 1% (w/v) Yeast extract, 2% (w/v) Peptone, 2% (w/v) glucose. Autoclaved

- Drop-out media for selective marker (SD-amino acid): 2% (w/v) Glucose, 1.5% (w/v) Yeast nitrogen base (amino acid and ammonium sulfate free), 5% (w/v) Ammonium sulfate, 1X amino acids except selected amino acid, 5X Adenine. Filter sterilized.
- For growth curve experiments:
    - MET25 promoter cassette selection (SD-MET + Clonat): 2% (w/v) Glucose, 1.5% (w/v) Yeast nitrogen base (amino acid and ammonium sulfate free), 0.1% (w/v) Monosodium glutamate, 1X amino acids except methionine, 5X Adenine, 300 mg/mL ClonNAT. Filter sterilized.
    - MET25 promoter, on: SD-MET 2% (w/v) Glucose, 1.5% (w/v) Yeast nitrogen base (amino acid and ammonium sulfate free), 5% (w/v) Ammonium sulfate, 1X amino acids except methionine, 5X Adenine. Filter sterilized.
    - For MET promoter shut-off (SD Complete): 2% (w/v) Glucose, 1.5% (w/v) Yeast nitrogen base (amino acid and ammonium sulfate free), 5% (w/v) Ammonium sulfate, 1X amino acids mix, 5 mM methionine, 5X Adenine. Filter sterilized.
- For nuclear transport arrest: 10 mM Sodium azide and 10 mM deoxy-d-glucose were added to appropriate media without glucose. (YP/sodium azide/deoxy-d-glucose or SD-MET/sodium azide/deoxy-d-glucose/without glucose)

Table IV: List of the antibiotics for appropriate yeast culture media

Antibiotic	Abbreviation	Concentration used (mg/mL)
Noursethricine	ClonNAT	300
Geneticin	G418	200 and 600

2.3 Plasmids

Table V: Plasmids used in this study

Name	Features	Source
pET21a peIB-VHH 16	Ilama nanobody, Amp, His6	Fridy et al., submitted
pFA6a-mCherry-KanMX6	mCherry, KanMX6	Zenklusen Lab
pNOY373	35S rDNA, Amp	[15]
pYM-N36	MET25::3XHA, clonNAT	[80]

2.4 Bacterial techniques

2.4.1 Expression and purification of recombinant anti-GFP nanobody

Anti-GFP nanobody needed to be purifying as a recombinant protein with the final aim of conjugating Dynabeads. To this end, transformation of pET21-peIB-VHH-16 plasmid into ArcticExpress cells (Agilent Technologies) and induction with IPTG was carried out.

2.4.1.1 Transformation of pET21-peIB-VHH plasmid into ArcticExpress (DE3) cells

Competent *E.coli* ArcticExpress cells have been used for their lack of the Lon protease, which can degrade recombinant proteins and for their Hte phenotype, which increases the transformation efficiency of the cell. Moreover, this host strain contains the pACYC-based plasmid that includes a gentamicin-resistance gene, which allows positive clone selection.

Table VI: ArcticExpress (DE3) cell genotype

Company	Catalog number	Host strain	Genotype
Agilent Technologies	230192	ArcticExpress (DE3) strain	*E.coli* B F^- *ompT hsdS*(r_B^- m_B^-) *dcm*$^+$ Tet^r *gal* λ(DE3) *endA* Hte [*cpn10 cpn60* $Gent^r$]

Transformation of pET21-peIB-VHH-16 plasmid into ArticExpress cell was carried out according to the manufacturer's instruction; on ice, 2 µL of 1:10 XL10-Gold β-mercaptoethanol were added to 100 µL of competent ArcticExpress cell and mixed every 2 min during 10 min. 25 ng of pET21-peIB-VHH-16 plasmid were added and the reaction was incubated on ice for 30 min. Thereafter, the reaction tube was incubated at 42 °C for 20 sec, and then on ice for 2 min, followed by an addition of 900 µL of preheated (42 °C) SOC medium to the reaction tube and incubation of the mixture for 1 hour at 37 °C, with agitation at 250 rpm. Finally, 200 µL of the reaction mix were spread onto an LB agar plate containing 100 µg/mL ampicillin.

2.4.1.2 Induction and expression of the anti-GFP nanobody

To express the nanobody clone VHH16 (pET21-peIB-VHH 16), 1L LB + 100 µg/ml amp was inoculated with 10 mL of an overnight culture (LB + 100 µg/ml amp + 20 µg/ml gentamicin that contained the selected clone). This culture was incubated at 37 °C until it reached an OD_{600} around 0.4 to 0.5 and was then transferred to 12°C until it reached an OD_{600} around 0.6 to 0.7. Thereafter, the expression was induced through addition of 0.5 mM IPTG. The culture was grown for ~ 20 h at 12 °C. IPTG concentration was determined by testing different concentrations and verifying the nanobody expression by coomassie staining gel and western blot.

A periplasmic preparation purification protocol was performed next day. Cells were harvested for 20 min, 4000 rpm at 4 °C, resuspended in TES buffer and incubated on ice for 30 min. The solution was spun down at 6000xg for 10 min, and the supernantant obtained centrifuged again at 48 000xg for 15 min. The resulting supernantant was incubated with 2 mL of His-Selected resin (Sigma cat. No. H0537) per liter of starter culture at 4 °C for 30 min with, 0.3 M NaCl and 20 mM imidazole. The sample was then passed over a column for binding, washed once with 6 column volumes high-salt buffer, and once with 2 column volumes low-salt buffer. The elution was carried out with 4 column volumes elution buffer, and the sample was dialyzed against PBS using 3,500 k MWCO tubing. Finally, the sample was concentrated using a 3 k MWCO centrifugal filter, and concentration was determined by Nanodrop measurement.

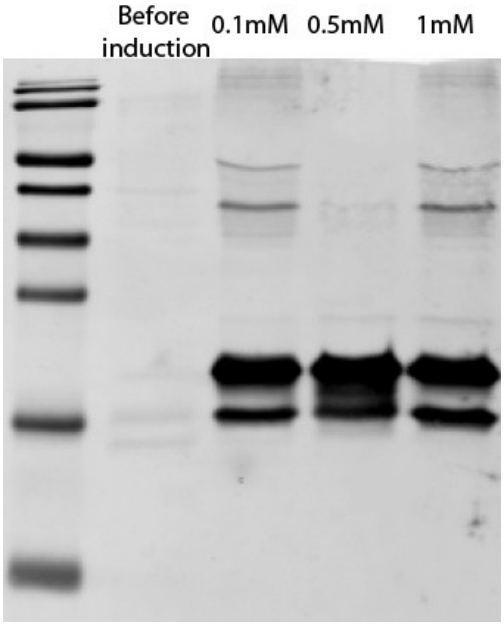

Figure 2.1: Testing different IPTG concentration in order to induce anti-GFP nanobody VHH-16

Cells containing pET21-peIB-VHH-16 plasmid were grow at 37°C in 1L LB + 100µg/ml amp until they reached an OD of 0.4-0.5. Then, cultures were transferred to 12°C until they reached an OD of 0.6-0.7. Thereafter, the induction was made by adding 0.1 mM, or 0.5 mM or 1 mM of IPTG and cultures were incubated for about 20 hours at 12°C.

2.4.2 Transformation of competent E.coli DH5-α cells

Competent *E.coli* DH5-α cells were used to amplify plasmids. On ice, 30 µL of competent cells were mixed with ~300 ng of plasmid, or with no plasmid as negative control. Samples were incubated on ice for 30 min. Thereafter, samples were heat shocked at 42 °C for 30 sec, and 900 µL pre-warmed LB medium was added immediately. Samples were then incubated 1 h at 37 °C and shaken at 650 rpms. After the incubation time, cells were centrifuged for 1 min at 13000 rpms, and the supernatant removed. Cells were resuspended in 100 µL of pre-warmed LB medium and spread onto appropriate plates. Plates were incubated upside-down at 37 °C for about 16 h.

2.5 Yeast techniques

2.5.1 Yeast strains

Table VII: Yeast strains used in this study

Name	Background	Genotype	Source
CML476a	-	*MAT*a *ura3-52 leu2Δ1 his3Δ200 GAL2 CMVp(tetR'-SSN6)::LEU2 trp1::tTA*	[81]
W303	-	*MAT*a : *leu2-3,112 trp1-1 can1-100 ura3-1 ade2-1 his3-11,15*	[82]
Noc1p-GFP	BY4741	*MAT*a his3-1 leu20 met150 ura30 *YDR060W-GPF-His3MX6*	[47]
Noc1p-GFP/Gar1p-mCherry	BY4741	*MAT*a his3-1 leu20 met150 ura30 *YDR060W-GPF-His3MX6 YHR089C-mCherry-KanMX6*	This study
Noc2p-GFP	W303	*MAT*a : *leu2-3,112 trp1-1 can1-100 ura3-1 ade2-1 his3-11,15 YOR206W-GFP-His*	Invitrogen
Noc2p-GFP/Gar1p-mCherry	W303	*MAT*a : *leu2-3,112 trp1-1 can1-100 ura3-1 ade2-1 his3-11,15 YOR206W-GFP-His5 YHR089C-mCherry-KanMX6*	This study
Noc3p-GFP	BY4741	*MAT*a his3Δ1 leu2Δ 00 LYS2 met15Δ ura3Δ *YLR002C-GFP-His3*	[31]
GFP-Noc3p	Offspring and isogenic of BSY420	*MAT*a, *ade2, can1, leu2, ura3, his3, trp1, noc3Δ::HIS3 + pNOPGFPIL-NOC3* (*ARS/CEN LEU2 GFP-NOC3*)	[47]
Rix7p-GFP/Ssf1p-TAP	DS1-2b	MATα his3-Δ200 leu2-Δ1 trp1-Δ63 ura3-52 SSF1-TAP::TRP1 RIX7-GFP::HIS3MX4	[45]
Rpl11p-GFP	W303	*MAT*a *leu2-3,112 trp1-1 can1-100 ura3-1 ade2-1 his3-11,15 YGR085C-GFP-His5*	[83]
pMET-NOC2/Noc1p-GFP/Gar1p-mCherry	W303	*MAT*a *leu2-3,112 trp1-1 can1-100 ura3-1 ade2-1 his3-11,15 ClonNAT-MET25::3XHA-YOR206W YDR00W-GPF-His3MX6 YHR089C-mCherry-KanMX6*	This study
pMET-NOC2/Rix7p-GFP/Gar1p-mCherry	W303	*MAT*a : *leu2-3,112 trp1-1 can1-100 ura3-1 ade2-1 his3-11,15 ClonNAT-MET25::3XHA-YOR206W* RIX7-GFP::HIS3MX4 *YHR089C-mCherry-KanMX6*	This study
pMET-NOC2/Noc3p-GFP/Gar1p-mCherry	W303	*MAT*a : *leu2-3,112 trp1-1 can1-100 ura3-1 ade2-1 his3-11,15 ClonNAT-MET25::3XHA-YOR206W YLR002C-GFP-His3 YHR089C-mCherry-KanMX6*	This study
pMET-NOC2/Rpl11p-GFP	W303	*MAT*a : *leu2-3,112 trp1-1 can1-100 ura3-1 ade2-1 his3-11,15 ClonNAT-MET25::3XHA-YOR206W YGR085C-GFP-His5*	This study

2.5.2 Yeast transformation and selection of positive clones

Yeast strains were transformed using the lithium acetate method [84, 85]. Yeast cells were first grown in media, selected based on strain background and selective marker, until they reached an $O.D_{600}$ between ~0.6 and 0.8. To prepare competent cells, yeast cells are washed four times with ddH_2O and spun down at 3000 rpm for 2 min. Thereafter, cells were washed three times with Tris/EDTA/LithiumAcetate (TELiAc) buffer and resuspended in 500 µL TELiAc buffer. For the transformation, 50 µL of cells were mixed with 5 µL of carrier DNA, 300 µL PEG3500 and 10 µL of PCR product, or 10 µL water for a negative control. These samples were incubated, shaking, at 30 °C for 30 min. After incubation, the cells were heatshocked at 42 °C for 15 min. Prior to plating, cells were spun down, the TELiAc buffer removed, and cells resuspended in 100 µL of 1X TE. Cells were finally plated on selective plates and incubated at 30 °C for 2 days.

- For MET promoter insertions, cells were plated on SD-MET plates and incubated at 30 °C for 2 days. 24 h later, colonies were replica-plated onto SD-MET + CloNAT and incubated at 30 °C for ~2 days.
- For GFP-tagging, cells were plated on SD-HIS plate and incubated at 30 °C for 2 days.
- For mCherry-tagging, cells were plated on YPD + G418 (200 µg/mL) and incubated at 30 °C for 2 days. 24 h later, colonies were replica-plated onto YPD + G418 (600 µg/mL) and incubated at 30 °C for about 2 days.

2.5.3 Serial dilution spot test

Yeast cells were grown in SD-MET media in a shaking incubator at 30 °C overnight. Next day, the O.D was measured to calculate the amount of cells required for a sample of an OD_{600} of 0.1. This first sample is used as the undiluted sample. Serial dilutions were made by mixing 100 µL of the previous dilution with 900 µL of sterile ddH_2O. Each dilution was then spotted by pipetting on either a SD-MET plate, as permissive media, or on YPD + 5 mM Methionine plate as repressive media. Plates were incubated 2 days at 30 °C.

2.5.4 Growth curves of genes under the control of a MET25 promoter

Strains under the control of an inducible MET25 promoter were grown in 250 mL of permissive media (SD-MET) until they reached an OD_{600} between 0.2 and 0.6. At time 0, an amount of culture required for a dilution to an OD_{600} ~0.2 was collected and spun down at 3000 rpms for 2 min at 4 °C. Yeast cells were washed twice with ddH_2O and resuspended in 250 mL repressive media (SD Complete + 5 mM Met) to obtain an OD_{600} of ~0.2. This dilution step is repeated for every time point thereafter to ensure that cultures do not exit log phase growth. For every time point, the OD_{600} before and after the dilution was measured and a graph of the relative OD_{600} against time was plotted by calculating the dilution factor ($DF_{tp} = DO_{600(before)} / DO_{600(after)}$), the cumulative dilution factor ($DF_{cum} = DF_{tp} \times DF_{cum(previous)}$) and the relative OD ($OD_{600} = DF_{cum} \times OD_{600}$ after dilution). The standard deviation of time points that were collected at least 3 times was calculated.

Moreover, for every time point, two separate culture volumes equivalent to 10 ODs were taken for western blot and qRT-PCR analysis; both samples were washed with water, spun and the cell pellets stored at -80 °C. In addition, 5 ODs of culture were taken for a Psoralen experiment (Section 2.6.6). Finally, 10 mL were taken for microscopic analysis (Section 2.9).

2.5.5 Nuclear transport arrest by metabolic poisoning

This experiment has been carried out according to Shulga et al. 1996 [78]. 500 mL of yeast culture were first grow in permissive media (depending on the strain) to an OD_{600} of ~0.8. Thereafter, 20 ODs were taken as the "non-poison sample" for western blot analysis and qRT-PCR. The remaining culture was washed twice with water containing 10 mM of both sodium azide and 2-deoxy-d-glucose. Then, cells were spun down at 4000xg for 5 min at 4 °C, resuspended in 500 mL of glucose-free media containing 10mM deoxy-d-glucose and 10 mM sodium azide, and incubated shaking at 30 °C. After 30 min and 1 hour incubations, 20 ODs were spun down for each time-point at 4000 rpms for 5 min, and the pellets were washed ice-cold once with ddH_2O/10 mM deoxy-d-glucose/10 mM sodium azide as the "30 min

poison sample" and "1 hour poison sample". The remainder of the culture was then resuspended in fresh permissive media and incubated at 30°C for 1 hour. 20 ODs were spin down at 4000 rpms 5 min and pellet was washed ice-cold with ddH_2O as "Re-induction sample". For every time-point and sample, 10 mL were also collected for microscopic analysis.

2.5.6 Harvesting of yeast cells and cryogenic cell lysis

Cell cultures were grown to ~ $3.0x10^7$ cell/mL and spun down at 4000xg for 5 min, 4 °C. Cells were washed twice in 50 mL ice-cold ddH_2O and spun down at 2600xg for 5 minutes, 4 °C. Thereafter, pellet was resuspended in an isovolume of ice-cold resuspension buffer and spun down at 2600xg for 15 min, 4 °C. The buffer was removed and the pellet spun down again at 2600xg for 15 min to ensure the entire buffer is removed prior to cryo-freexing. To make 'cryo-noodles', pellet was placed into a 10 mL syringe and presses into 50 mL Falcon tube filled with and cooled with liquid nitrogen. Finally, the liquid nitrogen is decanted, and the noodles stored at -80 °C or immediately subjected to cryo-lysis.

To cryo-lyse cells, frozen noodles were placed into a pre-chilled stainless steel grinding jar with pre-chilled stainless steel balls (20 mm diameter). By using PM100 Planetary Ball Mill (Retch) grinding was carried out over 8 cycles of 400 rpms, 3 min forward and 1 min reverse rotation, with no break between rotations. Between each cycle, the jar was removed and cooled in liquid nitrogen. After 8 cycles were completed, the yeast powder was removed using a pre-chilled spatula, and frozen cells grindate was stored at -80 °C.

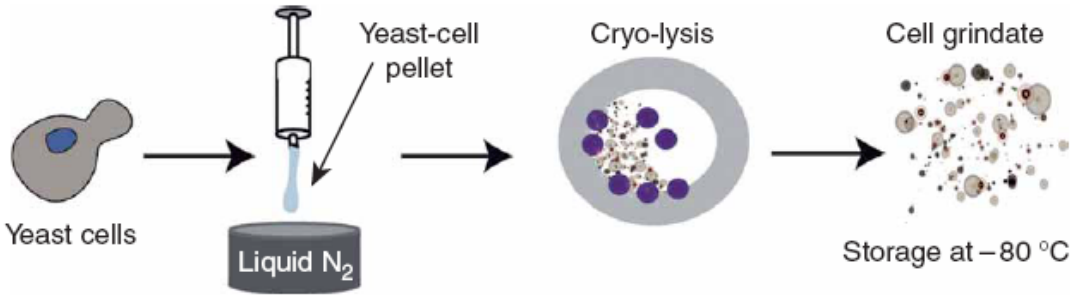

Figure 2.2. Schematic outline of harvesting cells and cryo-lysis protocol. [82]

2.6 DNA techniques

2.6.1 Plasmid purification

Plasmids were purified using the Wizard® *Plus* SV Minipreps DNA purification system from Promega and following the manufacturer's protocol. Plasmid -transformed *E.coli* DH5-α cells were first selected on plates by antibiotic, and grown o/n in selective liquid media. Next day, about 5 mL of the culture was spun down, and the pellet thoroughly resuspended in 250 µL of cell Resuspension Solution. Thereafter, 250 µL of Cell Lysis Solution were added and the sample mixed 4 times. 10 µL of Alkaline Protease Solution was added, the sample mixed 4 times and incubated at RT for 5 min. 350µL of Neutralization Solution was added, the sample mixed 4 times and centrifuged at RT for 10 min at maximum speed. The resulting cleared lysate was decanted into a Spin column supplied with the kit, and the sample washed once with 750 µL and once with 250 µL of Wash solution. The mixture was then centrifuged at maximum speed for 2 min and the flow-through discarded. Finally, 100 µL of Nuclease-Free water was added to the spin column, and the plasmid collected by centrifugation at RT for 1 min at maximum speed.

Plasmid was quantified by Nanodrop and visualized on a 0.5 % agarose gel using GelRed^{TM} (Biotium). The plasmid stock was stored at -20 °C.

2.6.2 Chromosomal DNA extraction from yeast cells

Cells were taken from plates and grown over night in 2 mL appropriate liquid media. Thereafter, ~2.5 OD_s of cells were spun down, resuspended in 200 µL breaking buffer, and then vortexed at maximum speed for 3 min. with 200 µL phenol/chloroform/isoamyl alcohol and 200 µL glass beads. 200 µL of 1X TE was then added to the mix, the sample vortexed briefly and centrifuged for 5 min at maximum speed. The top aqueous layer was transferred into a new tube and 1mL 100 % EtOH added. The solution was mixed by inversion and centrifuged for 10 min at maximum speed. The supernatant was removed and 500 µL 70 % EtOH was added. The sample was spun down 3 min at maximum speed, supernatant

removed, and the pellet air-dried. The DNA pellet was finally resuspended in 50 µL ddH_2O and quantified by Nanodrop. The chromosomal DNA was stored at -20 °C.

A final concentration of 250 ng/µL was used for control PCRs, and 100 ng/µL was used for cassette amplification.

2.6.3 Polymerase Chain Reaction

By using plasmids (Table V) or chromosomal DNA extracted from yeast strains (Table VII) as template in combination with specific primers (Table VIII), selected cassettes were amplified by Polymerase Chain Reaction (PCR). PCR elongation times were determined based on the size of the cassette to be inserted and its sequence.

Table VIII: Primers used in this study for strains construction.

Name	Segment not identical to the target sequence	Segment identical to the target sequence	Matrix DNA
5' pMET-NOC2 insertion	ATTTTTGAATTGTAAGAGAGATAGAGAA GGTCAACAATAGAATAAGTGGAGAT	CGTACGCTGCAGGT CGAC	pYM-N36
3' pMET-NOC2 insertion	AGTATGCTTCAAATGCTTCGATTGAAACT TCTTGGTCGATTTAGAAACTTTACC	CATCGATGAATTCTC TGTCG	pYM-N36
5' Control primer pMET-NOC2 insertion	-	AGATTCAACATTCCC GCATAT	chromosomal DNA form pMET-NOC2 strain
3' Control primer pMET-NOC2 insertion	-	TTCCTGATCAGTTTT GTTGCC	chromosomal DNA form pMET-NOC2 strain
5' Gar1-mCherry tagging	TCATTTAGAGGAGGATCTCGTGGCGGATC TCGTGGTGGTTTCAGAGGAGGTAGAAGA	CGGATCCCCGGGTT AATTAA	pFA6a-mCherry KanMX6
3' Gar1-mCherry tagging	GTGCTTCGGCAGATATAGTAAGTTGGAAG AAATGAAGAATTGTGAAAGATAAAGGAT	GAATTCGAGCTCGT TTAAAC	pFA6a-mCherry KanMX6
5' Control Primer Gar1-mCherry	-	GGTGGTAGTTCTTTC AGAGGA	chromosomal DNA from Gar1-mCherry strain
3' Control Primer Gar1-mCherry	-	ATAGTATACAGAAC AAACGGT	chromosomal DNA from Gar1-mCherry strain
5' Noc1-GFP cassette insertion	-	AAGTACAGCCTCTC ATGGAACAAT	chromosomal DNA from Noc1-GFP strain
3' Noc1-GFP cassette insertion	-	TAATCCTCTTAGGGT AAACAGGTG	chromosomal DNA from Noc1-GFP strain
5' Noc3-GFP cassette insertion	-	AGAATTCAACATTT TCTGAGAGGA	chromosomal DNA from Noc3-GFP strain
3' Noc3-GFP cassette insertion	-	AATAATAGCGCTTT TTCACTGAGG	chromosomal DNA from Noc3-GFP strain
5' Rix7-GFP cassette insertion	-	AATACCAAGTATCG TTTGAGTTCG	chromosomal DNA from Rix7-GFP/Ssf1-TAP strain
3' Rix7-GFP cassette insertion	-	GAGAAGACTCACTA GAGGTGAAAT	chromosomal DNA from Rix7-GFP/Ssf1-TAP strain
5' Rpl11-GFP cassette insertion	-	TTATTGTATTTTGCC CTCTCCTCA	chromosomal DNA from Rpl11-GFP strain
3' Rpl11-GFP cassette insertion	-	TTGTAATGGTTCCCT TGTTTTTGG	chromosomal DNA from Rpl11-GFP strain

PCR reaction mix used for MET25 promoter insertion and C-terminal mCherry tagging had the following final concentrations: 1X iProof buffer, 0.5pmol/µL of 5' and 3' primers, 200 µM of each dNTP, 2% DMSO, 1 ng/µL plasmid, 0.25 U/µL iProof Taq.

PCR program: MET25 promoter insertion [80]:

1 cycle: 97 °C for 4 min

10 cycles: 97 °C for 1 min, 54 °C for 30 sec, 72 °C for 1 min 30 sec

20 cycles: 97 °C for 1 min, 54 °C for 30 sec, 72 °C for 1 min 30 sec, and additional time of 10 sec/cycle

4 °C, forever

PCR program: C-terminal mCherry tagging

1 cycle: 94 °C for 5 min

30 cycles: 94 °C for 30 sec, 51 °C for 30 sec, 72 °C for 1 min 30 sec

1 cycle: 72 °C 10 min

4 °C, forever

PCR reaction mix used for testing for positive MET25 promoter cassette insertion had the following final concentrations: 1X iProof buffer, 0.5 pmol/μL of 5' and 3' primers, 200 μM of each dNTP, 2% DMSO, 1 μL of Chromosomal DNA extracted, 0.25 U/μL Taq.

PCR program: Control PCR for testing MET25 promoter insertion and mCherry tagging:

1 cycle: 94 °C for 5 min

30 cycles: 94 °C for 30 sec, 48 °C for 30 sec, 68 °C for 2 min 50

1 cycle: 68 °C for 10 min

4 °C, forever

PCR reaction mix used for GFP-tag cassette insertion as the AccuTaq™ LA DNA Polymerase procedure.

GFP-tag cassette insertion:

1 cycle: 98 °C for 30 sec

30 cycles : 96 °C for 15 sec, 55 °C for 20 sec, 68 °C for 4 min

1 cycle: 68 °C for 10 min

4 °C, forever

2.6.4 Phenol/chloroform/IAA DNA wash

Prior to transformation into yeast cells, PCR products were extracted and cleaned. To this aim, 350 µL of ddH_2O were added to the PCR reaction, followed by 400 µL of phenol/chloroform/IAA (Sigma). The mix was then vortexed for 30 sec and spun at maximum speed for 2 min. The resulting aqueous (top) phase (~300 µL) was taken off and mixed with 30 µL of a 3 M NaOAc pH 5.2 solution, 900 µL of 100% EtOH and 3 µL of glycogen solution (10 mg/µL). Thereafter, the sample was incubated at -80 °C for 30 min or o/n, then centrifuged for 10 min at 4 °C at maximum speed. The supernatant was discarded and the pellet washed with 500 µL of 70 % EtOH. Finally, the pellet was air-dried and resuspended in 11 µL of ddH_2O.

1 µL of purified PCR product was visualized on a 1% agarose gel, and 10 µL were used for transformation into yeast cells.

2.6.5 Agarose gel

DNA fragments were usually run on a 0.8%-1% agarose gel that contained 1X GelRed™ (Biotium). Samples were separated in 1X TBE and a voltage of 130 V.

2.6.6 Psoralen experiment

Psoralen experiments were carried out according to Griesenbeck et al., 2012 [86] with the following modifications:

Formaldehyde fixation and isolation of nuclei:

Cells were grown to ~ 0.5-0.7 $O.D_{600}$ and were not expressing the MNase fusion protein.

The *Chromatin endogenous cleavage* was omitted since composition of rDNA chromatin by using target protein fused with MNase was not studied.

Agarose gel electrophoresis and southern blotting:

DNA samples were separated for 6 h instead of 8 h.

Probe preparation, membrane hybridization, washing and membrane stripping:

DNA-labeling was performed once by following RadPrime DNA Labeling system (Invitrogen) and once by PCR according to Sambrook, J. and Russell D. W. (2006) [87], modified as follows:

PCR reaction:

5.0 µL 10X LA Taq buffer

10 mM dCTP, dGTP, dTTP

0.2324 mM dATP

2 µL of 25 pmol/µL 3474 primer

2 µL of 25 pmol/µL 3475 primer

9 ng pNOY373

50 µCi [α-^{32}P]dATP

0.25 µL LA taq DNA polymerase

H_2O to 50 µL

PCR program

1 cycle: 95 °C for 2 min 30 sec

30 cycles: 95 °C for 45 sec, 52 °C for 30 sec, 72 °C for 4 min

1 cycle: 72 °C for 1 min

4 °C, forever

Table IX: Primers for preparation of radio-labeled probes

Name	Sequence	Matrix DNA
3474 [15]	AAACGGCTACCACATCCAAG	pNOY373
3475 [15]	GTGGTGTCTGATGAGCGTGT	pNOY373

2.7 RNA techniques

2.7.1 RNA extraction [88]

About 15 ODs were spun down, resuspended in 500 µL Trizol (Invitrogen) and ~ 200 µL glass beads (DEPC treated, 0.4-0.5 mm diameter, Sigma), and vortex 20 min at maximum speed at 4 °C. Thereafter, the sample was incubated for 5 min at 65°C followed by 5 min at RT. The sample was spun down quickly, and 200 µL chloroform was added. The sample was then vortexed for 15 sec at maximum speed, and incubated for 3 min at RT. The sample was centrifuged for 15 min at 4 °C at maximum speed, and the top aqueous phase was transferred into a new tube. 500 µL isopropanol was added and the sample incubated for 10 min at RT. Thereafter, the sample was centrifuged for 15 min at 4 °C at maximum speed and the pellet then resuspended in 1 mL 70% EtOH and centrifuged again for 5 min at 4 °C, maximum speed. After air-drying the pellet, it was resuspended in 25 µL DEPC water. The RNA concentration was measures by Nanodrop and the RNA stored at -80 °C.

2.7.2 RNA Purification

Prior to qRT-PCR analysis, RNAs that were previously isolated by Trizol extraction were purified using a RNeasy® Mini Kit (QIAGEN) following the manufacturer's instruction.

2.7.3 Reverse transcription

In order to generate cDNA and perform qRT-PCR analysis, first-strand cDNA synthesis protocol was carried out according to the Invitrogen handbook; 100 ng of random

hexamers from Operon were mixed with 1 µg of RNA and 10 mM of each dNTP up to a final volume of 13 µL. This mixture was heated to 65 °C for 5 min and then quickly chilled on ice. Thereafter, 4 µL of 5X first-strand buffer and 2 µL of 0.1M DTT were added and the mixture incubated at 25 °C for 2 min. 200U of SuperScript™ II RT (Invitrogen) were added to the mixture, and it was once again incubated at 25 °C for 10 min. Finally, the sample was incubated at 42 °C for 50 min followed by 15 min incubation at 70 °C to inactivate the reaction.

For each RNA sample, a negative control was performed by adding dH_2O instead of SuperScript™ II RT.

2.7.4 qRT-PCR

Testing primers efficiency

In order to study specific gene expression, specific primers sets were required to discriminate genes from each other. To this aim, primers were designed by using NCBI/Primer-BLAST, where primers melting temperatures were selected close to 60 °C and the generated PCR products selected to be between 90 bps to 175 nucleotides in length.

Table X: Primers used in this study for qRT-PCR

Name	Sequence
5' Noc1	TTGGAAGTGCTTTCCCACGA
3' Noc1	TTCCTGCTCTGGTTGGTTGG
5' Noc2	GCGATTCAAAAGATGGCCCC
3' Noc2	TGCGACTTGACAATGGACGA
5' Noc3	GAGGTCCGTAAGGCTTTGCT
3' Noc3	AGCCCATCGACGAATTTGGA
5' Rix7	GAGGTGTTCTGTTGCATGGC
3' Rix7	CGCTTTCCCCAGACATACCA
5' H2b	AAGAAGCCAGCTGCCAAGAA
3' H2b	CAGTGTCTGGGTGAGTTTGC
5' H3	CGCTCAAGATTTCAAGACCGAC
3' H3	AGCGTGAATAGCAGCCAGAT
5' Hhf1	GCCAAGCGTCACAGAAAGATT
3' Hhf1	CGCTTGACACCACCTCTTCT
5' Nop7	CAAGGGCTCTACTGCACCAA
3' Nop7	CCCTACCCAAAGCCCTTGTT
5' Ssf1	ACAGTGCCGAATTTGCATCG
3' Ssf1	ACCGGTGTTCTTTGGGACTT
5'Ssf2	TCTCAAACTTCGCTGTCGCA
3'Ssf2	ACGTGGAGTTGGTTGCGAAT
5' Actine	ATGGTCGGTATGGGTCAAAA
3'Actine	TCCATATCGTCCCAGTTGGT
5' TDH3	CGGTAGATACGCTGGTGAAGTTTC
3' TDH3	TGGAAGATGGAGCAGTGATAACAAC
5' Ubc6	GATACTTGGCCTCCTGGCTGGTCTGTCTC
3' Ubc6	AAAGGGTCTTCTGTTTCATCACCTGTATTTGC
PolyT18	TTTTTTTTTTTTTTTTTT

Prior to qRT-PCR analysis, cDNA samples (from time 0) and negative control samples (from time 0) (Section 2.7.3) were used to test primer efficiency. First, 10 µL of these cDNA samples were mixed in parallel with 40 µL dH_2O. Then, 30 µL of these mixes were kept as a stock, and 20 µL once again diluted with 60 µL H_2O. These dilutions were considered the 'dilution 1'. Only for the positive cDNA sample (time 0), dilution 1 was further serial diluted to obtain dilutions 1/10, 1/100, 1/1000 and 1/10 000. Primers set were then tested by PCR in

96-well format using ViiA7. Primers sets were tested in duplicate for each positive cDNA dilution and for the negative cDNA 'dilution 1' in a 96 well-plate. Each PCR reaction contained 3 µL cDNA, 5 µL SYBR Select Master Mix (2X, from Applied Biosystems), 0.3 µL of each specific primer (10 µM working stock) and 1.4 µL of dH_2O. The PCR was followed by a melting curve analysis.

PCR program

1 cycle: 50 °C for 2 min

1 cycle: 95 °C for 2 min

40 cycles: 95 °C for 15 sec, 60 °C for 1 min

Figure 2.3 shows an example of qRT-PCR melting and standard curves obtained for a primer set, which target NOC2 mRNA. Indeed, melting curve analysis of each primer set showed that primers recognized only one gene, and are thus specific. In fact, each primer set showed the same T_m for every cDNA dilution of specific primer sets. Moreover, threshold PCR cycle values (C_T) were linearly correlated to the level of specific targeted cDNA and visualized in the standard curve. The slope value, the regression coefficient (R^2) and the amplification efficiency (Eff%) were checked for each primer set, to be sure about their efficiency. The slope and the Eff% values indicate the PCR amplification efficiency, where a slope of -32 indicates optimal 100% PCR amplification efficiency. In addition, R^2 indicates the closeness of fit between the standard curve regression line and the individual C_T values from standard reaction. Indeed, a R^2 value of 1.00 suggests a perfect fit.

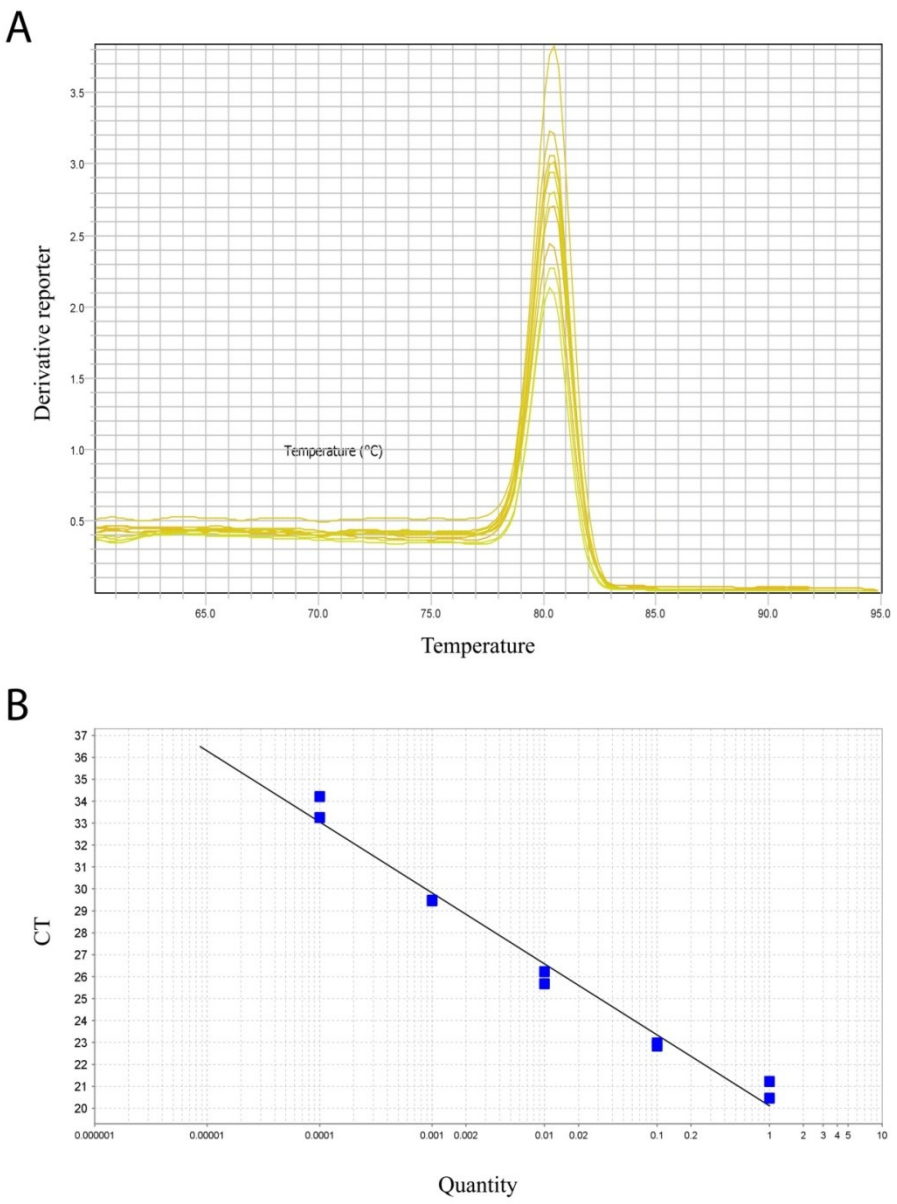

Figure 2.3. NOC2 qRT-PCR melting and standard curves using to test primers sets.

A) Melting curves showing Tm of NOC2 primer set. Tm values are between 80.265 and 10.462 °C. B) Standard curve of NOC2 primer set. Slope = -3.234 Eff% = 103.805 R^2 = 0.98 Y-inter = 20.114.

qRT-PCR

mRNA samples were normalized against ACT1, UBC6 and TDH3 [89]. For growth curve samples, mRNA levels at time 0 were assigned a value of 1, and detection of mRNA level changes at time 14 were compared to this value. For nuclear transport arrest samples, mRNA levels in normal condition (Before) were assigned a value of 1, and detection of mRNA level changes for "Poisoned mRNA" and "Re-induction mRNA" were compared to this value.

PCR program

1 cycle: 50 °C for 2 min

1 cycle: 95 °C for 2 min

40 cycle : 95 °C for 15 sec, 60 °C for 1min

2.8 Protein techniques

2.8.1 Preparation of yeast extracts for protein gel electrophoresis

Whole cell lysis

2 mL of yeast culture was spun down, the cell pellet resuspended in 240 µL lysis solution and then incubated on ice for 10 min. 240 µL of 50% TCA was added and the mixture incubated on ice for 10 min. The samples where then spun down at top speed, 4 °C for 10 min, and resuspended in 500 µL cold acetone. The mix was incubated at -20 °C for at least 20 min. Thereafter, the samples were spun down at top speed, 4 °C for 10 min and the acetone was aspirated. The pellet was finally resuspended in solution A, sonicated in a water bath for 10 min before solution B was added in an equal volume. Samples were incubated at 95 °C for 10 min prior to loading on an SDS gel.

Kushnirov post-alkaline whole protein extraction [90]

5 ODs of yeast cells were pelleted and resuspended in 100 µL H_2O and 100 µL 0.2M NaOH. Samples were incubated 5 min at RT and spun down at 3000 rpms for 1 min. Pellets were resuspended in 50 µL of modified Laemmli SDS sample buffer, incubated at 95 °C for 3 min and spun down quickly prior to loading on an SDS gel.

2.8.2 Polyacrylamide electrophoresis

Precast gel (CLEARPAGE^{TM}):

Tris-Glycine SDS ClearPAGE^{TM} (4-20%) precast gradient gels from C.B.S scientific company were used for separating proteins prior to visualization of separated proteins by sliver staining. The gel was run for 40 min in 1X MES buffer at 175 V.

Tris-glycine gel:

To test the expression of specifically tagged proteins or to test the efficiency of an affinity purification experiment, BioRad's Mini Protean's system was used to make Tris-glycine homemade gels. An 8% resolving gel (10 mL) was composed of 4.6 mL ddH_2O, 2.7 mL 30% acrylamide mix, 0.1 mL 10% SDS, 2.5 mL 1.5M Tris-HCl pH 8.8, 100 µL 10% ammonium persulfate and 6 µL TEMED. The 5% Stacking gel (5 mL) was composed of 3.4 mL dH_2O, 0.83 mL 30% acrylamide mix, 0.05 mL 10% SDS, 0.63 mL 1M Tris-HCl pH 6.8, 50 µL 10% ammonium persulfate and 5 µL TEMED. The gel was run in 1X Tris-Glycine at 120 V until the loading dye front reached the bottom of the gel.

2.8.3 Single-step affinity purification [82]

Conjugation of recombinant anti-GFP antibody to Dynabeads

The appropriate amount of Dynabeads was first resuspended in 0.1 M $NaP0_4$, pH 7.4 (60 µL per mg of beads) in a 15 mL falcon tube and shaken slowly for 10 min on a Nutator or rocking platform. The buffer was quickly aspirated by placing the tube into a magnetic rack until all beads were attached to the magnet. This wash step was repeated once again but

without the 10 min incubation. Thereafter, 2 mL of AB mix per 100 mg of beads were added to the beads and the mixture incubated on a rotating wheel at 30°C for at least 18 h but no more than 24 h.

The next day, the beads were vigorously washed to remove unbound antibody. For 100mg of beads, 4 mL of 100 mM Glycine HCl pH 2.5 were used for the first wash, 4 mL of 10 mM Tris pH 8.8 for the second wash, and 4 ml of fresh 100 mM Triethylamine for the third wash. For every wash, the tube was placed into a magnet rack and buffer aspired once all beads were attached against the magnet. Next, beads were washed 4 times for 5 min with 1X PBS, followed by 5 min and then 15 min with 1X PBS + 0,5% Triton X-100 and incubated on a Nutator or rocking platform. Finally, the beads were resuspended at a final concentration of 15 µg of beads per µL of solution (1X PBS/0.02% NaN_3/50% Glycerol) and stored at -20 °C.

Purifying RNP by single-step affinity purification technique

Yeast cryo-grindate was first weighed out into Falcon tubes chilled in liquid nitrogen (0.2g-0.5g depending on abundance of protein of interest), and Dynabeads (25 µL beads/0.5g cell powder) were pre-washed 3 times with extraction buffer. When the yeast grindate had thawed slightly, 4.5 mL extraction buffer/0.5g cell powder was added to the powder and the mixture vortexed for 30 sec. After, a hand polytron (7 mm probe) was used for 1 min to homogenize the lysate, and then the lysate was spun down at 3500 rpms for 10 min. Following that, the supernantant and conjugated Dynabeads were mixed together and incubated for 30 min at 4 °C, rotating. After binding, the tube was placed into a magnetic rack until the solution was cleared of the magnetic beads, and the supernatant was aspirated carefully. Beads were then washed quickly 4 times with 1 mL extraction buffer by pipetting, and once for 5 min with Last Wash Buffer. Finally, beads were eluted twice with 500 µL of elution buffer (Ingredients) for 20 min each time, at room temperature on Nutator. Eluates were pooled, and then isolated protein complexes were lyophilized in a speedvac overnight.

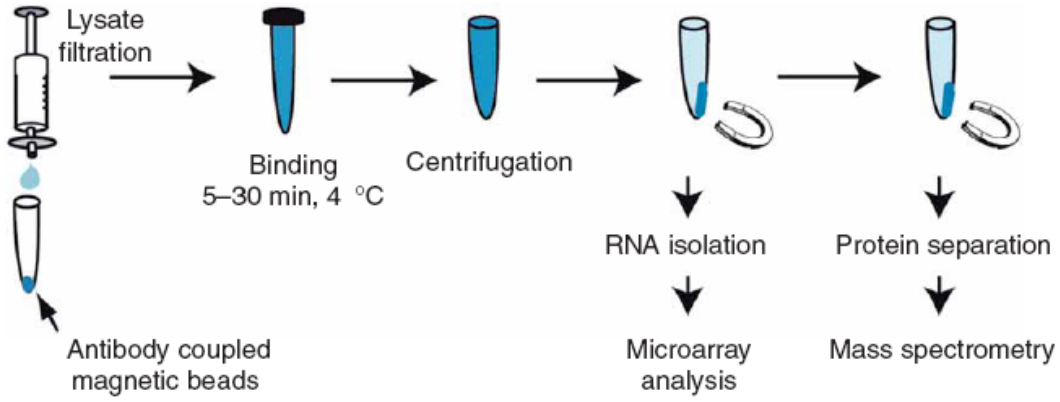

Figure 2.4. Schematic outline of the single-step purification technique. [82]

2.8.4 Silver staining of polyacrylamide gels

A fast staining protocol was performed by using SiverQuest™ Silver Staining Kit from Invitrogen, following the manufacturer's instructions. Briefly, after electrophoresis, the gel was rinsed with dH_2O, then submerged in 50 mL of fixative buffer (40% EtOH, 10% acetic acid), placed in microwave for 30 sec at maximum power setting, and then agitated at RT for 5 min. The fixative buffer was discarded and the same process was repeated using 30% EtOH. Thereafter, the gel was submerged in 50 mL of sensitizing solution (30% EtOH, 10% Sensitizer, supplied with the kit), placed into microwave for 30 sec at maximum power setting, and then agitated for 2 min at RT. The sensitizing solution was discarded and the same process repeated again twice with dH_2O. The gel was submerged after in 50 mL of staining solution (1% Stainer, supplied with the kit), placed into microwave for 30 sec at maximum power setting, and then agitated for 5 min at RT. The staining solution was discarded and the gel washed briefly with dH_2O. After that, the gel was submerged in 50 mL developing solution (10% Developer, 1 drop developer enhancer, both supplied with the kit), and agitated until the desired band intensity was achieved. 5 mL of Stopper (supplied with the kit) was added to stop the reaction, and the gel agitated at RT for 10 min. Finally, the solution was discarded and the gel washed with dH_2O at RT for 10 min, before visualization on a light box.

2.8.5 Western blotting

Precast gradient gels Tris-glycine (4-20%) were run at 185V for ~ 45 min in 1XMES buffer, and Tris-glycine at 100V for 1 h in Tris-Glycine buffer. Proteins were transferred onto a nitrocellulose membrane in 1X transfer buffer (20% Methanol and 10% 10X transfer buffer). The transfer was run at 4 °C at either 60V/240mA for 2 h, or 30V/120mA overnight. Once finished, the membrane was stained with Amido Black stain to visualize the gel loading. For destaining and preparation for antibody incubation, the membrane was rinsed with distilled water and blocked with 5 % milk in 1X TBST for 1 hour on an orbital shaker at RT. The membrane was then probed with the appropriate antibody (see Table XI) for either 1 h at RT or o/n at 4 °C. the antibody solution was discarded and the membrane was washed three times in 1XTBST prior to either incubation with a secondary antibody in in 1X TBST for 1 h at RT, or detection by Enhanced Chemiluminescence (ECL).

Detection

Membranes were scanned using Odyssey infrared imaging system (LI-COR Biosciences).

For ECL, 2mL Solution A were mixed with 6 μL 3% H_2O_2 and distributed over the entire membrane. The membrane was placed into a page protector and then into a film cassette; the membrane was exposed to film (what kind and from where) and developed in the dark room.

Table XI: List of antibodies used in this project

Antibody	Animal	Provider	Secondary antibody	Method of detection	Concentration used	Diluted in
α-HA	Mouse	Genscript	α-mouse	ECL	1:5000	TBST/milk
α-GFP	Mouse	ROCHE	α-mouse	ECL	1:1000	TBST/milk
α-Nop7	Rabbit	[36]	α-rabbit	Odyssey	1:7500	TBST/milk
α-β-actin	Mouse	Abcam	α-mouse	Odyssey	1:7500	TBST
α-H2B	Rabbit	Ab1790	α-rabbit	Odyssey	1:500	TBST/BSA
α-H4	Rabbit	Archambault Lab	α-rabbit	Odyssey	1:6000	TBST/BSA
α-mouse	Horseradish	GE healthcare	-	ECL	1:10000	TBST/milk
α-mouse Cy600 or Cy800	Llama	LI-COR	-	Odyssey	1:20000	TBST/milk
α-rabbit Cy600 or Cy800	Llama	LI-COR	-	Odyssey	1:10000	TBST/milk

2.9 Microscopy

2.9.1 Cell fixation

Fluorescently-tagged yeast cells were fixed in 4%Paraformaldehyde/100mMKPO_4, pH 7.4/3.4% sucrose and incubated, shaking, at RT for 30 min. Thereafter, cells were washed twice with 500 µL 100 mM KPi/Sorbitol, once with 200 µL KPi/Sorbitol/1% Triton for 2 min at RT, and twice more with 200 µL KPi/Sorbitol. Glass coverslips were flashed briefly over a flame and then placed into a "humid chamber". 0.1 mg/mL polylysine was spotted onto the coverslips, and left for 5 min. The polylysine was removed, and 50 µL of were spotted onto polylysin-coated coverslips and incubated for 10 min at RT and for 15 min in the humid chamber to adhere. Finally, 5 µL of Vectashield (Vector Laboratories Inc.) were added, the coverslip was mounted upside-down onto a glass slide and the edges sealed with clear nail polish.

2.9.2 Fluorescent microscopy

The fluorescently tagged proteins were visualized using a 100X objective on an inverted Fluorescence Microscope (Leica DM5500B); images were analyzed and put together using Adobe Creative Suite 6.

3 Results

Part 1: The effect of Noc2p depletion on early steps of 60S ribosome biogenesis

3.1 Studying the dynamic influence of Noc2p

The Noc proteins have been mostly studied at the beginning of 2000 and gave one of the first hints towards a potential spatio-temporal dynamic of ribosome biogenesis. In fact, mass spectrometry analyzes revealed that Noc1p and Noc2p form a heterodimeric complex at early stage during ribosome maturation, whereas Noc2p and Noc3p form such a complex at a later stage. Moreover, it has been shown by using *ts* mutants of the three proteins and fluorescent microscopy that the localization of Noc1p and Noc2p depends on the functionality of all the Noc proteins and that pre-60S particle transport is also linked to the functionality of all these proteins. Recently, it has been shown that under heat-shock conditions, many gene expression pathways are altered and ribosome biogenesis is, however briefly, switched off [75, 76]. Since almost all studies on the dynamic aspect of the Noc proteins have been obtained by using *ts* mutants and temperature shifts, it raises some questions about the reliability of the conclusions of these studies. In addition, these analyzes showed only a static picture of the Noc-complex exchange, due to a lack in number of time points taken after the temperature shift. Hence, the Noc proteins have been re-examined using an inducible/repressible promoter system in this study.

More precisely, only the influence of Noc2p depletion on the localization of Noc1p and Noc3p, their protein levels and their gene expression has been tested. In addition to the Noc proteins, Rix7 localization, its protein level and its gene expression have been studied under the depletion of Noc2p. It has been shown that all Noc proteins are involved in an overlapping step where Rix7p, an AAA-ATPase suggested to be involved in a particle rearrangement step during ribosome maturation, is also present. As Noc2p is the intermediate between these two complexes, a link between Noc2p and Rix7p has been examined. Despite knowing approximately at which stage Noc1-Noc2 and Noc2-Noc3 heterodimers are part of the 60S pre-ribosome, the exchange between Noc proteins and its mechanism is still completely undefined.

3.1.1 Strain construction

Synthesis of eukaryotic ribosomes has mostly been studied in the yeast *Saccharomyces cerevisiae* due to its easy experimental accessibility by biochemical and genetic methods. In *S. cerevisiae*, the NOC2 gene is located on chromosome XV and its expression is essential for cell growth [47]. Thus, study of this gene functionality has been made possible by generating a haploid yeast strain in which the expression of the NOC2 gene was placed under the control of the regulatable promoter.

In yeast, there are many choices for endogenous regulated promoter systems. The widely-used *GAL1* promoter, which is active in the presence of galactose and repressed by the addition of glucose, was not selected due to its tendency for overexpression and the possibility that changes in carbon source could cause undeterminable pleiotropic affects [77]. Three different regulatable promoters ($TetO_2$, $TetO_7$ and MET25) were tested instead in order to find the best system.

$TetO_2$ and $TetO_7$ promoters can be repressed by the presence of tetracycline (or its analog doxycycline), and contain two and seven tetracyclin operator binding sites, respectively [77, 81]. Thus under TetO expression control, a gene is known to be expressed in the absence of the antibiotic and to be not expressed in its presence [77, 81]. In order to use these TetO promoters, the haploid yeast strain CML476a, which contains a tetracycline transactivator (tTA) and a deficiency of KanMx4 marker, needed to be used as background strain [81]. However, due to its alterations, the strain has a very low basal growth rate. Moreover, as a high concentration of doxycycline was required for complete shutdown of NOC2 gene expression, experiments using the TetO promoters were found to be costly.

Efficiency of another promoter derived from genes encoding O-acetyl homoserine sulphydrylase, MET25, was tested in the same way as the TetO promoters [91]. The MET25 promoter is methionine-repressed, in the sense that a gene under the control of this promoter is expressed in the absence of methionine in the cell culture media (permissive media), and expression is repressed in the presence of methionine (repressive media) [91]. Compared to the TetO promoters, switching media from permissive to restrictive media was neither difficult

nor expensive, which is an advantage for long growth curves experiment, that can last up to 48 h during which methionine needs to be replenished within the medium. In addition, using W303 as the background strain to put NOC2 under to control of the MET25 promoter (PMet-Noc2), was again an advantage, as the basal growth rate of this strain was closer to what is normally expected in *S. cerevisiae* (~90 min). Therefore, the MET25 promoter was chosen for this study. Finally, an N-terminal HA epitope tag (3kDa) was also integrated into the cassette, which allowed the visualization of Noc2p levels by Western blot analysis [80].

The purpose of regulating NOC2 gene expression was to determine the effect on Noc1p, Noc3p and Rix7p. Combination strains have been created in W303 as the background strain, in each of which the NOC2 gene was placed under the control of the MET25 promoter. In addition, Gar1p was tagged with the fluorescent mCherry on its C-terminus to determine the structure of the nucleolus in these cells. As previously mentioned, Gar1p is part of box H/ACA snoRNPs, known to be exclusively located to the nucleolus in their steady state [23]. Hence, Gar1p has been chosen as a nucleolar marker for microscopy. Moreover, Noc1p, Noc3p and Rix7p have been GFP-tagged on their C-terminus and expressed from their endogenous promoter. In summary, these three different strains contained PMet-Noc2, Gar1-mCherry, and Noc1-GFP, Noc3-GFP or Rix7-GFP. In each of the strains, integration and functionality of the promoter and epitope cassettes were tested by PCR, Western blot and microscopic analyzes. In addition to these, another strain expressing methionine-repressible NOC2 as well as Gar1-mCherry and GFP-tagged Rpl11p was specifically constructed for ribosomal subunit export studies.

Besides efficient promoter integration, it was also crucial to test methionine sensitivity for each positive clone obtained to ensure efficient Noc2p depletion. Because the NOC2 gene is known to be essential for cell growth, it was simple to test its depletion by i) serial dilution of the strains on both permissive and restrictive media, and ii) by determining the cell growth in liquid [47]. For all strains in which the NOC2 gene had been placed under the control of the MET25 promoter, growth phenotypes looked closely like that of W303 in permissive media, showing that the promoter insertion is not affecting basal cell growth (Figure 3.1 A and C, Left pannel). Once in restrictive media, growth rate of these strains was strongly affected compared to wild-type, suggesting effective promoter repression (Figure 3.1 A and C, Right

pannel). However, increasing the amount of methionine from 2.5 mM to 5 mM in restrictive media was chosen due to a lower promoter sensitivity result obtained in a first spot test experiment (data not shown). Four different strains not containing the MET25 promoter but Noc1p, Noc3p, Rix7p or Rpl11p tagged with GFP have been used as control strains, and were also tested for their methionine sensitivity (Figure 3.1 B). Because some of these strains are derived from other background strains such as BY4741 and DS1-2b, their growth phenotype in permissive media differed slightly from W303. However, their growth rates in restrictive media resembled the growth rate of their respective P_{Met}-Noc2 strain in permissive media very closely. Finally, these strains were used as control for microscopy and Western blot analysis, but W303 wild-type was used for comparison of growth rates during growth curve experiments.

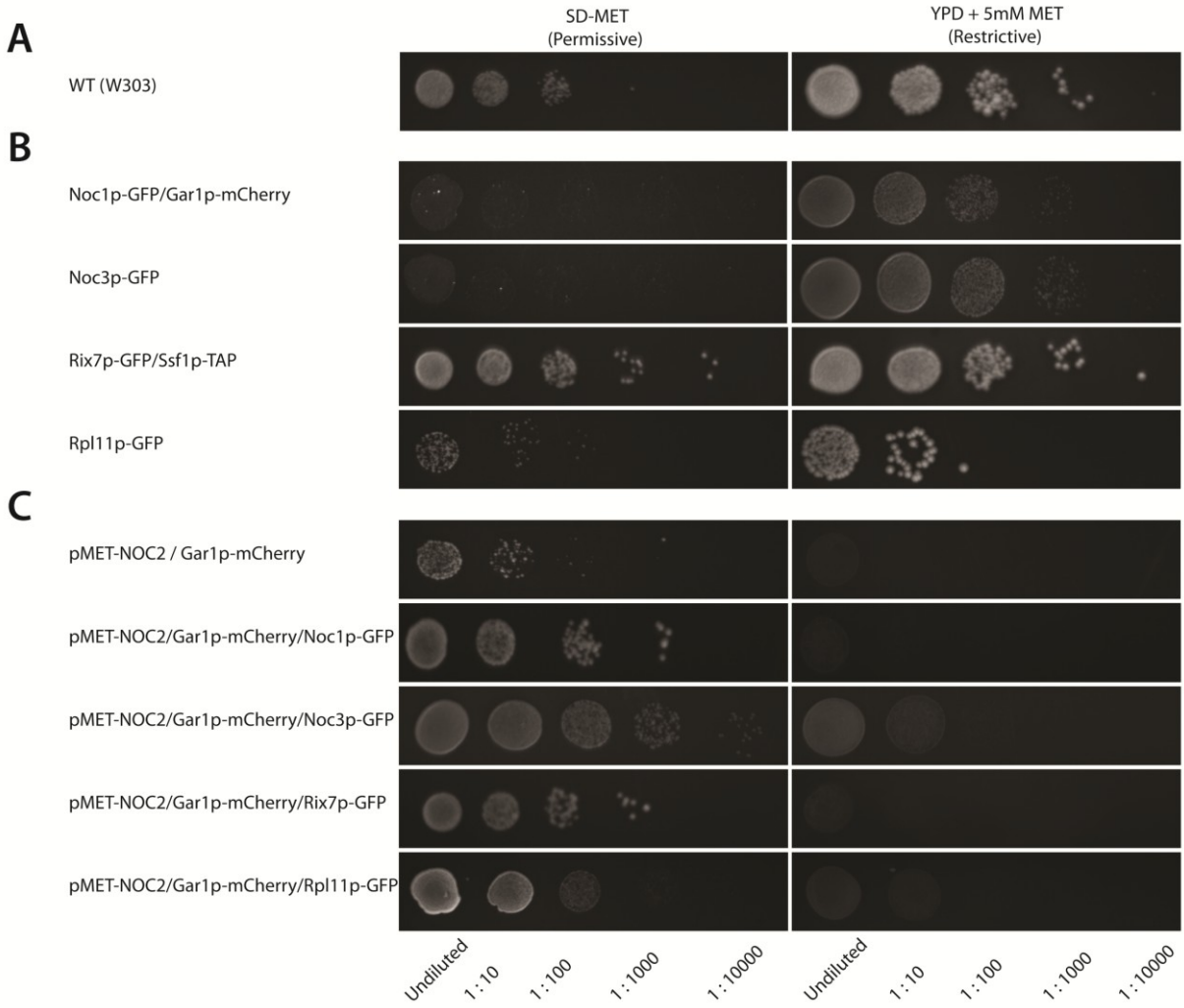

Figure 3.1. Testing MET25 promoter sensitivity and efficiency by spot test analysis.

Cells were grown o/n and an OD_{600} of 0.1 has been taken to make serial dilution on both SD-MET plate (permissive media) and YPD + 5mM MET (repressive media). Plates were incubated 2 days at 30 °C.

A) Background strain W303 used to create the five combination strains in the panel C. **B)** Four different strains used as control during growth curves analyzes and poison experiments. **C)** Combination strains used to test Noc2p influence.

3.1.2 Growth curves experiment

In order to look at the effect of Noc2p depletion on Noc1p, Noc3p and Rix7p in a dynamic fashion, independent growth curves have been performed. All PMet-NOC2 and the control strains derivative of W303 have been grown in liquid permissive media (SD-MET)

until they reached an OD_{600} of ~0.6, and were then diluted in repressive media (SD Complete + 5 mM MET) to obtain an OD_{600} of ~0.2. However, cells were washed twice with water before the dilution to make sure that all the permissive media was removed. Control strains that were not a derivative of W303, cells were grown in SD Complete media until they reached an OD_{600} of ~0.6, were washed twice with water and diluted into repressive media (SD Complete + 5 mM MET) to obtain an OD_{600} of ~ 0.2. Usually, cells were then diluted with fresh restrictive media to an OD_{600} of about 0.25-0.35 at every time point during the growth curve experiment in order to keep cells at in a logarithmic growth phase.

For the PMet-Noc2/Gar1-mCherry/Noc1-GFP and PMet-Noc2/Gar1-mCherry/Rix7-GFP strains, three independent growth curves have been performed, where the first one has been done over 20 h, and the second and third one over 60 h. More precisely, the second and the third growth curves followed the cell growth from time 0 to time 25 h, and samples for further experiments were taken at these time points. After 25 h, the cells appeared to be strongly affected by Noc2p depletion and were growing very slowly (doubling time of ~4.6 hours). Because it was unfeasible to continue diluting the cultures, for the second growth curve experiment cells were left to grow in restrictive media from 25 to 60 h after the shift to repressive conditions, without refreshing the media. Microscopy and western blot analyzes of these experiments will be discussed. In contrast, for the third growth curve experiment, restrictive media was refreshed every 4-5 h without diluting the cells, between 25 to 60 h after the shift. Microscopy, western blot and qRT-PCR analyzes of these growth curves will also be discussed. In comparison, doubling times between 0 to 25 h after the shift were nearly identical for all growth curves, with only marginal variations. However, in the second experiment cells were found to grow somewhat better than then those from the third experiment at 60 h after the shift (data not shown). At this point, the amount of methionine present in the repressing media needs to be considered for the continued depletion of Noc2p. Because cells have been growing in the same restrictive media for up to 35 h during the second experiment, while continuing to be in an exponential growth phase, it is likely that the level of methionine in the repressive media decreased to the point of being considered more like permissive media. NOC2 expression could have reinitiated, which could account for these differences in doubling time.

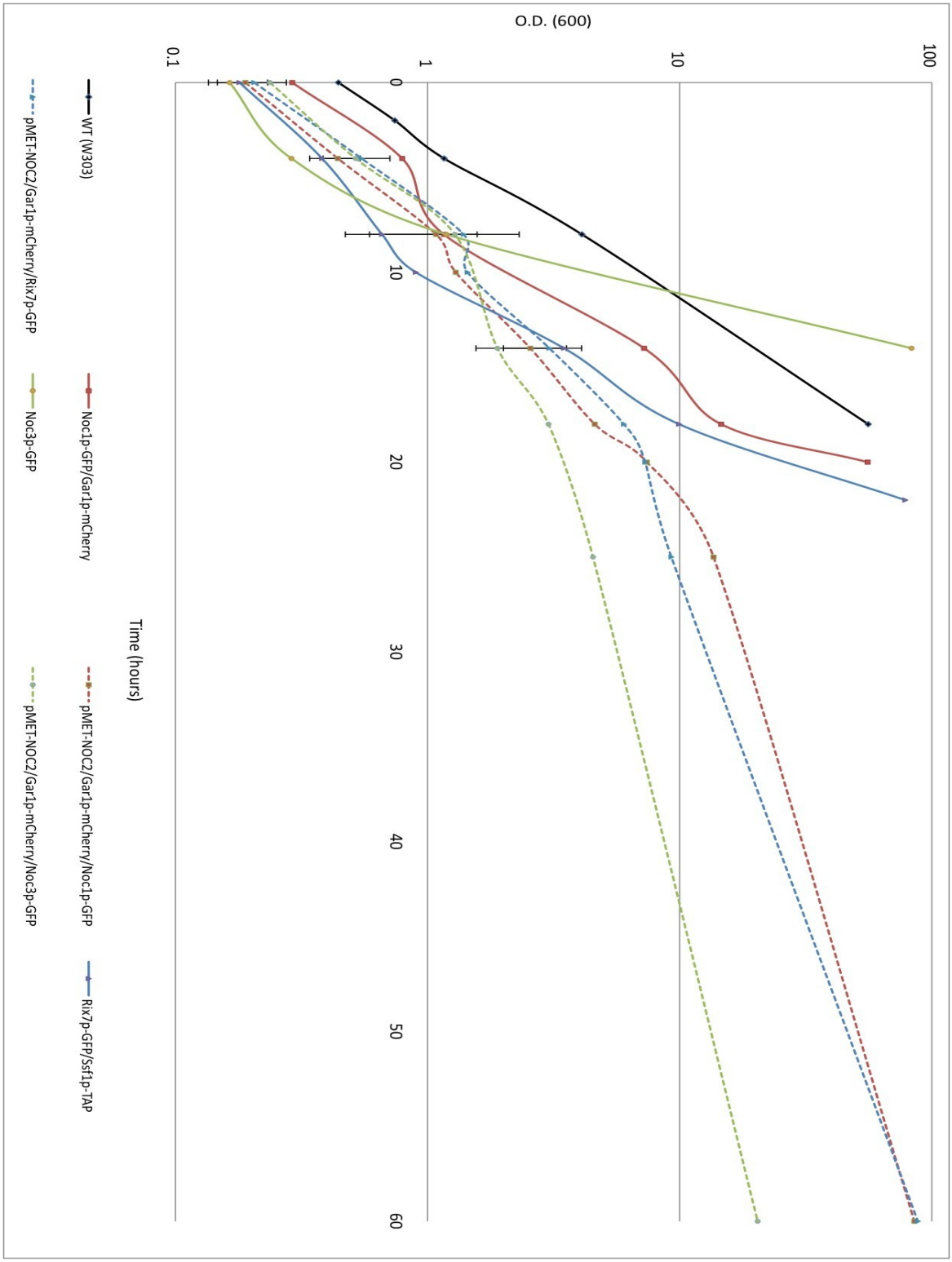
O.D. (600)
100
10
1
0.1
0
10
20
30
40
50
60
Time (hours)
WT (W303)
Noc1p-GFP/Gar1p-mCherry
pMET-NOC2/Gar1p-mCherry/Noc1p-GFP
Rix7p-GFP/Ssf1p-TAP
pMET-NOC2/Gar1p-mCherry/Rix7p-GFP
Noc3p-GFP
pMET-NOC2/Gar1p-mCherry/Noc3p-GFP

Figure 3.2. Noc2p depletion using a repressible MET25 promoter affects cell growth rate.

Cells were switched from permissive to restrictive media (time 0) and diluted at every time point. Here is a graph showing growth curves of the relative OD_{600} against time for every strain tested. The dotted lines indicate P_{Met}-Noc2-HA strains, and solid lines control strains (legend indicating lines colors related to strains names below the graph). Growth curves are the results of the means of every time point data from time 0 to 25 h that were performed independently more than one time. Standard deviations of time points that have been performed at least three times, have been calculated. For P_{Met}-Noc2-HA/Gar1-mCherry/Noc1-GFP and For P_{Met}-Noc2-HA/Gar1-mCherry/Rix7-GFP strains, time 60 h is the results of the third growth curves, where the restrictive media has been refreshed.

For the P_{Met}-Noc2/Gar1-mCherry/Noc3-GFP strain, only one growth curve experiment could be performed, where cells were diluted at every time point from time 0 to 25 h and repressive media has been refreshed every 4-5 h between 25 to 60 h after the shift, without diluting the cells.

Wild-type W303 and other respective control strains have also been used for growth curve analysis. However, their growth rates were so much faster than that of the P_{Met}-Noc2 strains that it has been difficult to perform a long experiment. In fact, it has been a manipulation problem in the sense that these strains required more dilution steps to allow cells to remain in an exponential phase. It has been difficult to match their dilution steps with their appropriate P_{Met}-Noc2 strain and to space it out in a way of good manipulating. Growth curves analyses of these strains have been stopped earlier (14-20 h).

Growth rates of every P_{Met}-Noc2 strains have been compared with the growth rate of W303 and even the appropriate control strains. As shown in Figure 3.2, the cell population of W303 has increased by more than 100 cell ODs in 18 hours. In contrast, the cell populations of P_{Met}-Noc2/Gar1-mCherry/Noc1-GFP and P_{Met}-Noc2/Gar1-mCherry/Rix7-GFP have only increased by ~10 ODs in 18 hours, and even less than 10 ODs for P_{M}et-Noc2/Gar1-mCherry/Noc3-GFP. The growth rate of these P_{Met}-Noc2 strains tends to slow down and no longer follow the original doubling time observed between 0 to 18 h after the shift. Although it has not been possible to dilute cultures between 25 and 60 h after shift to repressive media due to the extremely slow doubling times, the cell population continued to increase to a small

extent. Taken together, the detected growth phenotypes show the essential role of Noc2p for cell growth, however, it also demonstrates that it is not essential for cell viability as cells continue to divide, albeit slowly. This last phenotype could be also due to incomplete repression of the MET promoter and further analyses will need to be done.

Samples for subsequent experiments to look at the effect of Noc2p depletion on cell localization, protein level and expression of Noc1p, Noc3p and Rix7p were taken for almost every time point. The results are discussed throughout the next sections.

3.1.2.1 Noc protein localization affected by Noc2p depletion

Reconsidering Noc2p influence on Noc1p and Noc3p localization

As previously mentioned, the three Noc proteins were shown to each distinctly localize within cells. Noc1p localizes to the nucleolus, visible by a crescent-like signal and by colocalization with the nucleolar maker Nop1p [47, 54]. By contrast, Noc3p was shown to be distributed to ~40% in the nucleolus and to ~60% in the nucleoplasm [47]. Noc2p was shown to have a more intermediate distribution between the early nucleolar Noc1p and the late nuclear Noc3p, with ~60% nucleolar and ~40% nucleoplasmic [47]. This localization concurs with mass spectrometric data that shows Noc2p to form two complexes, Noc1p-Noc2p and Noc2p-Noc3p [47]. Influence of Noc2p function on the two other Noc proteins has already been tested by using *noc2-1 ts* mutant [47]. It has been shown that after shifting cells from 23 °C to 37 °C for 6 h, Noc1p was redistributed through the entire nucleoplasm, whereas Noc3p localization showed no significant change (Figure 1.10), suggesting that Noc1p needs to form a complex with Noc2p for its normal distribution [47]. However, *ts* mutants and temperature shifts are now reconsidering since heat-shock can altered gene expression pathways and ribosome biogenesis [75, 76]. For this reason, fluorescent microscopy analyses were performed on samples taken from our growth curve experiments, and the effect of Noc2p depletion using the MET25 promoter on Noc1p and Noc3p localization was determined. In addition, different from previous studies, strains used here also contained Gar1-mCherry as a nucleolar marker. Moreover, the effect has been looked at in a dynamic manner over time, in the sense that several samples were taken over 60 h following Noc2 depletion, instead of 6 h

using *ts* mutants. Effects on Noc1p and Noc3p localization have been visualized by fluorescent microscopy and results are shown and discuss separately in the following paragraphs.

In permissive media, in the presence of Noc2p, Noc1p was present in a crescent-like shape within the nucleus, representing the nucleolus, where it colocalized with the nucleolar marker Gar1-mCherry (Figure 3.3 A, time 0). This result is consistent with previous data were colocalization with the nucleolar marker Nop1p showed Noc1p to be a nucleolar protein [47, 54]. As mentioned, growth curve experiments using P_{Met}-Noc2/Gar1-mCherry/Noc1-GFP were performed by diluting the culture at each time point between 0 to 25 h after the shift to restrictive media, in order to keep the cells in a logarithmic growth phase, and to refresh the repressive media. As expected from previous data (Figure 1.10), Noc1p diffused all over the nucleus 14 h after the shift (Figure 3.3 A). However, by looking at Gar1-mCherry localization, a surprising and interesting phenotype could be observed; in the absence of Noc2p, we observed that Gar1-mCherry also diffused throughout the entire nucleus and its signal finally overlapped with the DAPI stained nucleoplasmic region, in the same manner as was observed for Noc1-GFP. Gar1p , as core component of H/ACA snoRNPs, is known to associate with pre-rRNA co-transcriptionally in the nucleolus [23]. The diffused localization of Gar1-mCherry raises several questions with regards to the redistribution of Noc1p throughout the nucleoplasm in the absence of Noc2p.

Interestingly, down-regulation of pre-rRNA transcription in a *ts* mutant of the Pol I transcription factor Rrnp3p, *rrn3-8*, exhibited the same phenotype, and Noc1p and the nucleolar marker Nop1p have been shown to present an intra-nuclear redistribution in the *rrn3-8* mutant, where both colocalized and overlapped significantly with the DAPI stained nucleoplasmic region [54]. The authors of this study proposed that the intra-nuclear redistribution is caused to putative changes in the nucleolus structure due to inhibition of Pol I transcription [54]. Moreover, the same phenotype has been visualized with another, later nucleolar protein, Nop7p, suggesting that problems in rDNA transcription have consequences for nucleolar structural and all nucleolar proteins, resulting in their re-distribution [54]. While previous data suggested that the Noc proteins exhibit a dynamic intranuclear distribution due to a potential shuttling between the nucleolus and the nucleoplasm [47], our results suggest a

different possibility. Given that the intra-nuclear redistribution of both Noc1p and Gar1p is a consequence of Noc2p depletion, it is possible that Noc2 has an important role for nucleolar integrity. Interestingly, a similar suggestion has been made for the human homolog of Noc2p, NIR, which will be discussed in more detail in part 4 of result.

Compared to previous localization analyses of Noc proteins, our growth curve experiment covered a much longer timeframe, allowing for observation of Noc1p localization even after 25 and 60 hours in repressive media. We observed that at 25 h of depletion, Noc1p seemed to be relocalized throughout the entire cell (Figure 3.3 A, time 25). In fact, Noc1p continued to colocalized with Gar1p in the nucleus, but was also present in the cytoplasm, while Gar1p was not. Curiously, we also observed some lighter foci in the cytoplasm possibly suggesting that Noc1p may be degraded [92, 93]. In addition, we observed an even stronger Noc1-GFP diffusion into the cytoplasm after 60 h, when the culture had been refreshed with restrictive media between 25 to 60 h after the shift (Figure 3.3 B). In these cells, the GFP signal was less defined and it was more difficult to detect. Interestingly, in these cells, even the cell structure seemed affected, which could also be due to the very slow growth rate. At this point, depletion of Noc2p seemed to cause a strong effect on Noc1p localization, nucleolar integrity, and cell structure overall.

In contrast, samples obtained after 60 h after shift to repressive media from cultures where cells have been left to grow without refreshing of methionine, showed a completely reverse phenotype. Noc1-GFP and Gar1-mCherry colocalized in a crescent-like distribution, which suggests nucleolar localization. Moreover, cell structure and the DAPI distribution appeared that observed in cells 0 to 10 h after the shift (Figure 3.3 A and C). We hypothesize that a significant amount of methionine that was present at time 25 h, was metabolized by the cells during the following 35 h, and therefore NOC2 was no longer repressed, but its expression gradually re-induced. Because samples between time 25 and 60 h have not been taken due to the low cell count, we have no clear picture of when and how gradually NOC2 expression may have resumed. However, we can conclude from these data points that Noc1p relocalization and perturbation of the nucleolar integrity is a reversible phenotype. We can further conclude that Noc2p is required for the intra-nuclear redistribution of Noc1 and that the NOC2 re-expression permits normal relocation of both Noc1p and Gar1p. However, it

remains to be determined if this is due to the interaction of Noc2p with Noc1p, or a different, unknown function of Noc2p that allows the restructuring of the nucleus.

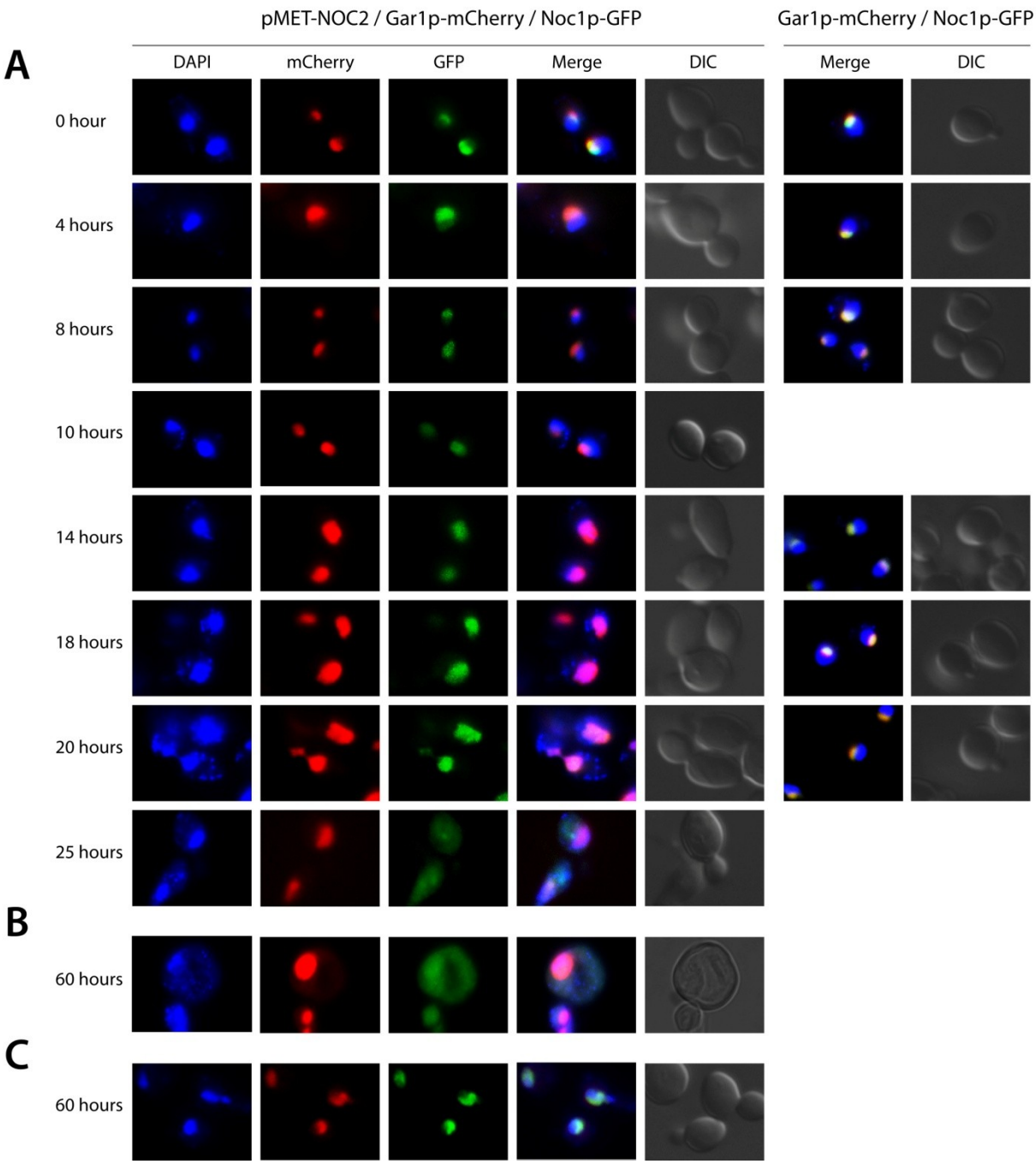

Figure 3.3. Noc1p and Gar1p are redistributed in cells in the absence of Noc2p.

A) The most representative samples taken from three different growth curves for P_{MET}/Gar1-mCherry/ Noc1-GFP and one growth curve for Noc1-GFP/Gar1-mCherry as control. **B)** Sample taken from the third growth curve, where restrictive media has been refreshed every 4-5 h from time 25 to 60 h. **C)** Sample taken from second growth curve, where cells have been left in the same restrictive media.

The same type of analysis has been carried out to determine the influence of Noc2p on Noc3p localization. In P_{Met}-Noc2/Gar1-mCherry/Noc3-GFP cells after shifting to repressive media, Noc3p localization was analysed between 0 to 25 h by diluting cells in fresh repressive media, and between 25 to 60 h by refreshing repressive media without diluting cells.

As previously observed, in permissive media, Noc3-GFP was localized throughout the nucleus, but it was enriched in the nucleolus and present at lower concentration in the nucleoplasm (Figure 3.4 time 0) [47]. Moreover, its nucleolar enrichment was confirmed by a strong co-localization with Gar1-mCherry. While previous analyses suggested that absence of Noc2p had no significant impact on Noc3p localization, our results suggested a more important role for Noc2, not only for the localization of both Noc1p and Noc3p, but also for nucleolar integrity. We observed that at early time point after shift to repressive medium and Noc2p depletion (Figure 3.4 time 4 and 8), nucleolar enrichment of Noc3-GFP seemed to be weaker, with a shift of its signal into the nucleoplasm. Hence, our results suggest that there is a relocation of Noc3p to the nucleoplasm upon Noc2p depletion.

Moreover, we examined other samples taken during the Noc2p depletion experiment by microscopy and observed the relocalization of Gar1-mCherry from the nucleolus to the nucleoplasm, similar to what we previously observed in the P_{Me}t-Noc2/Gar1-mCherry/Noc1-GFP strain (Figure 3.4 Time 18 and 25). This shows that this phenotype is not specific to just one strain, perhaps due to genomic manipulation issues, but instead is due to Noc2p depletion in both strains, and that the nucleolar integrity is affected in the absence of Noc2p. Likewise, Noc3p was also diffused throughout the nucleoplasm, colocalizing with Gar1-mCherry and the DAPI stained DNA. Our results suggest that the cellular distribution of Noc3p is dependent on Noc2p, with its absence leading to relocalization of Noc3p. However, it is still unclear if its relocation is due to its inability to form a heterodimer with Noc2p, or intra-nuclear rearrangement and the loss of nucleolar intergrity.

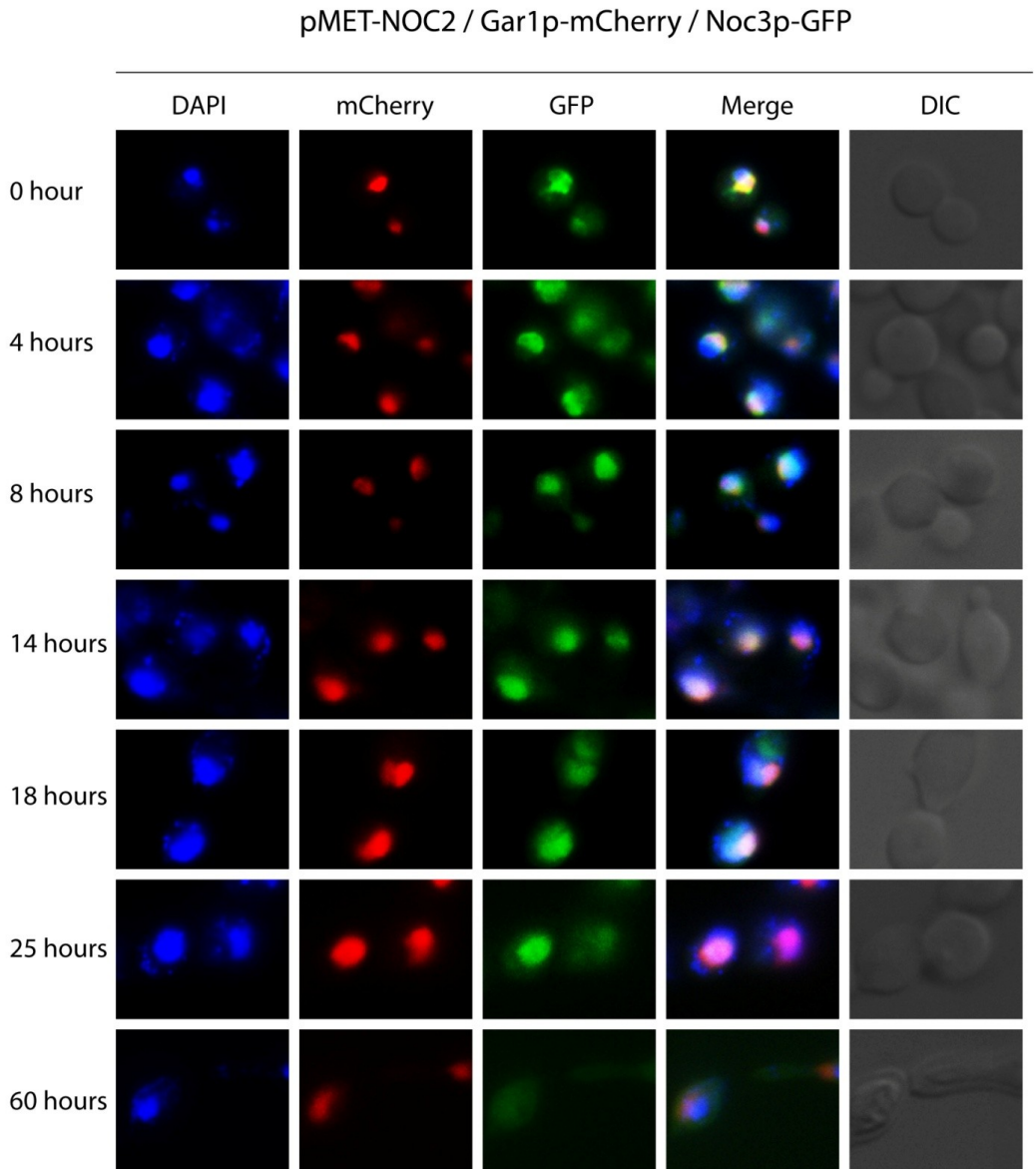

Figure 3.4. Noc3p and Gar1p are redistributed in cells in the absence of Noc2p.

Samples taken from one single growth curve experiment using PMet-Noc2/Gar1-mCherry/Noc3-GFP. Cultures were diluted in repressive media from time 0 to 25 h and restrictive media were refreshed every 4-5 h from time 25 to 60 h without diluting the cells.

Relocation of Noc3-GFP to the cytoplasm was observed at 25 h after shift to restrictive medium. However, its cytoplasmic distribution was not as strong as that observed for Noc1-GFP after 25 h of Noc2p depletion. As there were no samples taken between 25 and 60 h after shift to restrictive medium, we cannot confirm that Noc3p is relocated to the cytoplasm due to

Noc2p depletion. At 60 h, visualization of Noc3-GFP was rather difficult, however, we observed that Noc3-GFP was located throughout the cell and that Gar1-mCherry remained in a nuclear conformation, similar to Noc1p after 60 hours of Noc2p depeltion in strain P_{Met}-Noc2/Gar1-mCherry/Noc1-GFP. This suggests that when they are unable to form a complex with Noc2p, Noc1p and Noc3p are eventually exported to the cytoplasm for degradation.

With respect to these results and comparison to previous data, we suggest that Noc2p affects Noc1p and Noc3p localization, and its absence alters their nuclear distribution, over time leading to their recycling and degradation in the cytoplasm. It is also possible that Noc2p plays an important role in the exchange of Noc1p for Noc3p as well as the removal of Noc3p from pre-60S particles, and that those steps signify important stages along the pre-60S maturation pathway. Our results also highlight the possibility that Noc2p is required for the maintenance of an intact nucleolar structure, suggesting it is more important during ribosome biogenesis than previously thought.

Determining Noc2p influence on Rix7p localization

As previously mentioned, the AAA-ATPase Rix7p has been shown to be involved in removal of Nsa1p from pre-60S particles during ribosome maturation, which coincides with important compositional changes [45]. In fact, Noc1p and other early factors were shown to be present in the pre-60S particle, and to be lost after ATP hydrolysis by Rix7p, whereas some later factors were shown to be enriched at this stage. It is also believed that in this manner the subcomplex, Noc1p-Noc2p, is exchanged for Noc2p-Noc3p, coinciding with Rix7-triggered particle rearrangement. Because Noc2p is the intermediary between these two complexes, the effect of Noc2p depletion on Rix7p localization was tested.

Rix7p intranuclear localization was shown to change depending on the growth conditions and nutrient availability (Figure 1.5) [44]. In our set up, cells were first grown in permissive media until they reached an OD_{600} of ~ 0.6, keeping the culture in an exponential growth phase. In exponential phase, Rix7p is known to have an overall nuclear distribution compared to a nucleolar enrichment in stationary phase [44]. We observed that Rix7-GFP was located throughout the entire nucleus in permissive media, with enrichment in the nucleolus (Figure 3.5 A, time 0). At this point, Rix7p colocalized with the nucleolar marker Gar1-

mCherry and exceeded a little bit with the DAPI-stained nucleoplasmic regions near the nucleolus. This nucleolar enrichment is in agreement with the fact that Rix7p co-isolates with a large amount of nucleolar and intermediate nuclear complexes, such as the Nop7p and Nsa1p particles, but not with the later Rix1p or Arx1p particles (These particles have been discussed in Section 1.5.1 of the Introduction) [45]. However, during early stages of Noc2p depletion in restrictive media, an intranuclear diffusion of Rix7p and Gar1p could be observed, similar to those previously seen in P_{Met}-Noc2/Gar1-mCherry/Noc1-GFP and P_{Met}-Noc2/Gar1-mCherry/Noc3-GFP under Noc2 depletion (Figure 3.5 A, time 8-14). Similar to Noc1p and Noc3p, Rix7p changed its intranuclear distribution from nucleolus to entirely nucleoplasmic, in the same manner as Gar1p and in a Noc2p-dependent fashion. While the exact cause for this change is not known, it can be speculated that Noc2p has an important function for nucleolar integrity and its absence and redistribution of nucleolar structure causes this redistribution of Rix7p, as well as Noc1p and Noc3p from the nucleolus to the nucleoplasm.

During the later stages of Noc2p depletion, a fine cytoplasmic diffusion of Rix7-GFP could be observed (Figure 3.5 A, time 20 and 25). Our results suggest that Rix7p needs the structural integrity of the nucleolus and thus the presence of Noc2p to be localized within the nucleolus. Moreover, Rix7p may not be functional under these conditions and is subsequently exported to the cytoplasm to be degraded. Another possibility could be that it cannot enter into the nucleus after its synthesis in the cytoplasm. Moreover, after 60 hours of Noc2p depletion, we observed a change in the overall cell structure (Figure 3.5 B). At this point, Rix7p exhibited a peri-nuclear distribution. In fact, Rix7p had previously been shown to have a peri-nuclear distribution in cells that were reinduced with fresh media after having been in stationary phase [44]. Because our results were obtained after refreshing the restrictive media every 4-5 hours, new amount of glucose and amino acids could be the source of the effect, although according to optical density measurements, the culture continued to grow exponentially during this time, although slowly.

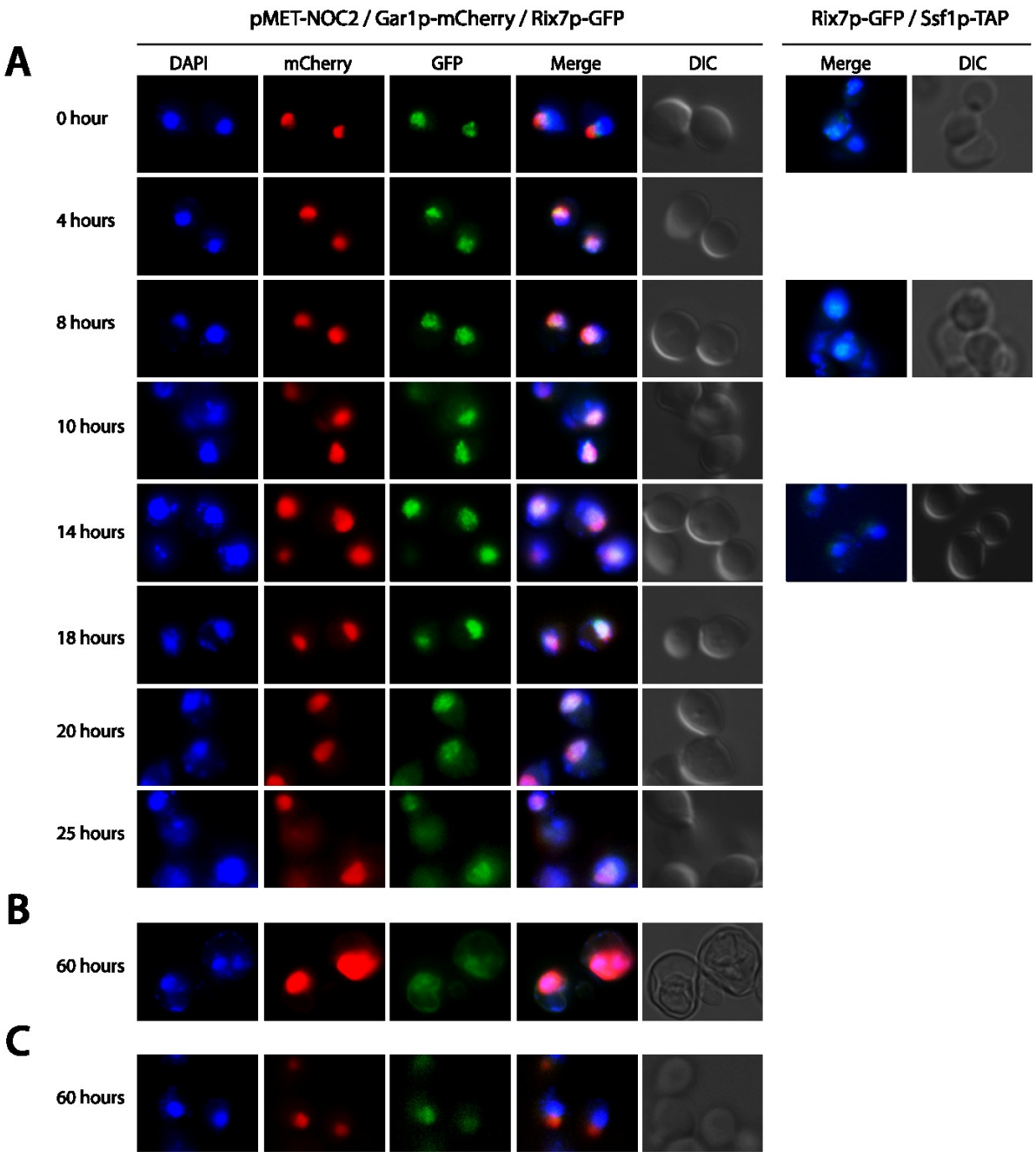

Figure 3.5. Rix7p and Gar1p are redistributed in Noc2p depleted cells.

A) The most representative samples taken from three different growth curves for P_{MET}-NOC2/Gar1-mCherry/Rix7-GFP and one growth curve for Rix7-GFP/Ssf1p-TAP as control. **B)** Samples taken during the third growth curve, where restrictive media has been refreshed every 4-5 hours between 25 to 60 hours after shift to restrictive media. **C)** Samples taken during the second growth curve, where cells have been left to grow in the same restrictive media.

During a second parallel experiment, cells were left in to grow in repressive media without media refreshment between 25 to 60 h after shift to restrictive media. In this case, we observed a relocalization of Rix7p into the nucleus instead of the cytoplasm (Figure 3.5 C). Once again, we believe that the methionine concentration in the repressive media decreased over time so that the methionine promoter, and thus expression of NOC2, was slowly re-induced. This suggests that Rix7p localization and/or function is indeed Noc2p-dependent, and that its inhibition is a reversible process.

In conclusion, Noc1p, Noc3p and Rix7p were observed to redistribute from the nucleolus to the nucleoplasm in a Noc2p-dependent manner. However, we do not know the mechanism of this redistribution and whether their redistribution is due to the relocalization of the individual proteins or of the pre-60S particles containing these proteins. In addition, our data suggest that Noc2p is not simply responsible for the redistribution of these proteins, but rather for the integrity of the nucleolus. Over time, Noc2p depletion causes the relocation (or retention) of Noc1p and Rix7p in the cytoplasm. In the cytoplasm, Noc1p was observed in small foci, suggesting its association with degradation machineries, while Rix7p was more diffused.

In contrast, Noc3p was somewhat diffused in the cytoplasm, but to be more enriched in the nucleus. Moreover, it appeared that the redistribution of Noc1p and Rix7p is a reversible process, as the decrease of methionine and reinduction of NOC2 expression from the methionine-regulated promoter reinstated normal nucleolar Noc1p and Rix7p localization. We would expect the same result for Noc3p localization and this need to be tested. Overall these results suggest that Noc2p is required for normal Noc1p, Noc3p and Rix7p localization. Moreover, our results suggest an important and unexpected role for Noc2p in the maintenance of nucleolar integrity.

3.1.2.2 Effect of Noc2p depletion on total protein levels

Since our microscopy results revealed the diffusion or retention of Noc1p, Noc3p and Rix7 in the cytoplasm upon Noc2p depletion, it is likely that these proteins are degraded. We therefore determined the total cellular proteins levels for Noc1p, Noc3p and Rix7p before and

at different time points after Noc2p depletion. Moreover, we also wanted to determine Noc2p protein levels over time, in order to follow its depletion. Samples were taken during the Noc2p depletion, always collecting the same amount of cells at each time point. In order to look at the different protein levels, western blot analyses were carried out using selected antibodies. Noc2p was visualized using its HA tag, while Noc1-, Noc3- and Rix7-GFP were detected using anti-GFP antibodies. Moreover, actin was used as loading control and H2B and H4 to look at different effects after Noc2p depletion.

By doing western blot analysis of samples collected from the different growth curves experiments processed on the three pMET-NOC2 strains, we were able to associate phenotype visualized by fluorescent microscopy with total protein level. In fact, we observed that Noc2p started to be significantly depleted 8 h after switching the media (Figure 3.6, anti-HA). This is in agreement with microscopy analyses, in which time 0 and time 4 h for all strains represented the wild-type localization of Noc1p or Noc3p or Rix7p. Thereafter, as long as Noc2p was depleted by diluting cells in repressive media and refreshing media with methionine, Noc1p, Noc3p and Rix7p protein levels seemed to be slightly decreased. A stronger decrease of Noc1p and Rix7p than Noc3p was observed, which could also be related to phenotype visualized with fluorescent microscopy. Indeed, Noc1p and Rix7 were found significantly enriched in the cytoplasm after 25 h of Noc2p depletion, which could suggest induction of their degradation pathway, which would be conform with the punctuate pattern of Noc1-GFP throughout the cytoplasm. In contrast, Noc3p levels decreased more slowly, and was still enriched in the nucleus at 25 h in restrictive media. Thus, we hypothesize that Noc1p and Rix7p are potentially degraded in the cytoplasm as an effect of Noc2p depletion, which can be visualize by fluorescent microscopy and by the decrease of total protein level by Western blot analysis. In the case of Noc3p, it is more difficult to speculate on its degradation due to the minor decrease in protein levels and its remaining nuclear localization. We suggest that Noc2p has a weaker influence on Noc3p, potentially due to it having a stronger effect on early stages of pre-60S maturation in the nucleolus and thus nucleolar proteins. More experiments with different nucleolar versus nucleoplasmic ribosome biogenesis factors would be needed to further test this hypothesis. However, in all cases, the decrease protein levels

could also be due to downregulation or degradation of their mRNA, which also remains to be tested.

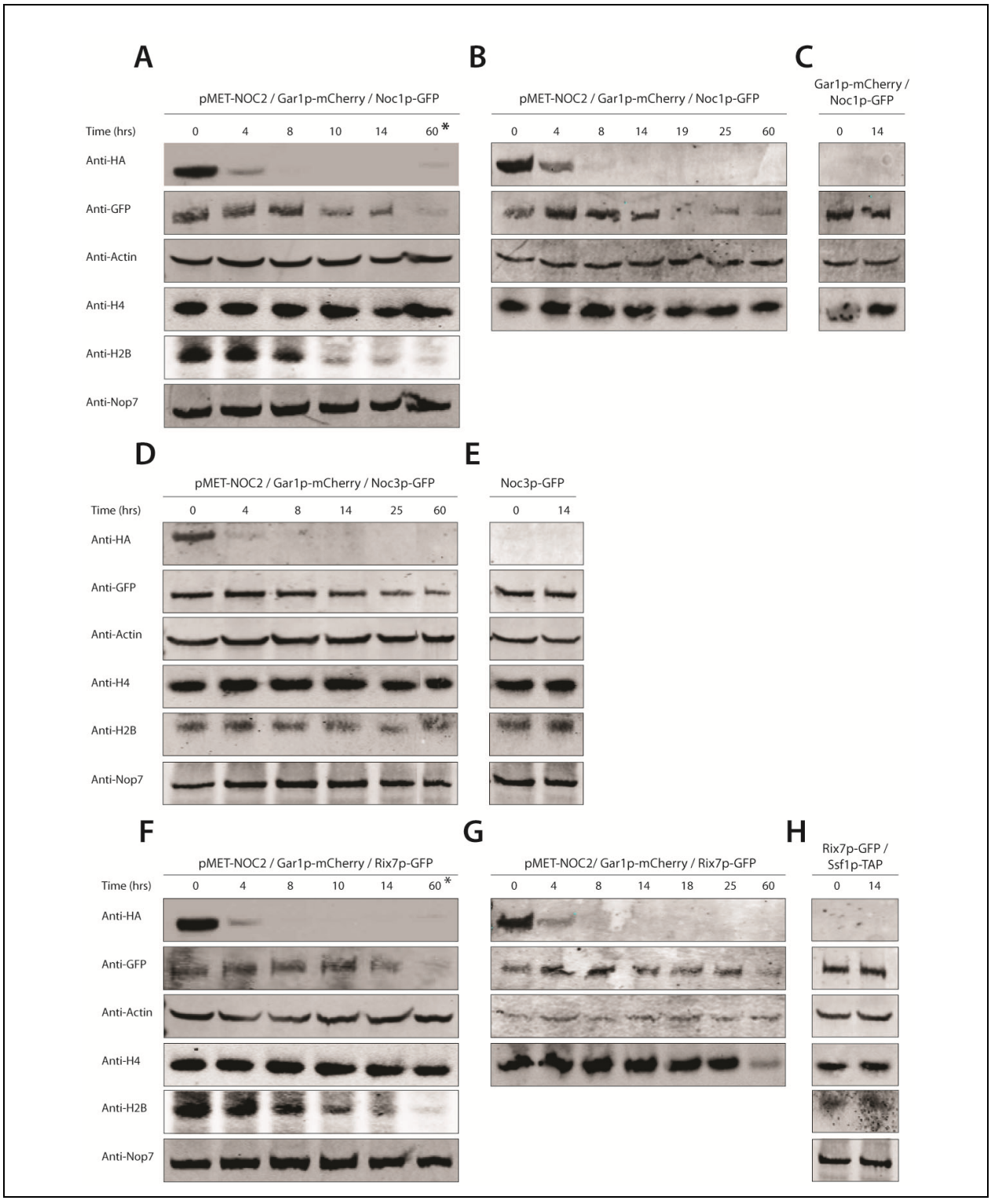

Figure 3.6. Noc2p depletion specifically influences proteins levels of the nucleolar factors Noc1p and Rix7p.

Kushnirov post-alkaline whole protein extraction was performed on each samples using five cell ODs for every time point from the Noc2 depletion experiment. Half of each sample was loaded on a pre-cast 4-12% Bis-Tris PAGE gel. **A, F)** Samples from Noc2 depletion experiments of either P_{Met}-Noc2/Gar1-mCherry/Noc1-GFP or P_{Met}-Noc2/Gar1-mCherry/Rix7-GFP when cells were left to grow in repressive media from time 25 to 60 h without media change. **B, D, G)** Samples from Noc2 depletion experiments when the repressive media was refreshed every 4 to 5 h between 25 to 60 h after the shift. **C, E, H)** Respective control strains. Control samples were run on the same gel as B, D and F.

As previously mentioned, in a second set of Noc2p depletion experiments performed with P_{Met}-Noc2/Gar1-mCherry/Noc1-GFP and P_{Met}-Noc2/Gar1-mCherry/Rix7-GFP, cells were left to grow in the same batch of restrictive media 25 to 60 h after the shift to repressive media, without changing the media or addition of methionine. By western blot analysis, we observed that Noc2p band was reappearing after 60 h, although finer than time 0 and 4 hours. At this point, longer exposition should be performed in order to obtain a stronger band and a better image quality. In addition, longer depletion time could increase the Noc2p reexpression phenotype. However, this supports our hypothesis in which the methionine contained in the repressive media was used up after 60 h, resulting in the re-induction of NOC2 expression from the MET25 promoter. Although at 60 h, we observed that both Noc1p and Rix7p localization was similar to that in permissive media at time 0 h by fluorescent microscopy, their protein levels continued to decrease. This may actually suggests that pre-60S particles are retained and proteins degraded in the nucleus, while under the continued repression of NOC2, freshly translated Noc1p and Rix7p may actually be retained in the cytoplasm for degradation and none or very little of it enters the nucleus. Nevertheless, this hypothesis needs to be investigated further.

In addition to our target proteins, we also determined the protein levels of other pre-60S factors upon Noc2p depletion. We looked at Nop7p level since the protein was shown to be both nucleolar and nuclear, and present in several intermediate and late pre-60S particles, such as those associated with Ssf1p, Nsa1p, Rix1p, Arx1p [45]. Moreover, the three Noc proteins and Rix7p have been found to co-purify by affinity purification mass spectrometry

using both Nop7p-PrA and Nop7-TAP as bait proteins (Oeffinger, unpublished data) [45]. In addition, the Ytm1p-Erb1p-Nop7p subcomplex was shown to be present in Nsa1p-associated complexes, which contained Rix7p, and in which the Noc1p-Noc2p to Noc2p-Noc3p exchange had taken place [2]. Hence, we were interested to see if Nop7p levels would be affected by the presence or the absence of Noc2p. However, we observed no change in Nop7p levels at any point during Noc2p depletion (Figure 3.6 D, anti-Nop7). Moreover, Nop7p level remained constant even when NOC2 was re-induced after 60 hours (Figure 3.6 A, F, anti-Nop7). Thus, Nop7p does not seem to be affected by loss of Noc2p, suggesting that the effect of Noc2p occurs during stages prior to Nop7p incorporation into pre-60S complexes.

The human Noc2p homolog, NIR, was shown to bind to the nucleosome and to block acetylation of core histones H3 and H4 [63]. Based on that observation, we wanted to test whether Noc2p depletion had any effect on the levels of different histone proteins. We therefore tested histone H4 levels as an indicator of the H3-H4 tetramer, and histone H2B as an indicator of the H2A-H2B dimer. Interestingly, western blot analyses of the different time points after Noc2p depletion showed changes in histone protein levels. In fact, H4 level was found to be slightly decreased upon Noc2p depletion (Figure 3.6, anti-H4). In contrast, H2B was strongly decreased upon Noc2p depletion in P_{Met}-Noc2/Gar1-mCherry/Noc1-GFP and P_{Met}-Noc2/Gar1-mCherry/Rix7-GFP strains, even after NOC2 re-induction (Figure 3.6 A,B,F,G, anti-H4). In P_{Met}-Noc2/Gar1-mCherry/Noc3-GFP cells, the decrease was less remarkable. This again points towards an effect of Noc2p depletion on chromatin structure. At this point, it is also unclear whether the decrease in histone levels is due to downregulation of histone mRNA, protein degradation or defect in chromatin assembly, and whether Noc2p has a similar function to its human homolog NIR.

In conclusion, our western blot results show that Noc2p depletion affects the protein levels of Noc1p, Rix7p and, to a lesser extent, Noc3p, consistent with our slow growth rate and protein redistribution phenotypes observed upon Noc2p depletion. Moreover, Noc2p seems to influence only a specific set of proteins, since Nop7p levels were not affected, even though it is known to be present in the same particles. However, H2B and H4 histone levels were, to different extents, found to be affected by Noc2p depletion, suggesting that Noc2p

could have a role in structure maintenance of chromatin, which would be supported by the fact that upon its depletion we observed a disruption in nucleolar integrity.

3.1.2.3 Effect of Noc2p depletion on gene expression

As shown by our results, we found Noc2p depletion to affect the localization and levels of our targeted proteins Noc1p, Noc3p and Rix7p. At this point, we were nonetheless unable to state whether the changes in protein levels were due to transcriptional regulation, post-transcriptional regulation or protein degradation. To this end, gene expression levels of NOC1, NOC3 and RIX7 were examined upon Noc2p depletion. QRT-PCR was performed to compare the mRNA levels of specific genes in permissive and restrictive media 14 hours after the shift in on P_{Met}-Noc2/Gar1-mCherry/Noc3-GFP, since we had more material for this strain and since global growth phenotype according to Noc2p depletion was the same for all strains. Later time points could not be studied due to insufficient numbers of cells and total RNA. However, by results obtained by microscopy and Western blot, we were confident that 14 h will be able to represent the phenotype related to Noc2p depletion.

Specific primers were designed to target specific genes such as NOC1, NOC2, NOC3, RIX7, NOP7, SSF1, SSF2, H2B, H3 and H4 and to determine their changes in expression. Since NOC2 expression was suppose to be modulated by repression of the MET25 promoter, we used this as a control. Moreover, NOP7 and SSF1 were chosen as genes expressing proteins that are known to be in an overlapping step of Noc2p in the ribosome biogenesis pathway. In addition, Ssf1p and Ssf2p are paralogs known to be expressed at different levels. Finally, H2B, H3 and H4 genes were chosen since the human Noc2p homolog has already been found to bind to the nucleosome and to block acetylation of H3 and H4, and because our western blot results revealed a potential influence of Noc2p on H2B and H4 expression. All primers were tested prior to qRT-PCR analysis by performing melting and standard curves (Material and methods section 2.7.4, Figure 2.3). Only primers targeting H4/HHF1 gene were rejected since they appeared not to be specific.

qRT-PCR was performed using primers targeting specific genes. RNA levels from time 0 were normalized as 100% of expression, and levels from 14 h were compared to this

standard. First, we observed that Noc2p depletion by MET25 promoter was efficient since only ~ 8.1% of NOC2 mRNA appeared to be present after 14 h in repressive media (Figure 3.7, NOC2). We believe that NOC2 expression continues to decrease over time, based on the phenotypical observations after 14 h in restrictive media. However, we cannot claim with certainty that NOC2 expression was zero after 60 h even when regularly refreshing the repressive media with methionine. Interestingly, we observed no significant change in the expressions of other tested genes. NOC1 mRNA levels were very close to 100% after 14 hours of Noc2p depletion, which is the opposite of what was observed for its protein levels. Thus, Noc1p seems to be affected by Noc2p depletion at the post-transcriptional level. In contrast, NOC3 and RIX7 expression levels appeared to be downregulated after 14 h of Noc2p depletion, but the levels were not significant. Thus, Noc3p and Rix7p may be affected by Noc2p depletion in a similar way than Noc1p, but their mRNA production or stability could also be affected. Later time points would provide a better indication of their regulation, however, larger cultures are required to collect sufficient material for these experiments.

Even more interesting, we observed a strong and significant increase in SSF1 expression and although SSF2 expression was not significantly increased upon Noc2p depletion. Ssf1p and Ssf2p are protein paralogs (94 % of sequence homology) that are expressed at different levels under normal growth conditions [51]. Recently, these two proteins were shown to function along separate pathways during ribosome biogenesis. Ssf1p particles were shown to contain the Noc proteins and Nop7p, whereas Ssf2p, unlike Ssf1p, was shown to interact with Rrp15p and Nop53p (Unpublished, Aguilar L.C) [45, 72]. In this regard, our qRT-PCR results are consistent with this data and suggest a relation between NOC2 expression and SSF1 expression. Moreover, our results also support the fact that Ssf1p and Ssf2p are not functionally linked or redundant, even if they are paralogs.

In addition, we analyzed NOP7 gene expression, however no significant change of NOP7 expression was found upon downregulation of NOC2 expression. This result is in agreement with our western blot analysis, in which we saw no change in Nop7p protein levels upon Noc2p depletion. We therefore conclude that Noc2p depletion has no effect on Nop7p synthesis.

As we observed a decrease in H2B protein levels, we also determined histone expression levels. However, H4 expression was not tested due to the primers redundancy as explained above. Interestingly, we observed a strong and significant increase of both H2B and H3 expression levels 14 hours after Noc2p depletion.

In conclusion, Noc2p depletion has no effect on the expression of NOC1, NOC3 and RIX7 genes. This suggests that the observed decrease in protein levels for these proteins could be caused by a protein degradation pathway in the nucleus or cytoplasm. Overall, we suggest that Noc2p has an influence on Noc1p, Noc3p and Rix7p and that its absence causes the degradation of these three proteins in different manners. In addition, we found that Noc2p may potentially be linked to Ssf1p, another protein known to be present in an overlapping step during early pre-60S maturation. Finally, Noc2p was found to affect histone levels. At this point, it is still unclear if these effects are direct or indirect and the mechanisms involved.

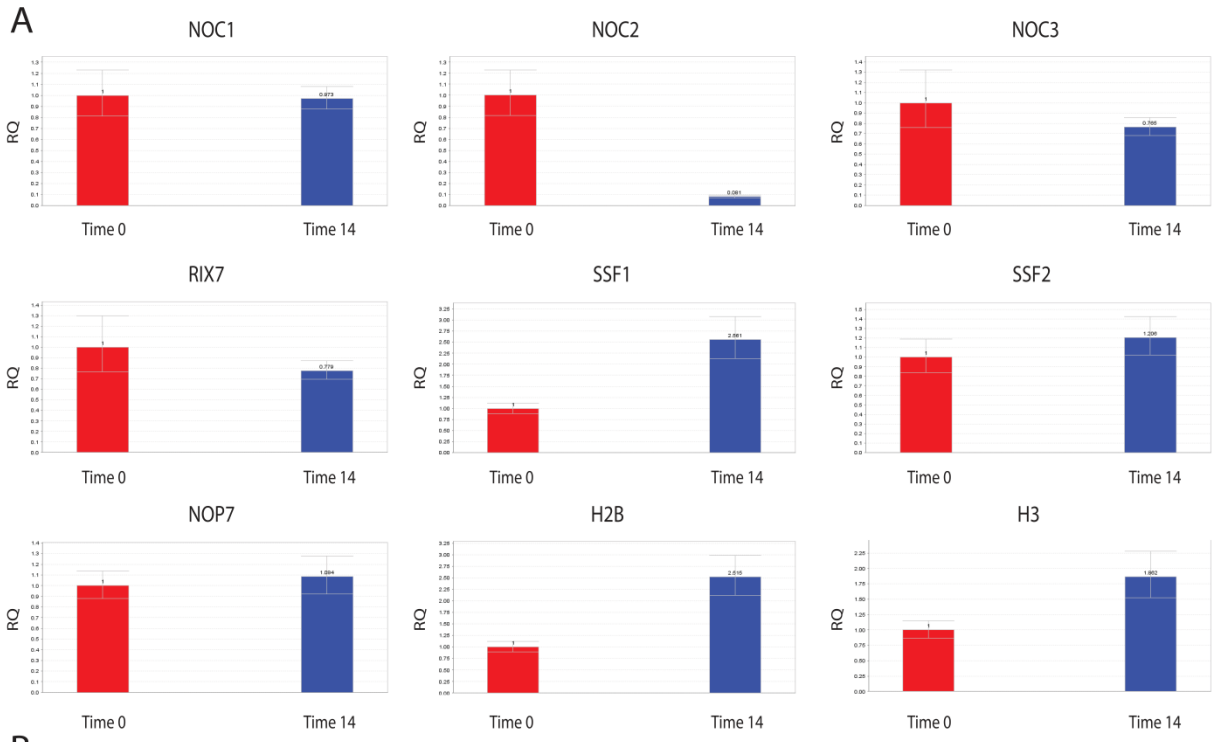

B

mRNA	Fold change	Significant
NOC1	0.973	No
NOC2	0.081	Yes
NOC3	0.765	No
RIX7	0.779	No
SSF1	2.561	Yes
SSF2	1.206	No
NOP7	1.084	No
H2B	2.515	Yes
H3	1.862	Yes

Figure 3.7. NOC2 level is influencing the genes expression of ribosomal factors and Histones.

Cells from P_{Met}-Noc2/Gar1-mCherry/Noc3-GFP in log phase at time 0 and 14 h were collected and reverse transcriptase II, random primers and RNA extracted were used to create cDNA. qRT-PCR analysis were performed using specific primers for each mRNA sequence. qRT-PCR results were normalized against UBC6, ACTIN and TDH3, and time 14 h for each mRNA were compared to time 0. A) qRT-PCR result illustrated as graphics. mRNA names are indicated on top of each graph. B) qRT-RCP results illustrated as significant fold change.

3.1.3 The effect of Noc2p depletion on pre-60S subunit export

Noc2p was first identified as a ribosomal export protein (Rix3p) and shown to be involved in pre-60S subunit transport [47]. Using a *rix3-1 ts* mutant and looking at Rlp25p-GFP localization, pre-60S particle were found to be retained in the nucleolus and the nucleoplasm [47]. Since then Rlp25-GFP has often been used as a marker to determine effects on pre-60S subunit export. Rpl25p is known to recognize and bind domain III of the 25S rRNA and was found in the same particle as Noc3p by affinity purification mass spectrometry, but not with Noc1p and Noc2p [72, 94]. We decided to use Rpl11p, another pre-60S export marker, instead of Rpl25p [83]. Rpl11p, which is encoded by the RPL11A and RPL11B genes, is bound to the ribosome interface [95, 96]. Rpl11bp was shown to have a cytoplasmic localization under normal condition by fluorescent microscopy [97], but was found to be localized in the nucleolus in *cic1-2 ts* mutant, showing a nucleolar block of pre-60S transport [97]. Since, Rpl11p has been found to be a good pre-60S particle marker and has been identified in the same particle as Noc1p but not Noc2p and Noc3p, we thought that it could be a useful marker to look at the pre-ribosomal transport [72]. In addition, Rpl11p is highly conserved, which not the case for Rpl25p [9].

In order to look at the effect of Noc2p depletion on pre-60S particle transport, a strain was constructed similar to the other P_{Met}-Noc2 strains, containing NOC2 under the control of the MET25 promoter, Gar1p tagged with m-Cherry under its own promoter, and Rpl11p tagged with GFP under its own promoter. Cells were grown in permissive media until they reached an OD_{600} of ~0.6, and were washed twice prior to shifting to restrictive media. Similar to other depletion experiments, cells were diluted every 4 to 5 h in order to stay in exponential phase and to refresh methionine within the restrictive media. At time 0 in permissive media, we observed that Rpl11p-GFP localized predominantly in the cytoplasm (Figure 3.8, time 0). This observation corresponds to previous visualization of Rpl11p-GFP at permissive temperatures [97]. Compared to previous data showing the accumulation of the marker Rpl25p in both the nucleolus and the nucleoplasm, our results did not show any pre-60S transport defect. In fact, after 14 h and 25 h in restrictive media, we observed that Rpl11p-GFP

remained in the cytoplasm (Figure 3.8). It is possible that we were able to visualize a minor nuclear accumulation at time 25 h. Nevertheless, it was not enough to suggest a pre-60S particle nuclear accumulation.

Considering our results, Noc2p depletion has no significant effect on transport of pre-60S subunits containing Rpl11p-GFP. However, this experiment needs to be repeated to allow the validity of the conclusion.

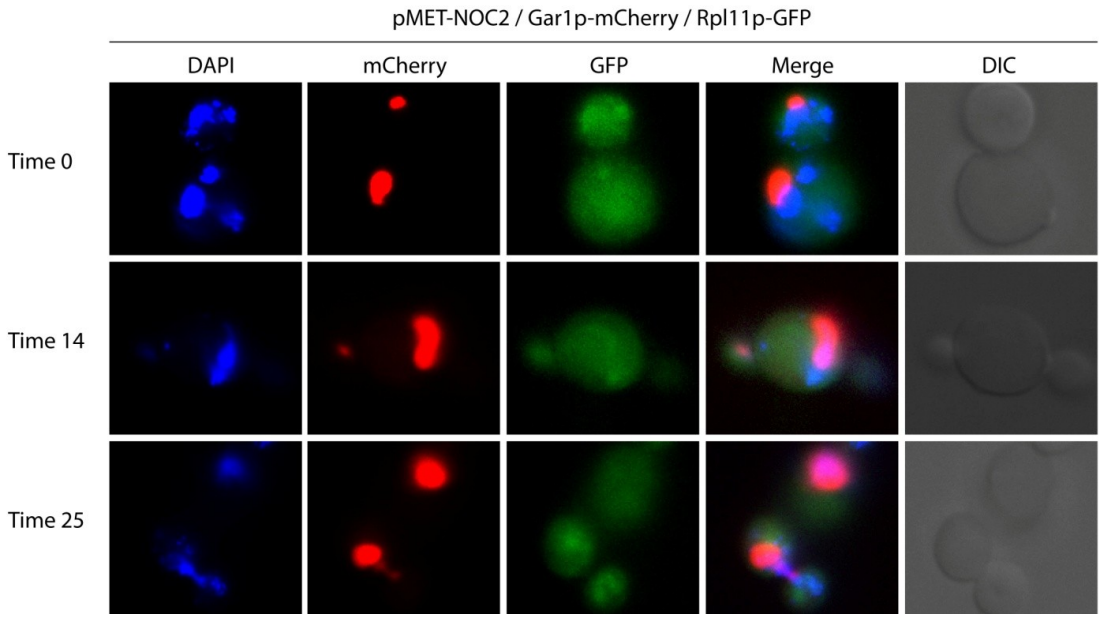

Figure 3.8. Rpl11p localization is not affected by Noc2p depletion.

Samples taken during a Noc2p depletion experiment using P_{Met}-Noc2/Gar1-mCherry/Rpl11p-GFP. Cultures were diluted in repressive media 0 to 25 h after the shift to repressive media.

Part 2: The Noc proteins during nuclear translocation of pre-60S ribosomes

3.2 The effect of reversible nuclear transport arrest on Noc protein exchange

As discussed in the introduction, about 20% of ribosome assembly factors are considered nucleoside triphosphate hydrolyzing enzymes, which are believed to provide energy needed to confer directionality to the ribosome maturation pathway [2, 40]. One of these factors, Rix7p, is a triple AAA-ATPase known to hydrolyzed ATP in order to remove and recycle Nsa1p from pre-60S particles [45]. This removing step has been found to coincide with a compositional change of pre-60S complexes, where early factors such as Noc1p are removed and later factors are integrated. We hypothesize that the Noc1p-Noc2p and Noc2p-Noc3p exchange occurs at this crucial step and that it requires ATP hydrolysis. Since there are several enzymes that are known to utilize energy, we decided to look first at the general influence of energy from nucleotide sources on the Noc proteins.

Therefore, we performed a reversible nuclear transport arrest using metabolic poison. Cells were grown in their normal medium containing 2% glucose until they reached an OD_{600} of ~0.6. Cells were then washed twice with water to ensure the removal of the glucose prior to the culture being diluted in media containing sodium azide and 2-deoxy-D-glucose [78]. Sodium azide was shown to effect mitochondrial oxidative phosphorylation by binding to cytochrome oxidase, which is known to induce ATP production [79]. 2-deoxy-D-glucose is a glucose molecule in which the 2-hydroxyl group is replaced by hydrogen, and therefore it cannot be metabolized by hexokinase, leading to a glycolysis block [98]. It has been proven that using these two components in appropriate concentration leads to a decrease of GTP content to as low as 2.58 to 1.85 nmoles/10^6, as ATP is required for GTP production [78]. Cells were grown in this metabolically poisoned media for 1 h, and two samples were taken, after 30 min and 1 hour of incubation. Thereafter, cells were transferred to normal YPD media containing 2% glucose, and were grown for 1 h before taking samples. For all samples taken, we again looked at protein localization, protein levels and gene expression levels to determine whether the absence of both ATP and GTP would affect the Noc protein exchange.

3.2.1 Effects of metabolic poison on protein localization.

The use of metabolic poison has shown that disruption of nuclear transport causes redistribution of certain late pre-ribosomal factors [31]. For example, Rrp17p, a 5'-3' exonuclease required for pre-60S rRNA processing, was shown to accumulate at the nuclear periphery in metabolically poisoned cells, whereas Rrp12p, which facilitates ribosome export, was found to be more cytoplasmic under these conditions [31]. This suggested a possible relation between pre-ribosome progression through the different nuclear sub-compartments and energy expenditure during ribosome biogenesis [31]. In addition, it has been suggested that ATP/GTP dependent steps may act as checkpoints for ribosome maturation, where energy-consuming proteins potentially release pre-ribosomes from one site of maturation within the nucleus to the next. This could be a possibility for the Noc proteins and Rix7p.

Noc protein localization upon metabolic poison treatment

Since the Noc proteins are believed to be involved in pre-60S ribosome nuclear transport, we decided to determine their localization during metabolic poisoning. Localization of Noc1p and Noc3p had already been determined previously under this condition [31]. However, only one condition had been tested (30 min of incubation in metabolically poisoned media) and the reversibly aspect of this arrest was not tested. Moreover, Noc2p localization had not been tested upon metabolic poisoning in previous studies.

First we examined at Noc1p localization in the four conditions mentioned above. As seen in our previous results (Figure 3.3 A, time 0) and in agreement with previous data, we observed that Noc1p was located in the nucleolus where it colocalized with Gar1p (Figure 3.9 A, Before) [47]. After switching cells into metabolically poisoned media for 30 minutes, we observed no significant change in Noc1p localization (Figure 3.9 A, 30 min), which is in agreement with previous experiments [31]. Moreover, we continued the incubation up to 1 hour, in order to look at a later change in phenotype. Once again, Noc1p was colocalized with Gar1p in the nucleolus (Figure 3.9 A, 1 hour). Indeed, these results suggest that Noc1p localization is not influenced by a decrease in free ATP/GTP in the cell or any energy-dependent steps. However, this result could also indicate the opposite, in the sense that Noc1p

could be blocked in the nucleolus because pre-60S ribosome transport is blocked. Similarly, it has previously been shown that nucleolar proteins involved in pre-rRNA processing, such as Noc1p, Noc2p and Ssf1p, remain in the nucleolus during glucose starvation without using sodium azide or deoxy-d-glucose, and it was hypothesized that their binding to specific mRNA retains the mRNA in the nucleolus under stress [92].

In samples from cells that were re-incubated for 1 hour in YPD, we observed an accumulation of Noc1p in discreet foci within the nucleolus (Figure 3.9 A, Re-induction). This phenomenon had already been observed in *noc3-1 ts* mutants, where Noc1-GFP was found to be strongly accumulated within nucleolar foci [47].

We also looked at Noc2p localization in metabolically poisoned cells. Previously Noc2p showed an intermediate distribution (60% nucleolar and 40% nucleoplasmic) under normal conditions [47]. Accordingly, we observed a predominant localization of Noc2p in the nucleolus, colocalizing with Gar1p (Figure 3.9 B, Before). However, there was a small population of Noc2-GFP diffused into the cytoplasm. After 30 min in metabolic poison, it was difficult to visualize that Noc2-GFP as the signal had become very weak. Its localization seemed to be enriched in the nucleolus, compared to normal conditions (Figure 3.9 B, 30 min). Furthermore, after 1 h in the metabolically poisoned media, signal in two different kinds of locations were observed depending on the cells, where in some cases the signal remains weak as observed at 30 min incubation, while in other cases the signal was stronger but exhibited a crescent-like nucleolar location (Figure 3.9 B, 1 hour). Regardless, Noc2-GFP signal was enriched in the nucleolus in both cases, in comparison to normal condition. This phenotype has already been observed in *noc3-1 ts* mutant cells, where Noc1-GFP and Noc2-GFP were found to predominantly accumulate in the nucleolus [47]. Indeed, it is possible that the lack of ATP/GTP causes or mimics the inability of Noc2p to bind to Noc3p. This hypothesis will be elaborated on in the discussion. In cells incubated for 1 h in YPD, the Noc2-GFP signal was stronger in every cell. While Noc2p remained enriched in the nucleolus it also appeared to diffuse into the nucleoplasm. We suggest that a longer incubation in YPD media would allow the complete redistribution of Noc2p to its wild-type localization.

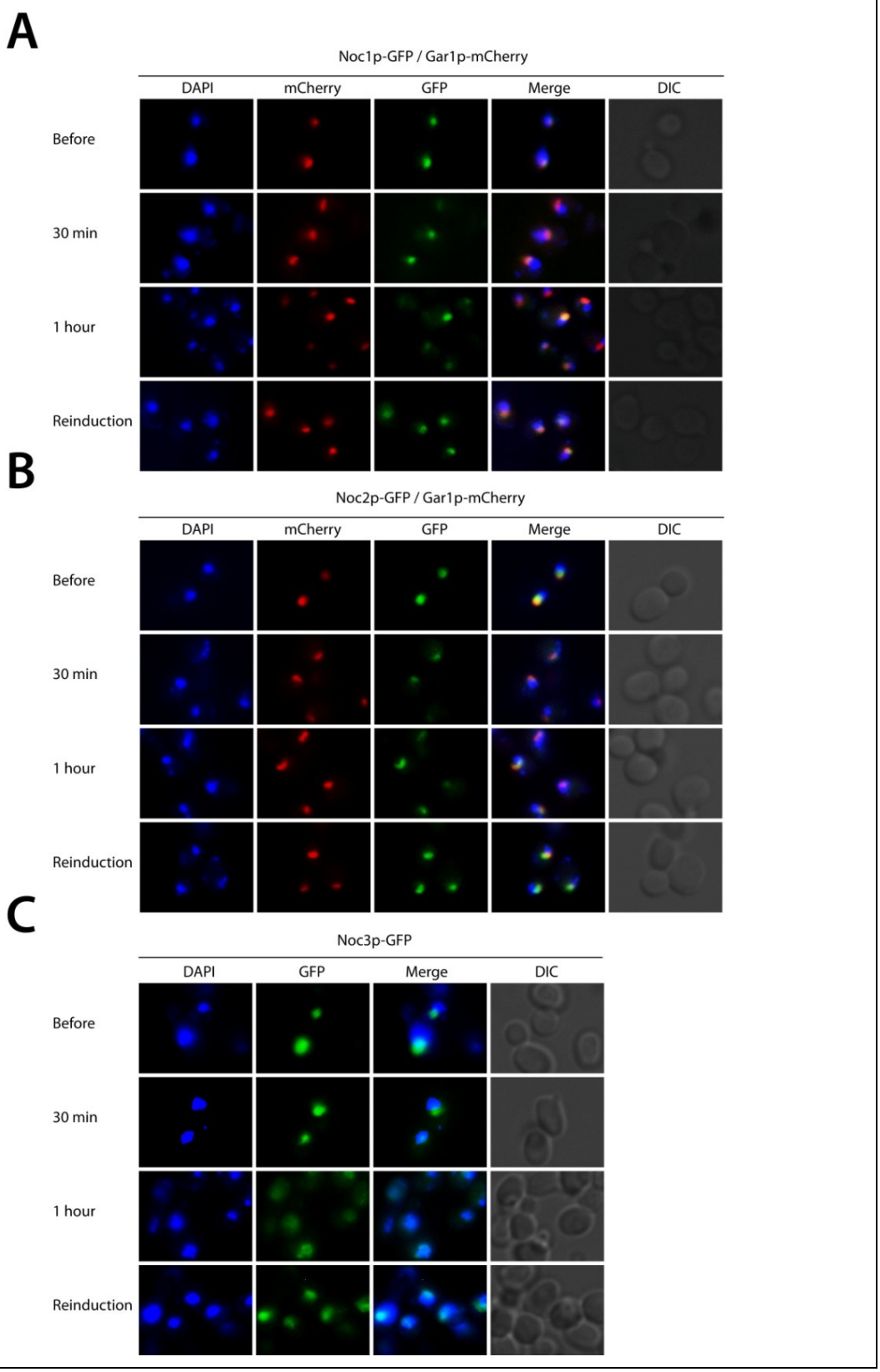
A
Noc1p-GFP / Gar1p-mCherry
DAPI
mCherry
GFP
Merge
DIC
Before
30 min
1 hour
Reinduction
B
Noc2p-GFP / Gar1p-mCherry
DAPI
mCherry
GFP
Merge
DIC
Before
30 min
1 hour
Reinduction
C
Noc3p-GFP
DAPI
GFP
Merge
DIC
Before
30 min
1 hour
Reinduction

Figure 3.9. Noc protein localization is energy-dependent.

Nuclear transport arrest was carried out according to Shulga et al. 1996 [78]. Cells were collected and fixed in normal yeast condition (Before), after 30 min (30 min) and 1 h (1 hour) incubation in glucose-free media containing 10 mM deoxy-d-glucose and 10 mM sodium azide and 1 hour after cells were resuspended in fresh permissive media (Reinduction). A) Noc1p-GFP/Gar1p-mCherry B) Noc2p-GFP/Gar1p-mCherry C) Noc3p-GFP**.** Experiments were performed twice

Finally, we determined Noc3p localization in metabolically poisoned cells. As previously seen by us and others, Noc3p was localized throughout the entire nucleus with a minor nucleolar enrichment [47]. It has already been shown that Noc3p redistributes to the nuclear periphery after 30 min in metabolic poison, similar to Rrp17p [31]. In contrast, we observed this phenotype only 1 h after transfer into poisoned media. Indeed, after 30 min of treatment, Noc3p retained its wild-type distribution (Figure 3.9 C, 30 min). After 1 h, we observed a punctate staining around the nuclear periphery (Figure 3.9 C, 1 hour). Thus, Noc3p localization is clearly affected by the absence of free energy in the cell. Moreover, after 1 h in YPD, Noc3p was more nucleolar than nuclear, exhibiting a crescent-like distribution (Figure 3.9 C, Re-induction).

In conclusion, we suggest that Noc1p-Noc2p and Noc2p-Noc3p complexes distribution could be linked to an ATP/GTP-dependent step. Although Noc1p remained in the nucleolus and did not appear to be affected by the ATP/GTP block, Noc2p and Noc3p were affected. Indeed, Noc2p was strongly enriched in the nucleolus, as previously seen in *noc3-1 ts* cells. In this way, Noc3p was redistributed at the nuclear periphery, unlike its usual nuclear localization. Together, we suggest that the complexes exchange were not able to exchange in the absence of free energy in the cell, causing the redistribution of Noc2p and Noc3p.

Rix7p localization upon metabolic poison treatment

Since Rix7p has been identified as a triple AAA-ATPase which hydrolyzes ATP during the period of Noc1p-Noc2p for Noc2p-Noc3p exchange, which has been suggested to act as checkpoint for ribosome export, we were interested in determining Rix7p localization upon treatment with metabolic poison treatment. As previously mentioned, Rix7p localization has been shown to change depending on growth condition and nutrient availability (Figure

1.5) [44]. Rix7p is located throughout the nucleus during exponential growth, enriched in the nucleolus during stationary phase, and has a perinuclear location when cells were reinduced by refreshing the media after having been in stationary phase [44]. To differentiate the nucleolus from the entire nucleus, Gar1p-mCherry was used as the nucleolar marker. We used our P_{MET}-NOC2-HA/Rix7-GFP/Gar1-mCherry strain, since the GFP and mCherry tags have already been integrated and tested. Thus, the strain was first grown in permissive media, in order to allow for synthesis of Noc2p. Thereafter, the experiment was carried out in the same way as for testing the Noc proteins, but in posioned SD-MET media.

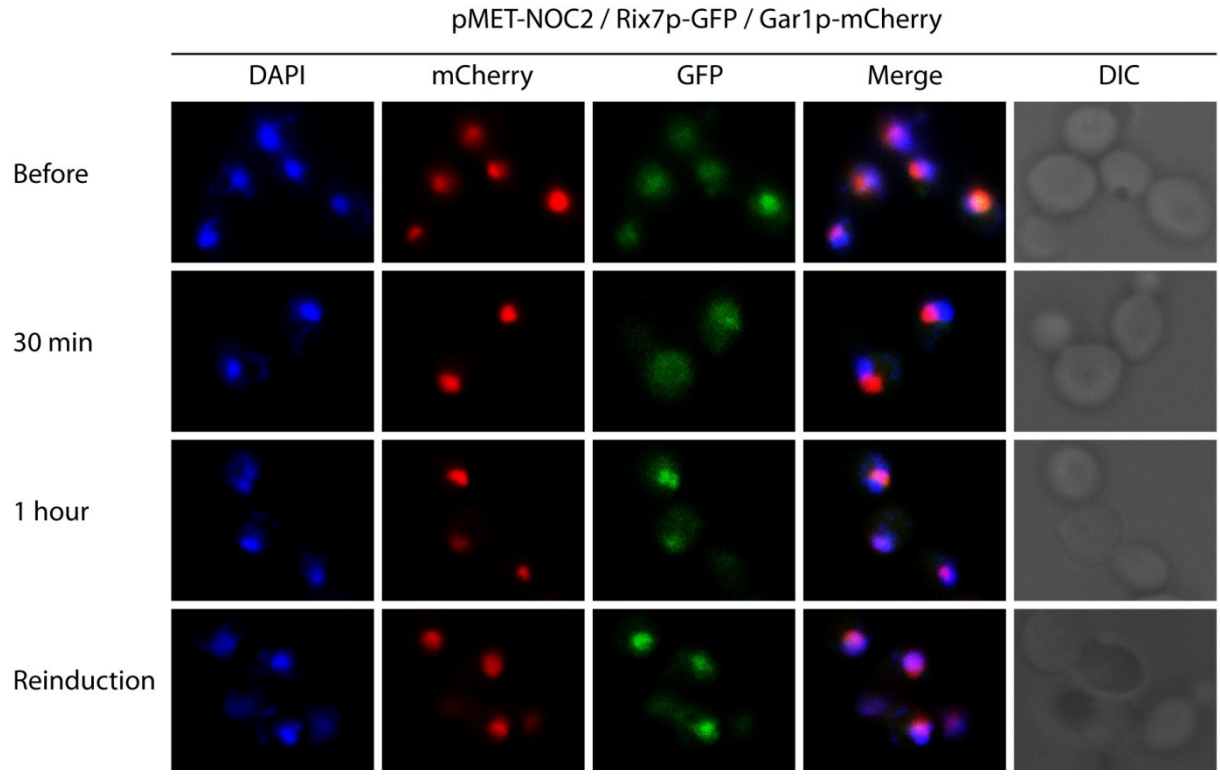

Figure 3.10. Rix7p localization may be influenced by lack of ATP and GTP.

P_{MET}-NOC2-HA/Rix7-GFP/Gar1-mCherry strain was grown in SD-MET media until they reached an OD_{600} of ~0.6. Nuclear transport arrest was carried out according to Shulga et al. 1996 [78]. Cells were collected and fixed in permissive media (Before), after 30 min (30 min) and 1 h (1 hour) incubation in glucose-free media containing 10 mM deoxy-d-glucose and 10 mM sodium azide and 1 h after cells were resuspended in fresh permissive media (Reinduction) Experiments were performed twice.

Under normal conditions, we observed that Rix7p was located throughout the nucleus, which is in agreement with its predicted localization during exponential growth (Figure 3.10, Before). After 30 min of incubation in poisoned media, the Rix7p-GFP signal was diffused throughout the nucleus and to some extent cytoplasmic (Figure 3.10, 30 min). Interestingly, after 1 h of incubation, the signal appeared to be enriched in the nucleolus (Figure 3.10, 1 hour). Since Rix7p localization is known to be affected by nutriment availability, its redistribution could be in agreement with the lack of glucose. Indeed, glucose levels are usually diminished when cells are in stationary phase. Thus, we cannot confirm that its relocalization is entirely due to glucose starvation or whether it is an effect of lack of ATP/GTP. After re-induction of ATP and GTP production by diluting cells in fresh glucose-SD-MET media, we observed that Rix7p was located throughout the entire nucleus, also colocalizing with Gar1p-mCherry and the DAPI nucleoplasmic stained region (Figure 3.10, Re-induction). This result conflicts with previous data, where Rix7p has been shown to be peinuclear when cells are re-induced to fresh nutrient rich media [44]. Indeed, smaller incubation time instead of 1 h could help us to visualize this perinuclear location. Alternatively, it could also indicate that the redistribution of Rix7p in metabolic poison is not due to lack of glucose, but absence of free energy. Even if we cannot confirm that the nucleolar concentration of Rix7p is not only due to glucose starvation, we can speculate that Rix7p is relocated in metabolically poisoned cells which blocks energy-dependant processes, and is not able to perform its function. Indeed, if we hypothesize that the Noc proteins require ATP hydrolysis by Rix7p to carry out the complexes exchange, these results would support this idea. In fact, we observed that Noc2p was enriched in the nucleolus, and Noc3p redistributed to the nuclear periphery, which suggests that the complex exchange is not occuring. At the same time, we observed that Rix7 relocalized to the nucleolus like Noc2p and Noc1p. Thus, the lack of ATP and GTP influences Noc2p, Noc3p and Rix7p localization.

3.2.2 Influence of nuclear transport on proteins level

Since we observed the redistribution of some proteins and diffusion of GFP signals of our target proteins, we decided to study their protein levels upon metabolic poisoning to determine whether it would modulate their protein levels in the same way as during Noc2p

depletion. In fact, the inability to perform the exchange between the Noc1p-Noc2p and Noc2p-Noc3p complexes could also modulate the level of these specific proteins.

In agreement with the microscopy results, in which Noc1p was found to remain in the nucleolus, we observed no change of Noc1p levels by western blot analysis (Figure 3.11 A). Moreover, no significant change was observed for Noc2p levels, despite the nucleolar redistribution and a minor decrease in GFP signal intensity (Figure 3.11 B). Interestingly, we observed a slight increase in Noc3p levels when cells had been incubated for 1 h in metabolically poisoned media (Figure 3.11 C). This coincided with the perinuclear redistribution that we observed by microscopy. However, Noc3p level decreased when cells were incubated for 1 h in YPD media. Finally, we were anticipating a reduction of Rix7p levels during incubation in poisoned media, since the GFP signal visualized by microscopy was very low at this point. We observed a very discrete decrease in Rix7p levels in metabolic poison and an increase after re-induction in YPD. However, these changes were minor and need to be quantified to confirm the effect of lack of free energy on Rix7p levels.

Thus, we conclude that only Noc3p and Rix7p levels are influenced by free energy levels in the cell and that it is a reversible effect.

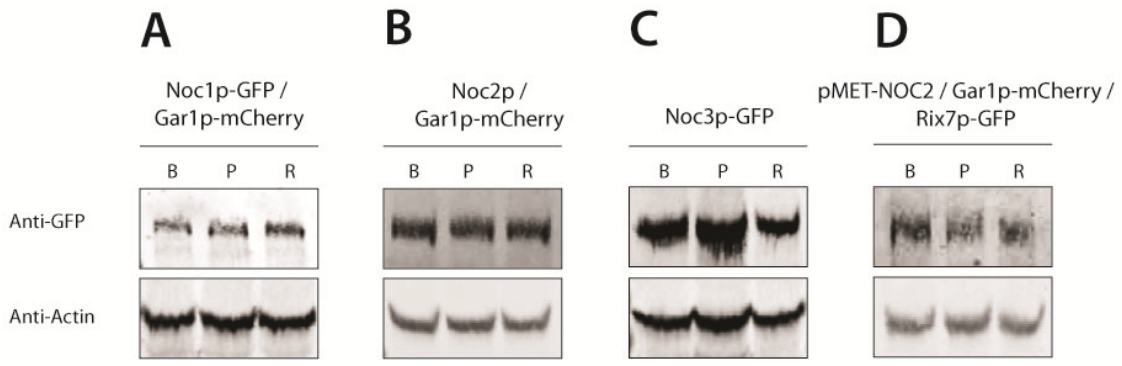

Figure 3.11. Total levels of the Noc proteins and Rix7p are influenced by metabolic poison.
Samples were taken during metabolic poison treatment and re-introduction of cells into YPD. B = Normal condition, P = 1 h of incubation in the metabolically poisoned media and R = Re-induction after 1 h incubation in noral condition. Samples taken from **A)** Noc1-GFP/Gar1-mCherry. **B)** Noc2-GFP/Gar1-mCherry **C)** Noc3-GFP **D)** P_{MET}-NOC2-HA/Gar1-mCherry/Rix7-GFP.

3.2.3 Influence of metabolic poison on mRNA levels

As shown by our microscopy and western blot analyses, absence of free energy can modulate localization of specific proteins and their overall levels. Since we observed some changes in protein levels, we also looked at gene expression level in order to understand if these changes were specifically due to transcriptional regulation, post-transcriptional regulation or proteins degradation. Indeed, we performed qRT-PCR experiments by comparing the mRNA abundances of selected genes of cells in normal condition with cells incubated for 1 h in metabolically poisoned media, and cells re-induced for 1 h in YPD. We used the same primers used previously to test the effect of Noc2p depletion on mRNA levels since they have already been tested and approved (Material and method section 2.7.4 Figure 2.3).

First, we determined the effect on NOC genes, and observed that NOC1 RNA level appeared significantly decreased in poisoned media, and significantly increase after re-induction (Figure 3.12, NOC1). Indeed, it seemed that cells downregulated NOC1 expression in the absence of ATP/GTP, and compensated this downregulation by a strong increase of NOC1 expression during the re-induction in YPD. In contrast, NOC2 and NOC3 RNA levels remained the same overall in metabolic poisoned and YPD media (Figure 3.12, NOC2 and NOC3). Indeed, the increase of Noc3p level observed by western blot in the poisoned cell is most likely due to post-transcriptional regulation, and not transcriptional regulation or mRNA stability.

Secondly, we observed that RIX7 RNA level was not affected by metabolic poisoning and the absence of ATP/GTP (Figure 3.12, RIX7). Indeed, the minor protein decrease seen by western blot could be due to protein degradation. In contrast, RIX7 expression significantly increased after re-induction into YPD media, suggesting that cells need to compensate by an increase in RIX7 expression. However, as seen by western blot, Rix7p levels remained the same after re-induction. Similar phenotypes were observed for NOP7 gene expression (Figure 3.12, NOP7). Interestingly, Nop7p (and theYtm1p-Erb1p-Nop7p complex) was shown to be removed from pre-60S particle by Rea1p, another AAA-ATPase, and co-associate with Rix7p in pre-60S complexes [43, 45].

Finally, we tested histone H3 and H2B RNA levels. We observed that H2B RNA level slightly increased, and H3 RNA level significantly increased in metabolic poisoned media (Figure 3.12 A, B). In comparison, we observed that both H2B and H3 mRNA levels significantly decrease after re-induction in YPD.

A

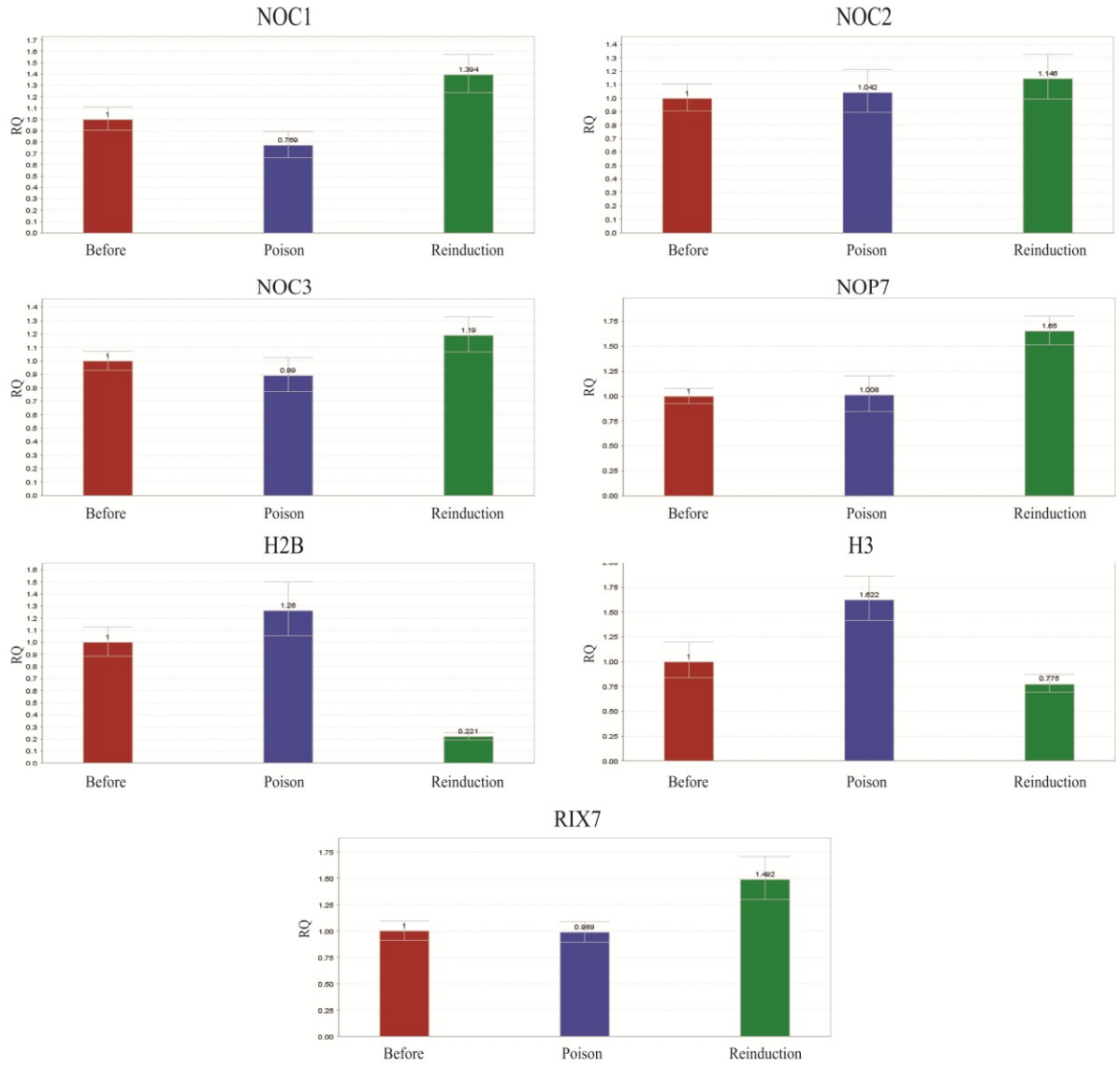

B

	Poison		Reinduction	
mRNA	Fold changes	Significant	Fold change	Significant
NOC1	0.769	Yes	1.394	Yes
NOC2	1.042	No	1.146	No
NOC3	0.89	No	1.19	No
NOP7	1.008	No	1.65	Yes
H2B	1.26	No	0.221	Yes
H3	1.622	Yes	0.775	No
RIX7	0.989	No	1.492	Yes

Figure 3.12. Metabolic poison affects gene expression levels.

Cells from P_{Met}-Noc2/Gar1-mCherry/Noc3-GFP in log phase in normal media (Before), after 1 h in poisoned media (Poison) and after 1 h of reinduction in fresh normal media (Reinduction) were collected and reverse transcriptase II, random primers and RNA extracted were used to create cDNA. qRT-PCR analysis were performed using specific primers for each mRNA sequence. qRT-PCR results were normalized against UBC6, ACTIN and TDH3, and Poison and Reinduction samples were compared to Before sample. A) qRT-PCR result illustrated as graphics. mRNA names are indicated on top of each graph. B) qRT-RCP results illustrated as significant fold change.

Thus, starvation of glucose and free energy in the cells caused significant decrease in NOC1 and H3 mRNA level. Thereafter, NOC1, NOP7 and RIX7 mRNA levels significantly increased upon re-induction in YPD. In contrast, H2B and H3 mRNA levels decreased compared to mRNA levels in poisoned media. Indeed, we suggest that histone mRNA levels are affected by the free ATP/GTP in the cell. Moreover, we suggest that the NOC1 gene is the only NOC gene influenced by this nuclear transport arrest, which could be linked to Noc1p being implicated in early steps of ribosome biogenesis.

Part 3: Determining compositional changes of selected pre-ribosomes

3.3 Studying Noc2p containing RNP complexes under different conditions

According to the BioGrid database, Noc2p was shown to have 181 physical interactions [72]. However, the majority of these interactions have been determined indirectly through studies with other proteins. Indeed, the only Noc2p affinity purification was only performed under highly stringent conditions in order to determine direct and strong interactions. It was found that Noc2p binds to both Noc1p and Noc3p and can also form the Rnp5p-Noc1p-Noc2p trimeric complex [47]. Nevertheless, it is important to study the proteins associated with Noc2p further in order to understand its role in ribosomal maturation and its link to the molecular composition of the pre-ribosome. Noc2p affinity purifications need to be performed using different buffer stringencies and different cellular conditions to gain a better picture of its environment and function. Affinity-purifications of Noc1p, Noc3p and Rix7p need to be performed in comparison, to pinpoint the Noc1p-Noc2p and Noc2p-Noc3p exchange, the possible role of Rix7p and to better understand the overall pre-ribosome environment.

To this aim, we decided to determine at first the difference between RNP composition of Noc1p-GFP, Noc3p-GFP or Rix7p-GFP associated complexes in the presence or absence of Noc2p, using the MET25 promoter. Indeed, the same strains were used for microscopy but grown in much larger cultures, in both permissive and restrictive media, in order to obtain sufficient amounts of cells to perform affinity purification of the GFP-tagged proteins. Samples in both permissive and restrictive conditions were collected for P_{MET}-NOC2-HA/Gar1-mCherry/Noc1-GFP and pMET-NOC2/Gar1p-mCherry/Rix7p-GFP. Purification of GFP-tagged proteins upon Noc2p depletion will allow us to determine changes within pre-ribosomal complexes by mass spectrometry. Moreover, we will be able to link mass spectrometric results with the observations made by microscopy, western blot and qRT-PCR.

In addition, we will also study the Noc1p, Noc2p, Noc3p and Rix7p interacting partners upon cellular energy depletion, which will result in an arrest of nuclear transport, and has so far been carried out for Noc1p-GFP/Gar1-mCherry and Noc2p-GFP/Gar1-mCherry and

remains to be done for Noc3p-GFP and pMET-NOC2/Rix7p-GFP/Gar1p-mCherry. Once again, purification of selected GFP-tagged proteins under the three different conditions during nuclear transport arrest (Normal, Poison and Re-induction) will allow us to determine changes in pre-ribosome composition by mass spectrometry.

3.3.1 Determining the composition of Noc2p-associated complexes under wild-type conditions

Since only one high-stringency affinity-purification of Noc2p has been performed in the past, nothing is known about the transient environment of Noc2p associated complexes. Indeed, we decided to first determine the Noc2p particle composition, using different purification buffers, allowing us to play with RNP complex integrity. Since Noc2p is very abundant (~29,000 molecules/cell according to [51]), we need to use only a small amount of yeast cryo-powder (0,2g-0,5g) collected from the Noc2p-GFP strain at an OD_{600} ~0.6. Different extraction buffers were used during the single-step affinity-purification, in order to identify buffers that would provide the minimal background without disturbing the RNP complex [82]. Indeed, we tested different salt concentration and types, detergents and pH ranges, based on different effects on surface tension and protein solubility [99]. Moreover, we used and modified buffers that had previously been used in affinity purifications where Noc2p had been identified by mass spectrometry [45, 47, 82]. Purified complexes were visualized on a silver-stained gel, which allowed us to determine distinct pre-ribosome migration patterns. Buffers used in conditions 1 and 6 were the same, except that buffer 6 contained 250 mM NaCitrate and was more stringent. By looking at the silver-stained gel, addition of NaCitrate significantly decreased RNP complex stability (Figure 3.13 A). Moreover, the buffer in condition 4 caused a high background compared to other conditions and the control (W303 yeast power). Indeed, looking at the different protein migration patterns, allowed us to select a first round of buffers that could provide interesting mass spectrometry results.

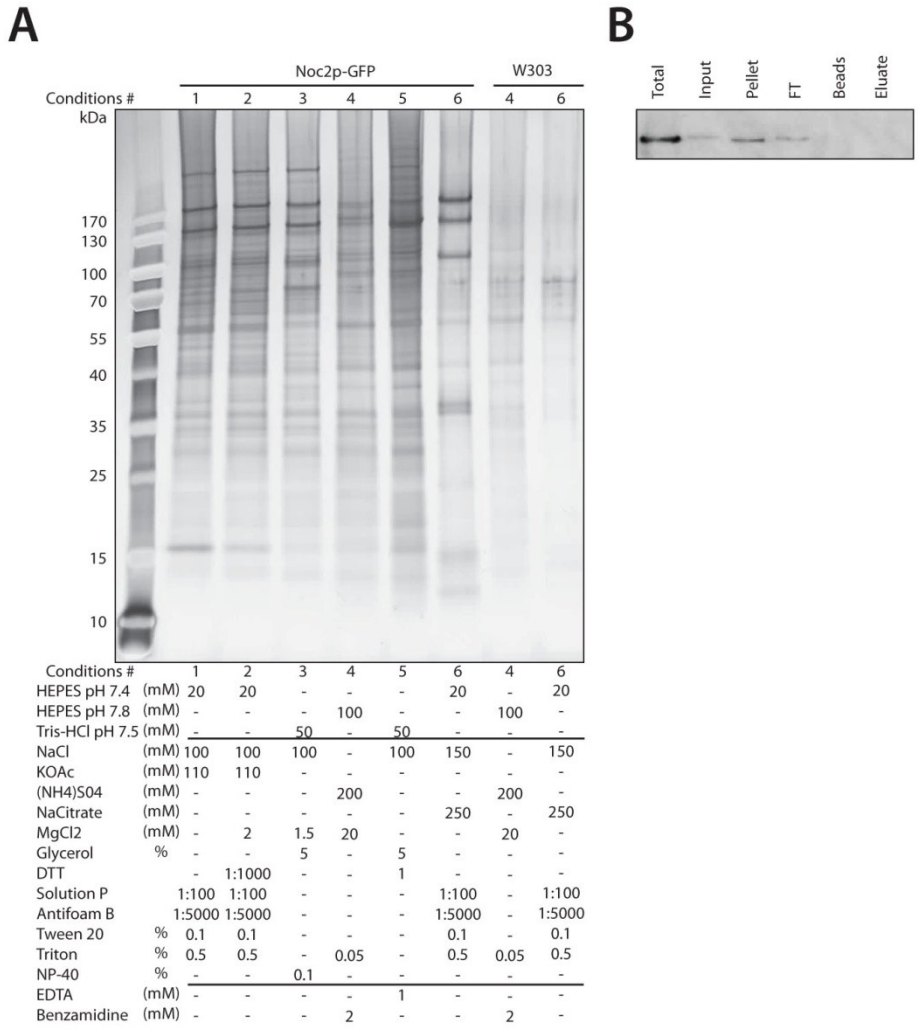

Figure 3.13. Affinity-purified Noc2p complexes using a GFP antibody and different buffer conditions.

Yeast Noc2p-GFP was grow in YDP media until it reached an OD_{600} ~0.6-0.7. Cells were harvested and cryo-lysed prior to purifying pre-ribsomes by single-step affinity purification. Dynabeads were conjugated with anti-GFP antibody no more than 7 days before use. The same procedures were carried out for the control, an untagged isogenic wild-type strain (W303). **A)** Silver stained gel after affinity purification of Noc2p-GFP and W303 as control. Conditions #1 and #2 from [82], #3 from [45], # 4 from [47], #5 from EMBL TAP-purification protocol site, and #6 modified from [82] **B)** Testing the efficiency of affinity-purification by looking at Noc2p-GFP loss or gain at different step of the single-step affinity purification procedure by Western blot analysis. This is an example of efficiency testing and protocol optimization using buffer condition #6.

In addition to visualizing protein migrations patterns, the purification efficiency was tested in order to ensure the purification of the entire Noc2p-associated pre-ribosome population. Samples were taken at key steps during the affinity purification and analyzed by western blot in order to determine the levels of Noc2p-GFP at each step. The analysis showed that the purifications were not efficient as much of the Noc2p-GFP was found to be lost in the pellet after centrifugation, or in the flow-through after the binding step. Indeed, we tried several optimization changes, such as homogenizing the lysate by polytron prior to the binding step, adding DNase into the RNP buffer and sonicating the pellet. However, none of these optimizations resulted in an efficient purification of the GFP-tagged Noc2p, visualized in the elution samples by Western blot analysis (Figure 3.13 B).

We therefore decided to switch to an anti-GFP nanobody from Ilama instead of our usually rabbit anti-GFP antibody. Nanobodies are composed of a single antibody VHH domain making them very small in size (14 kDa) and allowing them to bind antigens with the same affinity and specificity as conventional antibody [100]. However, nanobodies can be more densely conjugated to the magnetic beads, given their small size, increasing kinetic on-rates during the binding step of the affinity purification. Also, nanobodies have been shown to recognize epitopes located in clefts and protein cavities, which could be the case with Noc2p [100]. We are currently in the process of efficiently recombinantely expressing and purifying anti-GFP nanobody from plasmid pET21-peIB-VHH-16. To this purpose, we are using Arctic Express *E.coli* cells to induce and express our nanobody, to avoid the formation of aggregates during expression. We tried induction with different IPTG concentration and observed two strong bands independently of IPTG concentration (Figure 2.1). Indeed, the top one represents the unprocessed protein including the peIB leader sequence and the bottom one is the final secreted product after cleavage of the peIB sequence. Moreover, we observed two other bands when we induced with either 0.1 mM or 1 mM IPTG (Figure 2.1). These bands are suggested to be unspecific and allowed us to choose 0.5 mM IPTG as the concentration to use.

Thereafter, we performed a perilasmic prep/Ni-NTA purification (protocol obtained from the Rout laboratory) in order to obtain sufficient amounts of good quality nanobody. At

this point, we were not able to obtain the expected yields, in the sense that we lost much of the nanobody throughout the purification protocol. The anti-GFP nanobody construct includes a peIB leader sequence allowing the nanbody to be secreted and processed in the periplasm of the cell. This was suggested to increase the final nanobody stability and solubility, since the oxidative conditions in the periplasm help disulfide formation. However, it also means that only a fraction of the total protein is fully processed. Accordingly, we followed a purification protocol in which osmotic stress is used to cause the release of the nanobody from the periplasm. Following that, we needed to perform several centrifugations in order to discard non-processed nanobody. Nevertheless, we believe that those centrifugation steps also discard a bulk of the nanobody, which significantly decreases the final yield. Indeed, further optimization of the recombinant anti-GFP nanobody purification protocol is currently under way.

Once optimization is successful, pre-ribosomal complexes purified from Noc1p-GFP, Noc3p-GFP and Rix7p-GFP strains will be study under Noc2p depletion. Moreover, pre-ribosomes purified from these as well as Noc2p-GFP will be studying upon nuclear transport arrest. Thus, the environment of Noc2p and its partners will be determined by mass spectrometry under different cellular conditions.

Part 4: Noc2p and its human homolog NIR

3.4 Determining links between Noc2p and its human homolog NIR.

An NCBI Blast identified the protein NIR as the human homolog of Noc2p, with 31% sequence identity. Similar to Noc2p, NIR localizes predominantly to nucleoli, where it colocalizes with the nucleolar marker fibrillarin (human Nop1p), and to a lesser extent to the nucleoplasm [64]. Sucrose gradient centrifugation of nuclear extracts found NIR in fractions with both pre-40S and pre-60S particles [64]. Unlike Noc2p, NIR contains two independent INHAT domains, one at its N-terminal and one at its C-terminal end, that are known to bind to nucleosomes and block acetylation of core H3 and H4 [63]. Moreover, promoter-recruited NIR has been demonstrated to repress basal and activated transcription in a promoter-independent manner [64]. Knock down of NIR strongly inhibits cell growth and activates p53, possibly by de-repression of p53 acetylation [64].

In this study we observed that depletion of Noc2p caused a redistribution of Gar1p, which is part of the common core proteins of H/ACA snoRNPs and catalyzes site-specific pseudouridylation of pre-rRNA co-transcriptionally [23]. Upon Noc2p depletion, Gar1p was redistributed to the nucleoplasm (Figure 3.3; 3.4 3.5; 3.8; 3.9; 3.10). This kind of redistribution has already been observed with Nop1p/Fibrillarin, after down-regulation of pre-rRNA synthesis in Pol I mutant cells, where it was suggested that inhibition of Pol I transcription causes putative changes in the nucleolus structure [54]. This, together with our data, suggests that depletion of Noc2p induces a similar effect, and leads to the destabilization of nucleolar integrity.

Moreover, we observed by western blot that Noc2p depletion induced a slight decrease in histone levels and cells exhibited an extremely slow growth rate (Figure 3.2 and 3.6), consistent with previous data, which has shown that defects in histone expression lead to negative effects on transcription and cell fitness [101].

Finally, we also observed a strong and significant increase in both H2B and H3 mRNA levels upon depletion of Noc2p, which could indicate an arrest at START, before cells enter from G1 into S-phase of the cell cycle. Histone mRNAs level were shown to increase to upon

S phase entry to provide for the increased need of histones after DNA replication and during cell division [102].

3.4.1 Chromatin state influenced by Noc2p

In order to investigate a possible role of Noc2p in chromatin structure of transcription regulation, we looked at the co-existence of two distinct rDNA chromatin populations: silent and active. It is known that rRNA genes exist in two different chromatin states, where some are actively transcribing and depleted of nucleosomes, whereas others are transcriptionally inactive and assembled onto nucleosomes [86]. Our aim was to determine whether Noc2p depletion would influence one state or the other.

Therefore, samples were taken during Noc2p depletion experiments, cells were fixed and psoralen photocrosslinking was performed [86]. It has been shown that Psoralen photoreacts with double-stranded nucleic acids, allowing interstrand crosslinks [86]. In the past, it has been shown that the presence of nucleosomes on chromatin inhibits the extent of psoralen crosslinking, allowing the differentiation between the two chromatin states after a separation on a native agarose gel followed by Southern blot analysis [86]. For our experiment, we followed the *Griesenbeck, J. et al (2012)* protocol, performed cell fixation on our samples, followed by psoralen photocrosslinking and Southern blot analysis. However, we tried two different DNA-labeling systems in order to prepare the 3.5 kb rDNA probe used in the Southern blot. Unfortunately, no signal was obtained in either case on the membrane after hybridization. Therefore, this protocol needs to be re-evaluated before it will be repeated. Once the optimization is finish, we will be able to determine whether Noc2p depletion effects rDNA transcription.

4 Discussion and perspectives

Previous analyses on the Noc proteins have indicated a spatio-temporal dynamic aspect of ribosome biogenesis. Indeed, mass spectrometry analyses revealed that Noc1p and Noc2p form an early nucleolar complex during ribosome maturation, whereas Noc2p and Noc3p form a later nuclear complex, where their intra-cellular localizations depend on each other [47]. These three proteins are known to be important, since all NOC genes appear to be essential for cell growth and are well conserved from yeast to human [47]. More precisely, the Noc proteins were identified to be involved in pre-60S ribosome biogenesis in yeast, playing a role in intranuclear movement of the pre-60S subunit, which could be explain by their HEAT-repeats sequences that are predicted to form extended structures to protect rRNA surfaces [47, 50, 103].

However, it remains unclear how and why Noc2p dissociates from Noc1p to form another, later complex with Noc3p. In fact, Noc1p has been found to be more enriched in the early Nsa3-TAP associated particle and less prevalent in the more mature Nop7-TAP associated particle, whereas Noc3p was found in lower amounts in Nsa3-TAP and enriched in Nop7-TAP complexes [35]. Although it indicates the approximate timing of the Noc complex exchange, the causes or the prerequisites for this exchange is still unknown.

It is known that about 20% of the ribosome assembly factors are considered nucleoside triphosphate hydrolyzing enzymes, which are believed to provide the energy needed to confer directionality to the maturation pathway [2, 40]. In light of this information, energy-dependent events have been hypothesized to be linked to spatial progression and remodeling of pre-ribosomal particles. Indeed, it was suggested that the Noc complex exchange required an energy-dependent event in order to take place. The triple AAA-ATPase Rix7p, known to be involved in ribosome biogenesis, was found in an overlapping step with the Noc proteins [40]. It has also been shown that ATP hydrolysis by Rix7p coincides with a compositional change of the pre-60S particle, where some early factors such as Noc1p dissociate from the particle, and some later nuclear factors associate with the 60S pre-ribosome [40]. We hypothesize that the subcomplex exchange between Noc1p-Noc2p and Noc2p-Noc3p could coincide with this particle rearrangement.

With the intention of uncovering more details about the dynamic exchange of the Noc proteins, the influence of Noc2p on Noc1p, Noc3p and Rix7p was studied. Moreover, the effect of free energy level on intranuclear transport and Noc protein exchange and Rix7p function was studied by decreasing ATP and GTP levels in the cell.

4.1 Looking at the dynamic influence of Noc2p

In order to circumvent the problem associated with the use of *ts* mutants, the MET25 promoter has been chosen to regulate NOC2 gene expression in haploid yeast *Saccharomyces cerevisiae* cells. Since NOC2 has been previously shown to be essential for cell growth, efficiency of the MET25 promoter activity was tested by looking at the cell growth in two distinct ways. First, spot test analyses allowed us to determine if the MET25 promoter was sensitive to methionine or not. In fact, MET25 promoter sensitivity has been previously tested by looking at lacZ expression in the presence of increasing amounts of methionine and has been shown to respond in a logarithmic manner, dependent on methionine concentration [91]. In this previous study, 1 mM methionine was shown to allow ~10% of β-galactosidase activity due to its strong stability, whereas shorter half-life proteins were found in only ~1% [91]. Since the half-life of Noc2p is unknown, and based on our spot test analysis, we decided to increase methionine levels up to 5 mM for effective repression of MET25 promoter expression (Figure 3.1). Thereafter, this methionine concentration was used to perform several growth curve experiments by using combination strains containing NOC2 under the control of the inducible/repressible MET25 promoter, Gar1p mCherry-tagged as a nucleolar marker, and either GFP-tagged Noc1p, Noc3p or Rix7p. All strains were grown in permissive media (without methionine) until they reached an OD_{600} of ~0.6 and were then shifted into repressive media (containing methionine). Throughout the experiment, cells were diluted into fresh repressive media in order to keep them in an exponential phase and aliquots were collected.

Since Noc2p depletion affected cell growth rates strongly and negatively, the amount of cells decreased over the experiment, due to the collection of aliquots at selected time points. After some time, the growth rate was unable to compensate for the collected cells, in addition to the dilution or refreshing step with new repressing media, making it at some point impossible to either collect samples or dilute cells. Hence, in the future bigger starting cultures

must be use in order to compensate for the strongly decreased growth rate and to allow us to take samples at every time point.

However, this severe growth rate phenotype allowed us to more clearly understand previous data, in which NOC2 was determine to be essential for cell growth and not for cell viability, as cells continued to divide albeit extremely slow [47]. For every strain containing P_{MET}-NOC2, cell populations increased by only ~10 ODs after 18 h of NOC2 depletion, compared to the background strain W303, in which cell population increased by more than 100 ODs (Figure 3.2). Nevertheless, even after 25 h of depletion, the cell population continued to increase, showing the non-essential role of Noc2p in cell viability. However, it is impossible to claim that P_{MET} was completely repressed at this point. More qRT-PCR analyses will need to be performed in order to look at NOC2 RNA level. As mentioned previously, two kinds of growth curve experiments have been done on P_{MET}-NOC2/Gar1-mCherry/Noc1-GFP and P_{MET}-NOC2/Gar1-mCherry/Rix7-GFP. In one case, cells where left to grow in their repressive media from time 25 to time 60 h, whereas in the other case, the repressive media was refreshed every 4-5 h without diluting cells, the resulting difference that cells left in their media for a long period, undiluted grew faster rate. Indeed, it appears that in these cultures methionine concentration was decreased over time due to metabolical breakdown, which allowed the re-induction of NOC2, albeit at very low levels.

In order to verify both our hypothesis and the effect of Noc2p depletion, we performed Western blot and qRT-PCR analyses to look at Noc2p total levels and at NOC2 mRNA levels under the MET25 promoter at each time point taken. Indeed, Western blot analysis indicated that Noc2p levels in the cell decreased significantly after 8 hours of depletion in every strain. Moreover, NOC2 re-induction was confirmed by visualizing Noc2p at time 60 h in cells left to grow in the repressive media, without further refreshing methionine levels. However, the detected Noc2p levels were very low compared to permissive media. Indeed, longer exposure in addition to longer depletion time could reinforce this affirmation. Moreover, we performed qRT-PCR by comparing NOC2 mRNA levels in permissive media and after 14 h of depletion, and only 8.1% of NOC2 mRNA was present after 14 h, compared to 100% at time 0. Indeed, it is possible that at this point NOC2 expression is completely repressed; the detected mRNAs were synthesized prior to the shift to repressive media, or in the first few hours of depletion.

These mRNAs could be very stable and allowed synthesis of a non-significant amount of Noc2p, which were not visualized by Western blot analysis. However, it is possible that mRNA levels continue to decrease after 14 h when restrictive media is refreshed, and mRNAs gradually degraded. However, when methionine concentration decreases, allowing NOC2 re-induction, the mRNA pool is slowly replenished and Noc2p translated. However, since we do not know NOC2 mRNA half-life, this remains speculation at this point.

During our growth curves, several time points have been collected in order to perform microscopy, Western blot and qRT-PCR analyses. These studies allowed us to compared new data about Noc protein dynamics with previous data obtained by using *ts* strains, and also studying the effect and correlation between Noc2p function and Rix7p. Moreover, our data pinpointed a so far unknown role of Noc2p in nucleolar structural integrity.

4.1.1 The influence of Noc2p on nucleolar integrity

Eukaryotic cells were shown to contain a specialized subcompartment within the nucleus, called the nucleolus, which is known to be the site of rRNA synthesis, modification, processing and assembly [104, 105]. Using electron microscopy, specific components of this specialized structure were visualized, such as the fibrillar center (FC), which was shown to be surrounded by the dense fibrillar component (DFC). Both are embedded in the granular component (GC) [105]. Indeed, nascent rDNA transcripts were found to localize and elongate in the junction region between the FC and DFC, and to enter into the surrounding DFC region in order to be modified and processed, and to continue their intra-nucleolar migration through the GC region, while continuing to be processed and assembled [11, 105]. Interestingly, although condensed chromatin has been visualized in the nucleolus by electron microscopy, the overall amount of DNA is suggested to be low since DAPI DNA staining is excluded from the nucleolus [105]. Accordingly, this was confirmed by our microscopy results (Figure 3.3, 3.4, 3.5 and 3.8, 3.9 and 3.10). The DAPI stained region almost never colocalized with our nucleolar marker Gar1p. As mentioned previously, Gar1p has been identified to be part of box H/ACA snoRNPs, as well as Cbf5p, Nop10p and Nhp2p [23]. These box H/ACA snoRNPs are known to base pair with the pre-rRNA and to convert selected uridines to pseudouridines early during pre-rRNA maturation, whereas C/D box snoRNPs, containing

Nop1p, are known to 2'-O-methylate pre-rRNA [23]. Indeed, Gar1p and Nop1p have already been used as nucleolar component markers for the DFC, and are known to colocalize [106].

We tagged Gar1p with a mCherry tag at its C-terminal in order to visualize the nucleolus and to study nuclear non-ribosomal proteins. Indeed, we observed that Gar1p exhibited a nucleolar localization in every strain under normal conditions (Figure 3.3, 3.4, 3.5 and 3.8 Time 0; 3.9 A, B and 3.10 Before), where in some cases, clear crescent-like shapes were observed. Interestingly, after Noc2p depletion, we observed the diffusion of Gar1-mCherry all over the nucleus, while no more crescent shape nucleolus could be detected (Figure 3.3 A, 3.4 and 3.5 A, 3.8). In fact, we observed a distinct colocalization of Gar1p and the DAPI stained nuclear region. Since Gar1-mCherry was our nucleolar marker, it indicated that in these cells in the absence of Noc2p, the nucleolus had lost its structural integrity. In mammalian cells, the nucleolus can be disorganized at distinct and specific phases of the cell cycle. However, in yeast, the nucleolus is known to be active and structurally condesed throughout the entire cell cycle, which refutes any hypothesis that nucleolar redistribution visualized under Noc2p depletion is a normal cell cycle process or phenomenon [107]. Thus, different hypotheses may be formed with regard to the observed Gar1p redistribution, which will be discussed below.

Noc2p may be required for efficient processing of pre-RNA

One hypothesis could be that Noc2p depletion could lead to pre-rRNA redistribution or even degradation. In fact, Noc2p has been shown to form a hetero-trimeric complex, Rrp5p-Noc1p-Noc2p, in which Rrp5p and Noc1p were shown to be associated with the A_3 cleavage site and the 25S rRNA coding region of the 35S rDNA, respectively [25, 55]. Indeed, this could suggest that depletion of Noc2p causes the incapacity of the two other proteins to efficiently bind to the rDNA causing ineffective pre-rRNA processing. This could induce aberrant pre-rRNA synthesis and degradation by the polyadenylation and TRAMP targeting of pre-RNAs. However, pre-rRNA processing analyses performed using both *ts noc2-1* and P_{GAL}-NOC2 revealed only a mild processing delay [47, 55], thus this first hypothesis is unlikely.

Noc2p - a checkpoint for pre-rRNA passage from nucleolus to nucleus

The Noc proteins are known to be composed of HEAT-repeats that are predicted to form extended structures helping the protection of hydrophilic rRNA surfaces and allowing pre-ribosome transport [50, 103]. Indeed, Noc2p could play a role in a control checkpoint allowing transit of the pre-rRNA from the nucleolus to the nucleoplasm. Without Noc2p, pre-rRNA translocation is not timed and early pre-ribosomes can be found all over the nucleus, while continuing to be processed, which could explain the localization of Gar1p throughout the nucleus (Figure 3.3 A, 3.4 and 3.5 A, 3.8). In order to test this hypothesis, fluorescent *in situ* hybridization (FISH) experiments should be performed using specific Cy3-labeled probes targeting different pre-rRNA regions located within either the ITS1 or ITS2 region. Under normal conditions, ITS1 has been shown to be present in the early 35S, 32S and 20S pre-rRNA but absent from mature 18S rRNA as it is excised, which allows for its detection in the nucleolus and cytoplasm by FISH, the latter due to export of 20S pre-RNA. Indeed, it would be interesting to look at the efficiency of the 20S export. Especially, since Rrp5p is present in a trimeric complex with Noc2p and is known to be important for both 60S and 40S subunits synthesis just prior to separation of 20S and 27S precursors. In higher eukaryotes, hRrp5 is also known to interact with the human Noc2p homolog NIR [29, 50, 55, 64]. ITS2, on the other hand, was shown to be concentrated in the nucleolus and only weakly in the nucleoplasm and along the nuclear periphery [103]. Hence, it would be interesting to determine whether Noc2 depletion has an effect on the association of late processing steps at the nuclear periphery.

Noc2p may play a role in pseudouridylation machinery localization

Noc2p could also be required for the nucleolar localization of the pseudouridylation machinery, independent of pre-rRNA localization. It has been shown that disruption of Gar1p/Rnt1p interaction causes an impairment of the nucleolar localization of Gar1p, Cbf5p and Nhp2p. [108]. More precisely, these three proteins were shown to exhibit a cytoplasmic localization in Rnt1p mutants, suggesting that Gar1p needs to interact with Rnt1p in order to reach the nucleolus [108]. Moreover, this box H/ACA snoRNP redistribution was shown to cause a strong delay in rRNA processing, which is in agreement with the fact that rRNA modification by box H/ACA snoRNPs is carried out in the nucleolus [108]. Indeed, this study proved that one protein alone can dictate the intracellular localization of Gar1p and its

partners. Although our results did not show a cytoplasmic localization of Gar1-mCherry, Noc2p depletion induced an intranuclear redistribution of Gar1p. However, visualization of Cbf5p and Nhp2p over Noc2p depletion will be essential in order to determine if the effect seen here is similar to that of an Rnt1p mutant. If Cbf5p and Nhp2p redistribute under Noc2p depletion, it could suggest that Noc2p is required for the nucleolar localization/targeting of the pseudouridylation machinery. However, it has been shown by Northern blot analysis that pre-rRNA processing is not significantly affected in both *ts noc2-1* mutant and P_{GAL1}-NOC2 strains [47, 55]. Indeed, quantification of pre-rRNA base modifications would be a good way to look at a possible pseudouridylation defect [109].

Noc2p may be required for nucleolar integrity and rDNA regulation

As mentioned above, a previous study looked at Nop1p localization in an Rnt1p mutant in order to show that the mislocalization of Gar1p was not due to a general nucleolar disruption [108]. This lead us to propose another hypothesis, which is that Noc2p may be required to maintain the integrity of the nucleolar structure. Indeed, it has already been suggested that maintainance of nucleolar organization is a consequence of ribosome biogenesis activity and rDNA transcrition [104]. In fact, this link has been demonstrated in HeLa cells by inducing an arrest in rDNA transcription with actinomycin D [104, 105]. Under these conditions, the FC and DFC were shown to condense and migrate towards the nucleolar periphery in order to segregate with all nucleolar components and form a central body [104].. In yeast cells, down-regulation of pre-rRNA synthesis using a *ts* mutant expressing defective Pol I transcription factor Rrn3p has caused an intra-nuclear redistribution of Nop1p [54]. Both, the nucleolar marker Nop1p, and the early factors Noc1p and Nop7p were shown to redistribute in the *rrn3-8* mutant, by overlapping significantly with the DAPI stained nucleoplasmic region [54]. At this point, it had been suggested that this kind of intra-nuclear redistribution is caused by putative changes in the nucleolar structure due to inhibition of Pol I transcription [54]. Since our results show Gar1p nuclear diffusion under Noc2p depletion, similar to that of Nop1p redistribution in the *rrn3-8* cells, we hypothesize that Noc2p depletion affects rDNA transcription, inducing collapse of nucleolar integrity and intra-nuclear restructuration. The effect of Nop2p on nucleolar intergrity is supported by the fact that re-

induction of minimal amounts of Noc2p in non-replenished repressive medium, result in a reversal of the effect, and the re-formation of a nucleolus (Figure 3.3 and 3.5 C).

In order to test this hypothesis further, actinomycin D treatment should be performed in Gar1-mCherry strains and localization of this nucleolar marker should be compared to our previous data. Thereafter, electron microscopy analysis should be performed before and after Noc2p depletion in order to compare the normal nucleolar substructure and size to nucleoli in Noc2p depleted as well as actinomycin D treated cells. Since it has been shown that during nucleolar inactivation induced by transcriptional arrest, the perinucleolar compartment (PNC) and the SAM68 nuclear body disassemble, markers of these compartments could be used to study their redistribution in Noc2p depleted cells [110]. Finally, it could also be interesting to study pre-rRNP complexes purified with epitope-tagged Gar1p before and after Noc2p depletion, which could provide information about the effect of Noc2p on the components of early pre-60S complexes.

This hypothesis is also in agreement with the slow growth rate observed in Noc2p depleted cells (Figure 3.2). Moreover, it could also provide a link with the function of human Noc2p homolog, NIR. It has been shown that NIR contains an INHAT domain, which binds efficiently to nucleosomes and blocks acetylation of the core histones H3 and H4 [63]. Since histone acetylation is linked to actively transcribed genes, NIR appears to be involved in the repression of transcription, possibly of rDNA. Indeed, Noc2p could act as a transcriptional modulator of rDNA, with Noc2p depletion resulting in the de-repression of rDNA transcription, making more rDNA units actively transcribed and hence expanding the nucleolus out into the nucleoplasm.

4.1.2 Noc2p influence on Noc1p and Noc3p.

As previously mentioned, influence of Noc2p function on its partners Noc1p and Noc3p has been tested using a *ts noc2-1* mutant. These analyses showed a static picture of the Noc-complexes exchange due to the short duration of the experiment and limited number of time points. Here, we re-examined previous studies by using the MET25 promoter to regulate NOC2 expression and expanded the analysis.

Noc1p localization and protein level are influenced by Noc2p

Noc1p was shown to be nucleolar by its presence in a crescent-like structure within the nucleous, and colocalization with the nucleolar maker Nop1p [47, 54]. Under wild-type conditions, we observed the same Noc1p nucleolar distribution and its colocalization with the nucleolar marker Gar1p (Figure 3.3 A Time 0). Moreover, we also observed this nucleolar distribution in permissive conditions and up to 8 h after switching cells to repressive media. Noc2p can still be detected up to 8 h by Western blot. After 10 h Noc1p started to redistribute, and finally colocalize with the DAPI stained region after 14 h, which is in concurrence with a Noc2p decrease in the cells. This is also in accordance with previous results that showed Noc1p redistributed through the entire nucleoplasm in *ts noc2-1* mutants after switching cells from 23°C to 37°C for 6 h. Initially, our result appears to be similar to the previous studies, which suggested that Noc1p exhibits a dynamic intra-nuclear distribution in that it has the potential to shuttle between the nucleolus and the nucleoplasm [47]. However, upon closer examination, we realized that the nucleolar marker, Gar1p, no longer exhibited a crescent-like localization, but rather colocalized almost completely with the DAPI, in the same manner as Noc1p (Figure 3.3 A). Consistent with our hypothesis regarding to Gar1p diffusion and nucleolar integrity, we suggest that Noc1p is not shuttling between the nucleolus and the nucleoplasm, but rather its distribution changes to a collapse in nucleolar structures and it is therefore redistributed along with the rDNA and pre-rRNA. Noc1p diffusion has already been shown by down-regulation of pre-rRNA synthesis using a *ts* mutant expressing defective RNA Pol I transcription factor Rrn3p [54]. Moreover, the same phenotype has been observed with another, usually later, nucleolar protein, Nop7p, suggesting that this redistribution is not specifically related to Nop1p, Noc1p and Gar1p [54]. It thus supports the hypothesis that Noc2p influences rDNA transcription and /or nucleolar integrity, inducing a restructuring of the nucleus.

Furthermore, longer Noc2p depletion times allowed us to observe Noc1p in the entire cell. More precisely, Noc1p was found to be concentrated in foci, which do not correspond to either the nucleolus or the nucleus and are located in the cytoplasm (Figure 3.3 A 25 hours). Indeed, Noc2p depletion may induce cellular stress that causes either the sequestration or the degradation of excess levels of Noc1p in the cytoplasm. In comparison, we observed by

Western blot analysis that Noc1p levels decreased under Noc2p depletion while NOC1 mRNA levels remained constant (Figure 3.6 and 3.7). In fact, Noc1p is essential for cell viability and continuously transcribed [52, 111-113]. Moreover, since we observed no significant change in its mRNA level by qRT-PCR, we suggest that NOC1 mRNA stability is not affected by Noc2p depletion. Accordingly, post-transcriptional control, other than mRNA degradation, could be the result of this decrease of Noc1p level and this cytoplasmic relocation over Noc2p depletion. To confirm this, we should use known markers of stress granules and P-bodies, such as Pub1p and Edc3p, respectively, to determine if Noc1p and even NOC1 mRNA colocalize with one of them under Noc2p depletion [92]. In fact, NOC1 mRNA could be sequestered and stored in P-bodies under these conditions until re-initiation. Moreover, it is possible that Noc1p is degraded in proteasomes located in the cytoplasm. Since the foci corresponding to Noc1p were really close to the nucleus, we can also suggest that some nucleus-vacuole junctions were formed. It has been shown that under conditions of nutrient depletion, nucleus-vacuole junctions expanded and mediated a unique autophagic process which target specific portions of the nucleus for degradation [93]. This portion is known to contain nuclear envelope and nucleolar pre-ribosomes [93]. However, our results did not show a colocalization of Noc1p with Gar1p in these foci. Indeed, it appears to be Noc1p specific. To determine the identity of these foci, Vac8p and Nvj1p could be used as markers of nucleus-vacuole junctions, since they are formed through specific interactions between these two proteins, and determine whether Noc1p colocalizes with these proteins [93]. In addition to microscopic analysis, Noc1-GFP should be affinity purified under Noc2p depletion to determine whether it is found in complexes with components of the degradation machinery.

Since decrease of Noc1p levels seemed to be caused through post-translational regulation, we should further study its post-translational modifications. Hence, we could apply new methods developed in yeast *Saccharomyces cerevisiae* in 2013, allowing for the identification of protein isoforms that could be both phosphorylated and ubiquitinated, and targeted for protein degradation via the ubiquitin-proteasome system [114]. In fact, cross-regulation and substoichiometric balance between phosphorylation and ubiquitylation has been demonstrated and pushed forward the development of new approaches of investigation, combining nano-reversed-phase liquid chromatography (nRPLC) and mass spectrometry

(MS/MS), which would be useful here [114]. Indeed, we would be able to see if Noc1p post-translational modifications are affected or altered under Noc2p depletion.

Regardless, our results raise questions about previous conclusions, which were that Noc1p redistributes through the entire nucleoplasm when Noc2p is non-functional, due to its ability to shuttle [47]. In fact, it appeared that Noc1p stayed in the nucleolus under Noc2p depletion but that it is the nucleolus itself that reorganized. Indeed, Noc2p may have no direct role in Noc1p nucleolar localization, but rather a role in influencing nucleolar structure, by what mechanisms remains to be determined. However, the longer the depletion of Noc2p continues, cells seem to be extremely affected, shown by their slow growth rate and fitness. At this point, Noc1p should be degraded since ribosome biogenesis will be down regulated, which fits with the observation of Noc1p in the cytoplasmic foci. However, its mRNA level may remain constant to allow for a rapid response in case the stress will be lifted and re-induction of Noc2p expression is required.

Noc3p localization and levels are influenced by Noc2p

Under normal conditions, Noc3p was shown to localize throughout the nucleus, with some enrichment in the nucleolus [47]. Indeed, we confirmed the previous observation of nucleolar enrichment by observing its co-localization with the nucleolar marker Gar1p. By using *ts noc2-1* mutants, previous data reported no significant change in Noc3p localization [47]. In contrast, our results identified a fine distinction under Noc2p depletion; we observed a diffusion of Noc3p in the nucleoplasm from the beginning of the Noc2p depletion experiment (Figure 3.4). Since Noc3p has been suggested to be a component of pre-replication and post-replication complexes, and whereas it is known that Noc3p is bound to chromatin throughout the cell cycle at a constant level, we do not know the impact of this relocation on DNA replication or Noc3p interaction with chromatin [66]. As mentioned, Gar1p was shown to diffuse throughout the nucleus under Noc2p depletion. Indeed, we do not know if Noc3p relocation is due to the nucleolar collapse and rearrangement as suggested above, or whether it is redistributing upon compositional change of Noc3p associated complexes. Once again, it will be useful to affinity purify Noc3p associated complexes under Noc2p depletion, to study changes in its interactome. Decreased amounts of Mcm2p, Mcm5p and Orc1p, known to

normally precipitate with Noc3p and to be involved in DNA replication, or increase of nucleoplasmic proteins and components of the nuclear pore complex would provide insights about potential new functions of Noc3p in the absence of Noc2p.

Longer Noc2p depletion times allowed us to observe a cytoplasmic diffusion of Noc3p (Figure 3.4 25 h). However, this diffusion was less intense than that of Noc1p and a stronger Noc3-GFP signal was still present throughout the nucleus. Accordingly, Western blot analysis under Noc2p depletion did not show a strong decrease of Noc3p levels. Thus the question remains: does Noc2p depletion cause a functional incapacity or change of Noc3p to fulfill its role in DNA replication and induce relocation? Does Noc2p depletion induce Noc3p dissociation from the pre-ribosomes after cytoplasmic export, causing cytoplasmic diffusion? Again, affinity purification of Noc3p-associated complexes with provides additional indication about newly formed complexes, and may allow us to determine what happens with Noc3p and its associated partners. Similar to NOC1 mRNA levels, no significant change in NOC3 mRNA levels was detected. Nevertheless, we still observed a decrease in NOC3 mRNA levels 14 h after depletion. Although this decrease was not considered significant, further time points such as 25 h might provide more insight into NOC3 mRNA level changes. Indeed, we should consider a potential NOC3 mRNA regulation, such as transcriptional regulation or mRNA degradation upon Noc2p depletion. Thus, later time points must be analyzed. As mentioned for Noc1p, we could also test the effect on Noc3p post-translational modifications under Noc2p depletion by using new approaches that combines nano-reversed-phase liquid chromatography (nRPLC) and mass spectrometry (MS/MS) [114].

Unlike previous conclusions, suggesting that Noc2p functionality has no influence on Noc3p localization, our results showed a mild redistribution of Noc3p from an enriched nucleolar to a more uniformly nuclear distribution. Once again, an intra-nuclear rearrangement or the loss of nucleolar integrity may be involved and needs to be considered. Moreover, Noc3p protein levels must be re-evaluated using ImageQuant software, and its mRNA level must be re-evaluated at later time points after Noc2p depletion.

4.1.3 Noc2p depletion influences Rix7p intra-nuclear localization

Next, Rix7p was studied in order to pinpoint a possible link with Noc2p as well as Noc protein complex formation. In fact, all the Noc proteins and Rix7p have been identified as ribosome export factors (rix) [44, 47]. Moreover, Rix7p is an AAA-ATPase which has been shown to play a role in ribosomal particle rearrangement in an overlapping step where Noc1p-Noc2p and Noc2p-Noc3p exchange is thought to take place. In addition, this protein is known to be a homologue of Cdc48, which recognizes ubiquitinated proteins and dissociates them from non-ubiquitinated binding partners [45]. Since Noc2p is the intermediate and common protein between these two complexes, we were interested to see if Noc2p could have any influence on Rix7p.

Using the same approach as for Noc1p and Noc2p, we observed the localization, the total level and the gene expression of Rix7p under Noc2p depletion. Under normal conditions and exponential growth, Rix7p was distributed throughout the entire nucleus with enrichment in the nucleolus, consistent with the literature (Figure 3.5 A Time 0). In fact, Rix7p had been shown to have an overall nuclear distribution by fluorescent microcopy, but to co-precipitate with a large amount of nucleolar factors, such as Nop7p and Nsa1p-associated particles [44, 45]. However, we observed that the fluorescent signal was not uniform but rather in a dotted pattern. Indeed, it could be interesting to investigate this peculiar nuclear distribution by looking at associating proteins using affinity purification coupled with mass spectrometry, and by looking at its colocalization with selected markers. In fact, the nucleus is composed of specific sub-compartments such as the nuclear bodies, where proteins can accumulate [115]. Nuclear bodies have been proposed to refine several cellular processes by allowing and facilitating protein post-transcriptional modifications such as sumoylation [115]. Interestingly, the pre-60S assembly factor Nsa1p, previously shown to be removed from the pre-ribosome by Rix7p, is known to exist in both ubiquitinated and sumoylated forms [40]. Indeed, it has been proposed that these two post-transcriptional modifications can regulate its dissociation by Rix7p [40]. Accordingly, we should undertake future studies to look at a colocalization between Rix7p and a nuclear body marker.

By depleting Noc2p, Rix7p was less enriched in the nucleolus and colocalized with the DAPI stained region, similar to Gar1p, suggesting it is also affected by the intra-nuclear reorganization. After 20 and 25 hours of Noc2p depletion, Rix7p was distributed throughout the cell, with enrichment in the nucleus. Moreover, by depleting Noc2p, Rix7p levels decreases whereas its mRNA levels did not change significantly, which suggests, together with the microscopy analysis, that Rix7p is post-translational regulated under Noc2p depletion.

Since Rix7p is suggested to be involved in particle remodeling, it will be essential to look at its effect on the Noc proteins. In fact, the next step will be to put RIX7 under the control of the inducible promoter MET25, as done with NOC2, and look at its influence on the three Noc proteins tagged with GFP. Since it has been shown that mutation of Rix7p causes the incapacitation of Nsa1p to dissociate from pre-ribosomes and induces its relocalization in the cytoplasm, it is possible to imagine the same phenotype for the Noc proteins.

4.1.4 Noc2p depletion related phenotypes are reversible

Growth curve experiments were performed in two different manners. In one of them, media was always refreshed. In the second one, cells were left in the same repressive media for 25 to 60 h. In the latter, NOC2 expression was re-induced, most likely due to the decrease in methionine concentration in the repressive media over time. However, re-induced levels of Noc2p were very low at 60 h.

In this particular experiment, we observed that Gar1p, Noc1p and Rix7p localization had returned to wild-type distribution (Figure 3.3 and 3.4 C). However, their total protein levels did not return to a normal level (Figure 3.6 A, F). Indeed, we suggest that decreases in methionine concentration allowed NOC2 re-induction by MET25 which directly affect the new synthetized-proteins localization. Longer re-induction times should be performed in order to observe whether protein amounts will return to a wild-type level. Moreover, this particular experiment should be performed with the P_{MET}-NOC2/Gar1-mCherry/Noc3-GFP strain in order to see if relocation is also possible for Noc3p.

4.1.5 Noc2p depletion influences levels of other nuclear proteins

In addition to studying Noc1p, Noc3p and Rix7p, we decided to take a look at other proteins. Indeed, since Noc2p depletion seemed to cause a stronger effect than what was previously thought, we selected proteins known to be in an overlapping step with the Noc proteins. Moreover, due to the role of the human Noc2p homologue NIR on chromatin, we also looked at histone proteins.

Noc2p is not linked to Nop7p but significantly influences SSF1mRNA levels

At first, we looked at Nop7p. Nop7p has been shown to bind directly to the 5' coding region of 25S rRNA and to form a trimeric complex with Erb1p and Ytm1p, which is involved in $27SA_3$ pre-rRNA processing [36, 116]. Moreover, it has been found to be present in several particles, such as Ssf1p, Nsa1p, Rix1p and Arx1p particles and is believed to be a scaffold protein [45, 117]. In this way, the Noc proteins and Rix7p have been identified by performing a Nop7p-PrA and Nop7-TAP affinity purification coupled with mass spectrometry analysis (Oeffinger, unpublished data) [45]. Indeed, the Ytm1p-Erb1p-Nop7p subcomplex was shown to be present in isolated Nsa1p particles, which contained Rix7p, and in which the Noc1p-Noc2p to Noc2p-Noc3p complexes exchange had already been made [2]. We observed Nop7p protein levels and its mRNA levels under Noc2p depletion. Both protein and mRNA levels remained constant, suggesting that Noc2p is neither linked or does not influence Nop7p even if it is known to be in the same particle as Noc2p. However, it could be interesting to look at Nop7p localization and affinity partners under Noc2p depletion. It is interesting to note, that while Nop7p is also found in the nucleolus, it is mostly associated with later nuclear processing steps.

Ssf1p and Ssf2p are paralogs that have been found to be part of the Brix/Imp superfamily and to bind within the ITS1 region of the pre-rRNA. They are localized to the nucleolus. In addition to interacting with several assembly factors, these proteins have been shown to interact with histone modifiers and histone proteins. Indeed, Ssf1p is known to bind to H3 and H4 proteins, Sdc1p, which is involved in H2AZ to H2A exchange and to Eaf7p,

which is an acetylase of the H4 and H2A N-terminal tails [72, 118]. Ssf2p has been shown to interact with Rpd3p and Hda1p, which are histone deacetylases [72]. Since the human Noc2p homolog NIR has been shown to be potentially involved in histone modifications, we were interested to look at a potential link between Noc2p and Ssf1/2p. Indeed, we studied only their mRNA levels because we did not have antibodies to look at their proteins levels. Interestingly, although Ssf1/2 are known to be paralogs and to share 94% sequence homology, we found that while SSF1 mRNA levels increased significantly under Noc2p depletion, SSF2 mRNA levels did not change significantly. NIR has been shown to block acetylation of H3 and H4. Indeed, it could be possible that SSF1 mRNA synthesis or stability is linked to NOC2 synthesis, due to its potential relation with acetylation of histones. Moreover, it raises the question about the non-redundant function between Ssf1p and Ssf2p. Ssf1/2 protein levels and their localization under Noc2p depletion conditions should be determined, in combination strains such as the P_{MET}-NOC2/Gar1-mCherry/Ssf1-GFP and P_{MET} -NOC2/Gar1-mCherry/Ssf2-GFP.

Noc2p depletion influences histone protein and mRNA levels

As mentioned, NIR has been shown to bind efficiently to nucleosomes and to block acetylation of core histones H3 and H4 [63]. Indeed, we wanted to look at these proteins under Noc2p depletion in order to see if Noc2p could influence their protein and mRNA levels. Therefore, due to lack of antiboies, we only looked at H4 levels as an indicator of the H3-H4 tetramer, and at H2B levels as an indicator of the H2A-H2B dimer, contained in the core histone. We observed that both H2B and H4 protein levels decreased over time under Noc2p depletion. Histone levels can be regulated by degradation monitored by the kinase Rad53p [119]. Indeed, Rad53 can phosphorylate all four histone proteins prior to degradation by the proteasome [119]. It would be interesting to use phospho-antibodies in order to see if Noc2p depletion causes an increase in the phosphorylated forms of the histones. It has been shown that depletion of H2B causes defects in chromatin structure and nuclear segregation, which could be the case here, possibly due to an effect of Noc2p depletion of histone acetylation, which should be determined using acetyl-histone antibodies [120].

Thereafter, we looked at H2A and H3 mRNA levels since H4/HHF1 gene had to be excluded from the analysis due to unspecific primer hybridization. Indeed, we observed a

strong increase in both H2A and H3 mRNA levels upon Noc2p depletion. It has been shown by pulse-chase experiments that a peak in core histone mRNAs levels occurs normally later than during mRNA synthesis, indicating that core histone genes are regulated post-transcriptionally [119]. In fact, it has been determined that histone mRNA stability increases as cells enter S phase, whereas inhibition of DNA replication causes a reduction of the half-life of H2A and H2B mRNAs [119]. Indeed, Noc2p depletion may delay cells in S phase, which needs to be determined. Since histones are directly related to cell cycle, we should synchronize our cells and perform another growth curve experiment in order to determine the role of Noc2p on histones during the cell cycle. There are three common ways to synchronize yeast cells early during the cell cycle; one is to use the mating pheromone α-factor, which is known to inhibit Cdc28p activity leading to an arrest at the G1/S phase boundary; the second hydroxyurea, which is known to inhibit ribonucleotide reductase and blocks cells in early S phase [121]. Lastly, early G1/S phase cells can be isolated by elutriation centrifugation, where cells are separated by size.

As previously mentioned, we hypothesized that one reason for the Noc2p depletion could be due to an inhibition or down regulation of RNA polymerase I, which could induce a slow growth rate and a potential intra-nuclear restructuring. RNA polymerase I activity has been shown to be constant over the entire cell cycle under normal conditions [122]. However, efficient rDNA transcription requires several factors such as the TATA-binding protein, Rrn3p, the core factor and the upstream activating factor (UAF). In relation to a potential transcription inhibition, UAF has been shown to be composed of six polypeptides, in addition to H3, H4 and Uaf30p [123]. Therefore, effects on histones H3 and H4 could affect transcription rates since binding of UAF to the promoter is necessary to recruit both core factor and the RNA polymerase I-Rrnp3 complex [123]. Since it is known that rDNA repeats are excised as extra-chromosomal circles over the life span of a yeast cell, which are then transcribed by RNA Pol II, it is possible that ribosomes synthesized from these circles keep cells viable in case of an effect of Pol I transcription rates, which would also result in a collapse of nucleolar integrity [124]. Previous data, where pre-rRNA was synthesized from Pol II transcribed plasmids in the absence of Pol I transcription, cause a viable, slow growth phenotype [125].

Moreover, histones are known to be components of nucleosomes. Thus, alteration of their levels may affect chromatin structure. An alternate hypothesis is that, quite the opposite, an effect on chromatin structure could lead to more open confirmation of rDNA and thus loss of nucleolar integrity. Indeed, we are currently optimizing a Psoralen-crosslinking protocol in order to look at the co-existence of the two distinct rDNA chromatin populations. It is known that rDNA exists in two different chromatin states, where some are actively transcribed and depleted of nucleosomes, whereas others are transcriptionally repressed and assembled with nucleosomes [86]. NIR was shown to be a histone acetyltransferase inhibitor, which inhibits transcription. Indeed, by looking at the chromatin states using this method and the acetyl-histones state by performing western blot analysis under Noc2p depletion, we will determine a potential link between Noc2p and NIR function. However, by looking at the slow growth rates and the intra-nuclear redistribution, transcription seemed to be decreased under Noc2p depletion, which would be in contradiction with and absence of NIR function.

4.2 Influence of reversibly depletion of free cellular energy

About 20% of ribosome assembly factors are considered nucleoside triphosphate hydrolyzing enzymes, which are believed to provide the energy needed to confer directionality to the ribosome maturation pathway [2, 40]. One of them, Rix7p, is an AAA-ATPase known to hydrolyze ATP in order to remove and recycle Nsa1p from pre-60S particles [45]. This removing step has been found to coincide with compositional change of pre-60S particles, where early factors such as Noc1p were identified to be removed and where some later factors were identified to be integrated. Indeed, we hypothesize that the Noc1p-Noc2p and Noc2p-Noc3p exchange may be performed at this crucial step and that it may involve ATP hydrolysis. Since there are several enzymes that are known to utilize energy prior to and around the same time as Rix7p and the Noc protein exchange, we decided to first study the general influence of free energy from nucleotide sources on Noc proteins. To this aim, we performed reversible depletion of free cellular energy using metabolic poison, which is a glucose media that contains sodium azide and deoxy-d-glucose, leading to a decrease of free ATP and GTP production in the cell.

Noc1p-Noc2p and Noc2p-Noc3p exchange could be related to energy-dependent intranuclear translocation

First, we looked at the localization of Noc proteins under these conditions. Consistent with previous result, we observed that Noc1p remained in the nucleolus, which suggests that its localization is not influenced by ATP or GTP-dependent steps [31]. However, it could also be due to some complex reorganization since pre-60S translocation between sub-nucleolar compartments as well as the nucleolus and the nucleoplasm could be blocked, effectively trapping Noc1p in the nucleolus. It has been shown that under glucose starvation, the majority of mRNP proteins relocalized into P-bodies and stress granules [92]. Some of them, such as Bfr1p and Scp160, also dissociated from the ER or moved into vacuoles (Scw4p) [92]. However, nucleolar proteins involved in pre-rRNA processing, such as Noc1p, Noc2p, Nop7 and Ssf1p, were shown to remain in the nucleolus during glucose starvation without using

sodium azide or deoxy-d-glucose [92]. Indeed, Noc1p interactors may be affected by a decrease of free energy in the cell, but this phenotype may not be observable by fluorescent microscopy. Affinity purification of Noc1-GFP coupled with mass spectrometry analysis upon cellular energy depletion must be performed in order to identify interactions changes.

We also observed that Noc3p relocated at the nuclear periphery energy depletion conditions, which has already been seen in a previous study [31]. Indeed, this suggests that Noc3p could associate at some stage with pre-ribosomes at the nuclear periphery and that it requires ATP or GTP to be recycled back to associate with earlier pre-ribosomes, or to dissociate from pre-ribosomes prior to export. Furthermore, we observed that Noc2p redistributed under these conditions. In fact, its localization appeared to be strongly concentrated in the nucleolus, compared to an intermediate localization under normal conditions. A similar phenotype has been already seen in *noc3-1 ts* mutant cells where Noc1-GFP and Noc2-GFP were found to be highly concentrated in the nucleolus [47]. Indeed, it could be possible that depletion of free energy causes the incapacity of Noc3p to bind to Noc2p, inducing a reorganization of the Noc proteins complexes, or that either ATP or GTP is needed to translocate Noc1p-Noc2p containing pre-ribosomes to the nucleolar sub-compartment, where they dissociate and Noc2p binds to Noc3p. Once again, affinity purification of the three proteins will be essential to distinguishing compositional changes of these particles. Interestingly, we re-induced ATP and GTP synthesis by incubating cell in fresh media containing 2% glucose. At this point, Noc1p was shown to concentrate in the nucleolus, whereas Noc2p was shown to redistributed to its normal localization, while displaying a stronger signal. By contrast, Noc3p, which is usually nuclear, was shown to have a nucleolar crescent-like distribution. Indeed, Noc3p nucleolar redistribution could be due to compensate for accumulated pre-ribosomal stages.

Moreover, we were interested to see if depletion of free energy could modulate protein levels in the same way as Noc2p depletion. In fact, we were thinking that the incapacity of performing the Noc1p-Noc2p and Noc2p-Noc3p complex exchange could also modulate the levels of the selected proteins studied above. Indeed, no significant changes of Noc1p and Noc2p levels were observed in either stress or re-induction conditions. In contrast, NOC1 gene expression seemed to be strongly influenced by the available free energy in the cell. In fact,

its gene expression decreased significantly in poisoned media and increase significantly after re-induction (Figure 3.12 NOC1). Indeed, it seemed that cells need to downregulate NOC1 mRNA level, by transcriptional regulation, mRNA degradation pathways or by segregation in P-bodies or stress granules, when ATP and GTP were depleted. Thereafter, cells need to compensate for this down-regulation with a strong increase in NOC1 mRNA levels during the re-induction, either through an increase in mRNA synthesis or stability. Interestingly, we observed a slight increase of Noc3p levels when cells were incubated for 1 h in the metabolically poisoned media (Figure 3.11 C). This coincided with the perinuclear redistribution that we observed by microscopy, previously associated with nutrient starvation. Thereafter, we observed that Noc3p level decreased when cells were incubated for 1 h in normal condition. This suggests that Noc3p levels are modulated by the availability of free energy in the cell. In contrast, no significant changes were observed for either NOC3 or NOC2 mRNA levels. Indeed, the increase of Noc3p levels observed by western blot in the poisoned cells could be due to post-translational regulation, and not transcription regulation or mRNA stability. It could be useful to perform radioactive pulse-chase analysis in order to determine if Noc3p half-life is affected. Nevertheless, it is interesting to see that cells require more Noc3p during the decrease of free ATP/GTP, indicating another potential role for this protein, or that cells try to compensate the lack of ATP and GTP by re-routing pre-ribosomes during late stages of the maturation to preserve translation capability. It should be noted that whereas most pre-ribosome export pathways are GTP-dependent, the GTP-independent exporter Mex67p has also been implicated in export of pre-ribosome to the cytoplasm and could provide an alternative export pathway under these conditions.

Rix7p mRNA levels are strongly affected upon depletion of free energy

Since Rix7p has been identified as an AAA-ATPase, which hydrolyzes ATP, possibly aiding Noc1p-Noc2p and Noc2p-Noc3p exchange, we were curious to study both its localization and its protein and mRNA levels upon depletion of free ATP and GTP. Unfortunately, Rix7p localization is known to be affected by nutrient availability [44]. We observed that Rix7p was enriched in the nucleolus under these conditions, compared to its normal nuclear localization. Even if we cannot state that the nucleolar enrichment of Rix7p is not only due to glucose starvation, we can stipulate that Rix7p is not able to perform its

function, which is to release and exchange factor on the pre-ribosome under ATP depletion condition. The fact that Rix7p is accumulated in the nucleolus, suggests that its function and the rearrangement may be coupled to a nuclear translocation event during pre-60S maturation.

The fact that we also observed Noc2p enriched in the nucleolus and Noc3p redistributed at the nuclear pore complex, suggests that the complex exchange is not performed. At the same time, we observed that Rix7 was accumulated in the nucleolus, similar to Noc2p and Noc1p. Thus, free energy is required for Noc2p, Noc3p and Rix7p localization as well as Rix7p function, whereby its capacity of ATP hydrolysis enables rearrangements of pre-60S ribosomes, and, most likely the Noc1p for Noc3p exchange. After diluting cells in fresh glucose-SD-MET media, we observed that Rix7p was redistributed in the entire nucleus, since it colocalizaed with Gar1-mCherry and the DAPI stained regions (Figure 3.10 Re-induction). This result discords with previous data, where Rix7p has been shown to be perinuclear when cells are re-induced into fresh media after glucose starvation [44]. Indeed, we should try shorter incubation times in order to really pinpoint the dynamic redistribution.

By looking at Rix7p protein and mRNA levels during this nuclear transport arrest, we observed a small decrease in its protein levels and no significant change in its mRNA levels. However, RIX7 mRNA levels significantly increased upon re-induction into normal conditions. A similar phenotype was observed for NOP7 (Figure 3.12 NOP7). Indeed, the Ytm1p-Erb1p-Nop7p complex is known to be removed from pre-60S particles by Rea1p, another AAA-ATPase, and co-precipitate with Rix7p [43, 45]. In this regard, Nop7p or NOP7 is subject to modulaion by free ATP/GTP in the cell. Moreover, H2B and H3 mRNA levels were found to increase upon depletion of free energy, and to significantly decrease after re-induction. Our first phenotype could be linked to the fact that histone mRNAs levels are known to reach their highest peaks in S phase, due to an increase of their stability [119]. After re-induction, decrease of mRNA levels could be linked to a global inhibition of DNA replication known to cause reduction of half-live of the H2B mRNA [119]. Indeed, we suggest that histone mRNA levels are affected by the free ATP/GTP in the cell, caused by different replication ratio due to cell cycle arrest.

At this point we should definitely perform affinity purifications of the three Noc proteins and Rix7p to study their associated proteins under a decrease of free energy in the cell. Indeed, it will allow us to see potentially distinct enrichments of proteins due to energy-dependent check points such as Rix7-induced rearrangements, but also those involving the GTPase Nog1p and the ATPase Rei1p, which are also involved in ribosome biogenesis at steps overlapping with the Noc proteins. Moreover, we should design mutants of Rix7p within its two different AAA ATPase domains (D1 and D2) that are known to act differently with ATP [41]. Regardless, by looking once again at the Noc proteins, we will be able to pinpoint the potential role of Rix7p activity on Noc proteins complex exchanges, and possibly the role of Noc proteins overall.

5 Bibliography

1. Palade, G.E., *A small particulate component of the cytoplasm.* J Biophys Biochem Cytol, 1955. **1**(1): p. 59-68.
2. Kressler, D., E. Hurt, and J. Bassler, *Driving ribosome assembly.* Biochim Biophys Acta, 2010. **1803**(6): p. 673-83.
3. Venema, J. and D. Tollervey, *Ribosome synthesis in Saccharomyces cerevisiae.* Annu Rev Genet, 1999. **33**: p. 261-311.
4. Woolford, J.L., Jr. and S.J. Baserga, *Ribosome Biogenesis in the Yeast Saccharomyces cerevisiae.* Genetics, 2013. **195**(3): p. 643-81.
5. Fromont-Racine, M., et al., *Ribosome assembly in eukaryotes.* Gene, 2003. **313**: p. 17-42.
6. Wilson, D.N. and J.H. Doudna Cate, *The structure and function of the eukaryotic ribosome.* Cold Spring Harb Perspect Biol, 2012. **4**(5).
7. Ben-Shem, A., et al., *Crystal structure of the eukaryotic ribosome.* Science, 2010. **330**(6008): p. 1203-9.
8. Wimberly, B.T., et al., *Structure of the 30S ribosomal subunit.* Nature, 2000. **407**(6802): p. 327-39.
9. Korobeinikova, A.V., M.B. Garber, and G.M. Gongadze, *Ribosomal proteins: structure, function, and evolution.* Biochemistry (Mosc), 2012. **77**(6): p. 562-74.
10. Trumtel, S., et al., *Assembly and functional organization of the nucleolus: ultrastructural analysis of Saccharomyces cerevisiae mutants.* Mol Biol Cell, 2000. **11**(6): p. 2175-89.
11. Cheutin, T., et al., *Three-dimensional organization of active rRNA genes within the nucleolus.* J Cell Sci, 2002. **115**(Pt 16): p. 3297-307.
12. Panse, V.G. and A.W. Johnson, *Maturation of eukaryotic ribosomes: acquisition of functionality.* Trends Biochem Sci, 2010. **35**(5): p. 260-6.
13. Hamperl, S., et al., *Compositional and structural analysis of selected chromosomal domains from Saccharomyces cerevisiae.* Nucleic Acids Res, 2013.
14. Nogi, Y., R. Yano, and M. Nomura, *Synthesis of large rRNAs by RNA polymerase II in mutants of Saccharomyces cerevisiae defective in RNA polymerase I.* Proc Natl Acad Sci U S A, 1991. **88**(9): p. 3962-6.
15. Wittner, M., et al., *Establishment and maintenance of alternative chromatin states at a multicopy gene locus.* Cell, 2011. **145**(4): p. 543-54.
16. Johnson, J.M., et al., *Rpd3- and spt16-mediated nucleosome assembly and transcriptional regulation on yeast ribosomal DNA genes.* Mol Cell Biol, 2013. **33**(14): p. 2748-59.
17. Merz, K., et al., *Actively transcribed rRNA genes in S. cerevisiae are organized in a specialized chromatin associated with the high-mobility group protein Hmo1 and are largely devoid of histone molecules.* Genes Dev, 2008. **22**(9): p. 1190-204.
18. Turowski, T.W., *The impact of transcription on posttranscriptional processes in yeast.* Gene, 2013. **526**(1): p. 23-9.
19. Hamperl, S., et al., *Chromatin states at ribosomal DNA loci.* Biochim Biophys Acta, 2013. **1829**(3-4): p. 405-17.
20. Karbstein, K., *Role of GTPases in ribosome assembly.* Biopolymers, 2007. **87**(1): p. 1-11.
21. Kos, M. and D. Tollervey, *Yeast pre-rRNA processing and modification occur cotranscriptionally.* Mol Cell, 2010. **37**(6): p. 809-20.

22. Kufel, J., B. Dichtl, and D. Tollervey, *Yeast Rnt1p is required for cleavage of the pre-ribosomal RNA in the 3' ETS but not the 5' ETS.* RNA, 1999. **5**(7): p. 909-17.
23. Watkins, N.J. and M.T. Bohnsack, *The box C/D and H/ACA snoRNPs: key players in the modification, processing and the dynamic folding of ribosomal RNA.* Wiley Interdiscip Rev RNA, 2012. **3**(3): p. 397-414.
24. Choque, E., et al., *The nucleolar protein Nop19p interacts preferentially with Utp25p and Dhr2p and is essential for the production of the 40S ribosomal subunit in Saccharomyces cerevisiae.* RNA Biol, 2011. **8**(6): p. 1158-72.
25. Dembowski, J.A., B. Kuo, and J.L. Woolford, Jr., *Has1 regulates consecutive maturation and processing steps for assembly of 60S ribosomal subunits.* Nucleic Acids Res, 2013. **41**(16): p. 7889-904.
26. Oeffinger, M., et al., *Yeast Rrp14p is required for ribosomal subunit synthesis and for correct positioning of the mitotic spindle during mitosis.* Nucleic Acids Res, 2007. **35**(4): p. 1354-66.
27. Campbell, M.G. and K. Karbstein, *Protein-protein interactions within late pre-40S ribosomes.* PLoS One, 2011. **6**(1): p. e16194.
28. Peifer, C., et al., *Yeast Rrp8p, a novel methyltransferase responsible for m1A 645 base modification of 25S rRNA.* Nucleic Acids Res, 2013. **41**(2): p. 1151-63.
29. Lebaron, S., et al., *Rrp5 Binding at Multiple Sites Coordinates Pre-rRNA Processing and Assembly.* Mol Cell, 2013.
30. Xue, Y., et al., *Saccharomyces cerevisiae RAI1 (YGL246c) is homologous to human DOM3Z and encodes a protein that binds the nuclear exoribonuclease Rat1p.* Mol Cell Biol, 2000. **20**(11): p. 4006-15.
31. Oeffinger, M., et al., *Rrp17p is a eukaryotic exonuclease required for 5' end processing of Pre-60S ribosomal RNA.* Mol Cell, 2009. **36**(5): p. 768-81.
32. van Hoof, A., P. Lennertz, and R. Parker, *Three conserved members of the RNase D family have unique and overlapping functions in the processing of 5S, 5.8S, U4, U5, RNase MRP and RNase P RNAs in yeast.* EMBO J, 2000. **19**(6): p. 1357-65.
33. Dez, C. and D. Tollervey, *Ribosome synthesis meets the cell cycle.* Curr Opin Microbiol, 2004. **7**(6): p. 631-7.
34. Lebreton, A., et al., *60S ribosomal subunit assembly dynamics defined by semi-quantitative mass spectrometry of purified complexes.* Nucleic Acids Res, 2008. **36**(15): p. 4988-99.
35. Nissan, T.A., et al., *60S pre-ribosome formation viewed from assembly in the nucleolus until export to the cytoplasm.* EMBO J, 2002. **21**(20): p. 5539-47.
36. Tang, L., et al., *Interactions among Ytm1, Erb1, and Nop7 required for assembly of the Nop7-subcomplex in yeast preribosomes.* Mol Biol Cell, 2008. **19**(7): p. 2844-56.
37. Ciganda, M. and N. Williams, *Eukaryotic 5S rRNA biogenesis.* Wiley Interdiscip Rev RNA, 2011. **2**(4): p. 523-33.
38. Perez-Fernandez, J., et al., *The 90S preribosome is a multimodular structure that is assembled through a hierarchical mechanism.* Mol Cell Biol, 2007. **27**(15): p. 5414-29.
39. Warner, J.R., *The economics of ribosome biosynthesis in yeast.* Trends Biochem Sci, 1999. **24**(11): p. 437-40.
40. Strunk, B.S. and K. Karbstein, *Powering through ribosome assembly.* RNA, 2009. **15**(12): p. 2083-104.

41. Pratte, D., et al., *Mak5 and Ebp2 Act Together on Early Pre-60S Particles and Their Reduced Functionality Bypasses the Requirement for the Essential Pre-60S Factor Nsa1.* PLoS One, 2013. **8**(12): p. e82741.
42. Kong, K.Y., et al., *Cotranscriptional recruitment of yeast TRAMP complex to intronic sequences promotes optimal pre-mRNA splicing.* Nucleic Acids Res, 2014. **42**(1): p. 643-60.
43. Kressler, D., et al., *The power of AAA-ATPases on the road of pre-60S ribosome maturation--molecular machines that strip pre-ribosomal particles.* Biochim Biophys Acta, 2012. **1823**(1): p. 92-100.
44. Gadal, O., et al., *A nuclear AAA-type ATPase (Rix7p) is required for biogenesis and nuclear export of 60S ribosomal subunits.* EMBO J, 2001. **20**(14): p. 3695-704.
45. Kressler, D., et al., *The AAA ATPase Rix7 powers progression of ribosome biogenesis by stripping Nsa1 from pre-60S particles.* J Cell Biol, 2008. **181**(6): p. 935-44.
46. Fath, S., et al., *Association of yeast RNA polymerase I with a nucleolar substructure active in rRNA synthesis and processing.* J Cell Biol, 2000. **149**(3): p. 575-90.
47. Milkereit, P., et al., *Maturation and intranuclear transport of pre-ribosomes requires Noc proteins.* Cell, 2001. **105**(4): p. 499-509.
48. Milkereit, P., et al., *A Noc complex specifically involved in the formation and nuclear export of ribosomal 40 S subunits.* J Biol Chem, 2003. **278**(6): p. 4072-81.
49. Dlakic, M. and D. Tollervey, *The Noc proteins involved in ribosome synthesis and export contain divergent HEAT repeats.* RNA, 2004. **10**(3): p. 351-4.
50. Oeffinger, M., M. Dlakic, and D. Tollervey, *A pre-ribosome-associated HEAT-repeat protein is required for export of both ribosomal subunits.* Genes Dev, 2004. **18**(2): p. 196-209.
51. Ghaemmaghami, S., et al., *Global analysis of protein expression in yeast.* Nature, 2003. **425**(6959): p. 737-41.
52. Edskes, H.K., Y. Ohtake, and R.B. Wickner, *Mak21p of Saccharomyces cerevisiae, a homolog of human CAATT-binding protein, is essential for 60 S ribosomal subunit biogenesis.* J Biol Chem, 1998. **273**(44): p. 28912-20.
53. Carroll, K. and R.B. Wickner, *Translation and M1 double-stranded RNA propagation: MAK18 = RPL41B and cycloheximide curing.* J Bacteriol, 1995. **177**(10): p. 2887-91.
54. Merl, J., et al., *Analysis of ribosome biogenesis factor-modules in yeast cells depleted from pre-ribosomes.* Nucleic Acids Res, 2010. **38**(9): p. 3068-80.
55. Hierlmeier, T., et al., *Rrp5p, Noc1p and Noc2p form a protein module which is part of early large ribosomal subunit precursors in S. cerevisiae.* Nucleic Acids Res, 2013. **41**(2): p. 1191-210.
56. Altschul, S.F., et al., *Gapped BLAST and PSI-BLAST: a new generation of protein database search programs.* Nucleic Acids Res, 1997. **25**(17): p. 3389-402.
57. Lum, L.S., et al., *A cloned human CCAAT-box-binding factor stimulates transcription from the human hsp70 promoter.* Mol Cell Biol, 1990. **10**(12): p. 6709-17.
58. Lum, L.S., et al., *The hsp70 gene CCAAT-binding factor mediates transcriptional activation by the adenovirus E1a protein.* Mol Cell Biol, 1992. **12**(6): p. 2599-605.
59. Schuler, G.D., S.F. Altschul, and D.J. Lipman, *A workbench for multiple alignment construction and analysis.* Proteins, 1991. **9**(3): p. 180-90.

60. Li, N., et al., *SLOW WALKER2, a NOC1/MAK21 homologue, is essential for coordinated cell cycle progression during female gametophyte development in Arabidopsis.* Plant Physiol, 2009. **151**(3): p. 1486-97.
61. Gadal, O., et al., *Nuclear export of 60s ribosomal subunits depends on Xpo1p and requires a nuclear export sequence-containing factor, Nmd3p, that associates with the large subunit protein Rpl10p.* Mol Cell Biol, 2001. **21**(10): p. 3405-15.
62. Ohmayer, U., et al., *Studies on the Assembly Characteristics of Large Subunit Ribosomal Proteins in S. cerevisae.* PLoS One, 2013. **8**(7): p. e68412.
63. Hublitz, P., et al., *NIR is a novel INHAT repressor that modulates the transcriptional activity of p53.* Genes Dev, 2005. **19**(23): p. 2912-24.
64. Wu, J., et al., *Transcriptional repressor NIR functions in the ribosome RNA processing of both 40S and 60S subunits.* PLoS One, 2012. **7**(2): p. e31692.
65. Heyne, K., et al., *NIR, an inhibitor of histone acetyltransferases, regulates transcription factor TAp63 and is controlled by the cell cycle.* Nucleic Acids Res, 2010. **38**(10): p. 3159-71.
66. Zhang, Y., et al., *Noc3p, a bHLH protein, plays an integral role in the initiation of DNA replication in budding yeast.* Cell, 2002. **109**(7): p. 849-60.
67. Huo, L., et al., *The Rix1 (Ipi1p-2p-3p) complex is a critical determinant of DNA replication licensing independent of their roles in ribosome biogenesis.* Cell Cycle, 2012. **11**(7): p. 1325-39.
68. Houchens, C.R., et al., *Schizosaccharomyces pombe Noc3 is essential for ribosome biogenesis and cell division but not DNA replication.* Eukaryot Cell, 2008. **7**(9): p. 1433-40.
69. Tominaga, K., et al., *Fad24, a mammalian homolog of Noc3p, is a positive regulator in adipocyte differentiation.* J Cell Sci, 2004. **117**(Pt 25): p. 6217-26.
70. Jakob, S., et al., *Interrelationships between yeast ribosomal protein assembly events and transient ribosome biogenesis factors interactions in early pre-ribosomes.* PLoS One, 2012. **7**(3): p. e32552.
71. Wild, T., et al., *A protein inventory of human ribosome biogenesis reveals an essential function of exportin 5 in 60S subunit export.* PLoS Biol, 2010. **8**(10): p. e1000522.
72. Chatr-Aryamontri, A., et al., *The BioGRID interaction database: 2013 update.* Nucleic Acids Res, 2013. **41**(Database issue): p. D816-23.
73. Dragon, F., et al., *A large nucleolar U3 ribonucleoprotein required for 18S ribosomal RNA biogenesis.* Nature, 2002. **417**(6892): p. 967-70.
74. Ben-Aroya, S., et al., *Making temperature-sensitive mutants.* Methods Enzymol, 2010. **470**: p. 181-204.
75. Fehling, E. and M. Weidner, *Temperature characteristics and adaptive potential of wheat ribosomes.* Plant Physiol, 1986. **80**(1): p. 181-6.
76. Volkov, R.A., Panchuk, II, and F. Schoffl, *Heat-stress-dependency and developmental modulation of gene expression: the potential of house-keeping genes as internal standards in mRNA expression profiling using real-time RT-PCR.* J Exp Bot, 2003. **54**(391): p. 2343-9.
77. Gari, E., et al., *A set of vectors with a tetracycline-regulatable promoter system for modulated gene expression in Saccharomyces cerevisiae.* Yeast, 1997. **13**(9): p. 837-48.

78. Shulga, N., et al., *In vivo nuclear transport kinetics in Saccharomyces cerevisiae: a role for heat shock protein 70 during targeting and translocation.* J Cell Biol, 1996. **135**(2): p. 329-39.
79. Schwoebel, E.D., T.H. Ho, and M.S. Moore, *The mechanism of inhibition of Ran-dependent nuclear transport by cellular ATP depletion.* J Cell Biol, 2002. **157**(6): p. 963-74.
80. Janke, C., et al., *A versatile toolbox for PCR-based tagging of yeast genes: new fluorescent proteins, more markers and promoter substitution cassettes.* Yeast, 2004. **21**(11): p. 947-62.
81. Yen, K., et al., *An improved tetO promoter replacement system for regulating the expression of yeast genes.* Yeast, 2003. **20**(15): p. 1255-62.
82. Oeffinger, M., et al., *Comprehensive analysis of diverse ribonucleoprotein complexes.* Nat Methods, 2007. **4**(11): p. 951-6.
83. Stage-Zimmermann, T., U. Schmidt, and P.A. Silver, *Factors affecting nuclear export of the 60S ribosomal subunit in vivo.* Mol Biol Cell, 2000. **11**(11): p. 3777-89.
84. Gietz, D., et al., *Improved method for high efficiency transformation of intact yeast cells.* Nucleic Acids Res, 1992. **20**(6): p. 1425.
85. Gietz, R.D. and R.A. Woods, *Transformation of yeast by lithium acetate/single-stranded carrier DNA/polyethylene glycol method.* Methods Enzymol, 2002. **350**: p. 87-96.
86. Griesenbeck, J., et al., *Chromatin endogenous cleavage and psoralen crosslinking assays to analyze rRNA gene chromatin in vivo.* Methods Mol Biol, 2012. **809**: p. 291-301.
87. Sambrook, J. and D.W. Russell, *Radiolabeling of DNA probes by the polymerase chain reaction.* CSH Protoc, 2006. **2006**(1).
88. Bellemer, C., et al., *Genetic interactions show the importance of rRNA modification machinery for the role of Rps15p during ribosome biogenesis in S. cerevisiae.* PLoS One, 2010. **5**(5): p. e10472.
89. Teste, M.A., et al., *Validation of reference genes for quantitative expression analysis by real-time RT-PCR in Saccharomyces cerevisiae.* BMC Mol Biol, 2009. **10**: p. 99.
90. Kushnirov, V.V., *Rapid and reliable protein extraction from yeast.* Yeast, 2000. **16**(9): p. 857-60.
91. Mumberg, D., R. Muller, and M. Funk, *Regulatable promoters of Saccharomyces cerevisiae: comparison of transcriptional activity and their use for heterologous expression.* Nucleic Acids Res, 1994. **22**(25): p. 5767-8.
92. Mitchell, S.F., et al., *Global analysis of yeast mRNPs.* Nat Struct Mol Biol, 2013. **20**(1): p. 127-33.
93. Kvam, E. and D.S. Goldfarb, *Nucleus-vacuole junctions in yeast: anatomy of a membrane contact site.* Biochem Soc Trans, 2006. **34**(Pt 3): p. 340-2.
94. van Beekvelt, C.A., et al., *Domain III of Saccharomyces cerevisiae 25 S ribosomal RNA: its role in binding of ribosomal protein L25 and 60 S subunit formation.* J Mol Biol, 2000. **296**(1): p. 7-17.
95. Miyoshi, K., et al., *Normal assembly of 60 S ribosomal subunits is required for the signaling in response to a secretory defect in Saccharomyces cerevisiae.* J Biol Chem, 2002. **277**(21): p. 18334-9.

96. Kressler, D., P. Linder, and J. de La Cruz, *Protein trans-acting factors involved in ribosome biogenesis in Saccharomyces cerevisiae.* Mol Cell Biol, 1999. **19**(12): p. 7897-912.
97. Fatica, A., et al., *Cic1p/Nsa3p is required for synthesis and nuclear export of 60S ribosomal subunits.* RNA, 2003. **9**(12): p. 1431-6.
98. Wang, Q., et al., *2-Deoxy-D-glucose treatment of endothelial cells induces autophagy by reactive oxygen species-mediated activation of the AMP-activated protein kinase.* PLoS One, 2011. **6**(2): p. e17234.
99. Zhang, Y. and P.S. Cremer, *Interactions between macromolecules and ions: The Hofmeister series.* Curr Opin Chem Biol, 2006. **10**(6): p. 658-63.
100. Salema, V. and L.A. Fernandez, *High yield purification of nanobodies from the periplasm of E. coli as fusions with the maltose binding protein.* Protein Expr Purif, 2013. **91**(1): p. 42-8.
101. Singh, R.K., et al., *Histone levels are regulated by phosphorylation and ubiquitylation-dependent proteolysis.* Nat Cell Biol, 2009. **11**(8): p. 925-33.
102. Marzluff, W.F. and R.J. Duronio, *Histone mRNA expression: multiple levels of cell cycle regulation and important developmental consequences.* Curr Opin Cell Biol, 2002. **14**(6): p. 692-9.
103. Dez, C., J. Houseley, and D. Tollervey, *Surveillance of nuclear-restricted pre-ribosomes within a subnucleolar region of Saccharomyces cerevisiae.* EMBO J, 2006. **25**(7): p. 1534-46.
104. Hernandez-Verdun, D., *The nucleolus: a model for the organization of nuclear functions.* Histochem Cell Biol, 2006. **126**(2): p. 135-48.
105. Hernandez-Verdun, D., *Nucleolus: from structure to dynamics.* Histochem Cell Biol, 2006. **125**(1-2): p. 127-37.
106. Gadal, O., et al., *Rlp7p is associated with 60S preribosomes, restricted to the granular component of the nucleolus, and required for pre-rRNA processing.* J Cell Biol, 2002. **157**(6): p. 941-51.
107. Sirri, V., et al., *Nucleolus: the fascinating nuclear body.* Histochem Cell Biol, 2008. **129**(1): p. 13-31.
108. Tremblay, A., et al., *A physical interaction between Gar1p and Rnt1pi is required for the nuclear import of H/ACA small nucleolar RNA-associated proteins.* Mol Cell Biol, 2002. **22**(13): p. 4792-802.
109. Zhao, X. and Y.T. Yu, *Detection and quantitation of RNA base modifications.* RNA, 2004. **10**(6): p. 996-1002.
110. Leung, A.K. and A.I. Lamond, *The dynamics of the nucleolus.* Crit Rev Eukaryot Gene Expr, 2003. **13**(1): p. 39-54.
111. Pramila, T., et al., *The Forkhead transcription factor Hcm1 regulates chromosome segregation genes and fills the S-phase gap in the transcriptional circuitry of the cell cycle.* Genes Dev, 2006. **20**(16): p. 2266-78.
112. Spellman, P.T., et al., *Comprehensive identification of cell cycle-regulated genes of the yeast Saccharomyces cerevisiae by microarray hybridization.* Mol Biol Cell, 1998. **9**(12): p. 3273-97.
113. Cho, R.J., et al., *A genome-wide transcriptional analysis of the mitotic cell cycle.* Mol Cell, 1998. **2**(1): p. 65-73.

114. Swaney, D.L., et al., *Global analysis of phosphorylation and ubiquitylation cross-talk in protein degradation.* Nat Methods, 2013. **10**(7): p. 676-82.
115. Lallemand-Breitenbach, V. and H. de The, *PML nuclear bodies.* Cold Spring Harb Perspect Biol, 2010. **2**(5): p. a000661.
116. Granneman, S., E. Petfalski, and D. Tollervey, *A cluster of ribosome synthesis factors regulate pre-rRNA folding and 5.8S rRNA maturation by the Rat1 exonuclease.* EMBO J, 2011. **30**(19): p. 4006-19.
117. Oeffinger, M., et al., *Yeast Pescadillo is required for multiple activities during 60S ribosomal subunit synthesis.* RNA, 2002. **8**(5): p. 626-36.
118. Kaluarachchi Duffy, S., et al., *Exploring the yeast acetylome using functional genomics.* Cell, 2012. **149**(4): p. 936-48.
119. Eriksson, P.R., et al., *Regulation of histone gene expression in budding yeast.* Genetics, 2012. **191**(1): p. 7-20.
120. Clark-Adams, C.D., et al., *Changes in histone gene dosage alter transcription in yeast.* Genes Dev, 1988. **2**(2): p. 150-9.
121. Futcher, B., *Cell cycle synchronization.* Methods Cell Sci, 1999. **21**(2-3): p. 79-86.
122. Sebastian, J., I. Takano, and H.O. Halvorson, *Independent regulation of the nuclear RNA polymerases I and II during the yeast cell cycle.* Proc Natl Acad Sci U S A, 1974. **71**(3): p. 769-73.
123. Grummt, I., *Life on a planet of its own: regulation of RNA polymerase I transcription in the nucleolus.* Genes Dev, 2003. **17**(14): p. 1691-702.
124. Lewinska, A., et al., *Links between nucleolar activity, rDNA stability, aneuploidy and chronological aging in the yeast Saccharomyces cerevisiae.* Biogerontology, 2014.
125. Musters, W., et al., *A system for the analysis of yeast ribosomal DNA mutations.* Mol Cell Biol, 1989. **9**(2): p. 551-9.

6 Annexe

Expression and purification of anti-GFP nanobody

TES:	0.2M Tris-HCl, pH 8.0
	0.5mM EDTA, pH 8.0
	0.5M Sucrose
High-salt wash buffer:	20mM sodium phosphate, pH 8.0
	1M NaCl
	20mM imidazole, pH 8.0
Low-salt wash buffer:	20mM sodium phosphate, pH 8.0
	500mM NaCl
	20mM imidazole, pH 8.0
Elution buffer:	20mM sodium phosphate, pH 8.0
	500mM NaCl
	300mM imidazole, pH 8.0

Conjugation of recombinant anti-GFP nanobody to dynabeads

Dynabeads M270 Epoxy (invitrogen)

AB mix	10μg nanobody per mg of beads
	0.1M Sodium Phosphate pH 7.4- depending on the volume of nanobody, add the amount needed to have a total reaction volume of 2.0ml per 100 mg beads.
	1M Ammonium sulfate

Harvesting cell and cryogenic disruption

Resuspension buffer:	1.2% PVP-40
	20mM Hepes pH 7.4
	1:100 PIC
	1:100 Solution P
	1:1000 DTT
Solution P	2mg Pepstatin A
	90mg PMSF
	5ml absolute ethanol
	Store at -20°C, discard after 3 weeks

Protein extraction

Modified Laemmli SDS sample buffer :	0.06M Tris-HCl pH 6.8
	5% glycerol
	2% SDS
	4% βmercaptoethanol
	0.0025% bromophenol blue
Lysis solution :	1.85mL 10N NaOH
	740 µL βmercaptoethanol
	7.41mL ddH_2O
Solution A:	0.5M Tris Base
	5% SDS
Solution B :	37.5mM glycerol
	12.5mL ddH_2O
	0.96g Dithothreitol (DTT)
	0.05% bromophenol blue

Western blot

Solution A (ECL):	5mL 1M Tris-HCl pH 8.5
	45mL ddH_2O
	110µL 90mM Cumaric acid
	280µL 250mM Luminol
Solution B (ECL):	3% H_2O_2
Stripping buffer:	0.1M Glycine pH 2.5

10X TBST, 1L:	24.2g Tris
	80g NaCl
	21mL Tween20 brought to pH 7.6 with HCl

10X SDS-Tris glycine running buffer, 1L:	30.3g Tris Base
	144g Glycine
	10g SDS

10X TE : 10mM Tris Base, 1mM EDTA

Chromosomal DNA extraction

Breacking buffer, 10mL :	2% Triton X-100
	1% SDS
	100mM NaCl
	10mM Tris-HCl pH 8.0
	1mM EDTA pH 8.0
10X DNA loading buffer, 50mL :	30% glycerol
	10mg Orange B
10X TBE, 1L:	108 g Tris Base
	55g Boric acid
	40mL 0.5M EDTA pH 8.0